CRANFIELD UNIVERSITY

SIPENG SONG

MULTI-OBJECTIVE OPTIMAL LONGITUDINAL FLIGHT CONTROL SYSTEM DESIGN FOR A LARGE FLEXIBLE TRANSPORT AIRCRAFT

SCHOOL OF AEROSPACE, TRANSPORT AND MANUFACTURING
Aerospace

MSc by research
Academic Year: 2017–2018

Supervisor: Dr M.M.Lone / Dr J.F.Whidborne
May 2018

CRANFIELD UNIVERSITY

SCHOOL OF AEROSPACE, TRANSPORT AND MANUFACTURING
Aerospace

MSc by research

Academic Year: 2017–2018

SIPENG SONG

Multi-objective Optimal Longitudinal Flight Control System Design for a Large Flexible Transport Aircraft

Supervisor: Dr M.M.Lone / Dr J.F.Whidborne
May 2018

This thesis is submitted in partial fulfilment of the requirements for the degree of MSc by research.

© Cranfield University 2018. All rights reserved. No part of this publication may be reproduced without the written permission of the copyright owner.

Abstract

This thesis presents a multi-objective evolutionary algorithm design of a longitudinal optimal controller for a large flexible transport aircraft. The algorithm uses a mixed optimization approach based on a combination of Linear Quadratic Regulator(LQR) control and a Multi-Objective Genetic Algorithm (MOGA) to search over a set of possible weighting function structures and parameter values in order to satisfy a number of conflicting design criteria. The proposed approach offers a number of potential optimal solutions lying on or near the Pareto optimal front of competing objectives. The approach is explained in this thesis and some results are presented.

Keywords

Multi-objective Optimisation; Flexible Aircraft; MOGA; LQR; Handling Quality.

To my beloved grandparents

Contents

Abstract **iii**

Contents **v**

List of Figures **vii**

List of Tables **ix**

List of Abbreviations **x**

Acknowledgements **xi**

1 Introduction **1**
1.1 Motivation 1
1.2 Aim and Objectives 2
1.3 Outline of the Thesis 3
1.4 Contributions 4
1.5 Dissemination of Results 4

2 Literature Review **6**
2.1 Aircraft Modelling 6
2.2 Design Specifications 8
2.3 Multi-objective Optimisation 17
2.4 Mixed Optimisation Problem 24
2.5 Conclusion 27

3 System Modelling **29**
3.1 AX-1 model 29
3.2 Trim and Linearisation 30

4 Controller Design Process **44**
4.1 Controller Structure 44
4.2 Performance Objective Functions 47
4.3 Non-linear Constraints 54
4.4 Conclusion 56

5 Results Analysis **57**
5.1 Linear Results 57
5.2 Non-linear Simulation Results 69

6 Conclusions and Future Work **85**
6.1 Summary 85
6.2 Achievements 86
6.3 Challenges and Limitations 87
6.4 Recommendations for Further Work 89

A AX-1 Open-loop State-space Model **90**

References **92**

List of Figures

2.1 Collars Aeroelasticity Triangle [Wright and Cooper, 2007] 7
2.2 Bandwidth Definition [Cook, 2012] 9
2.3 Bandwidth Requirements (Category C) [MIL-STD-1797A, 1997] . . . 10
2.4 C* Time Response Envelopes [Field, 1993] 11
2.5 Short Period Dynamic Requirements of Large Aircraft [MIL-STD-1797A, 1997] 12
2.6 Generic Short Period Pitch Time Response [Gibson, 1999] 13
2.7 Dropback Criterion Assessment [Mooij, 1985] 14
2.8 Pareto Front [Liu et al., 2002] 19

3.1 AX-1 Aircraft Model [Portapas et al., 2017] 30
3.2 CA^{2}LM framework Structure [Portapas et al., 2017] 31
3.3 Mode Shapes 35
3.4 Pitch Rate Responses Comparison 38
3.5 Pitch Rate Error between Different Model 39
3.6 Pitch Rate Error between Different Input 39
3.7 Normal Acceleration Responses Comparison 40
3.8 Normal Acceleration Error between Different Model 41
3.9 Normal Acceleration Error between Different Input 41

4.1 Controller Structure 45
4.2 Definition of $q_{\max}$, q_{ss} and DB terms 47
4.3 Definition of Rise Time 50
4.4 Equivalent Controller Structure (Wind Disturbance) 51
4.5 Equivalent Controller Structure (Control Effort) 52
4.6 Equivalent Controller Structure (Comfort) 54

5.1 Tradeoff between f_1 ($q_{\max}/q_{\text{ss}}$) and f_5 (Rise Time) 58
5.2 Multi-objective Trade-off Diagram 59
5.3 Multi-objective Trade-off Diagram (non-diminated solutions) 59
5.4 Tradeoff between f_1 ($q_{\max}/q_{\text{ss}}$) and f_5 (Rise Time) 60
5.5 Tradeoff between f_1 and f_5 60
5.6 Tradeoff between f_1 and f_5 61
5.7 Tradeoff between f_1 and f_5 (detail) 62
5.8 Tradeoff between f_1 and f_5 62
5.9 Gibson Pitch Attitude Dropback Assessment 63
5.10 Gibson Pitch Attitude Dropback Assessment 64

5.11 Gibson Criteria Pitch Rate Response 64
5.12 Normal Acceleration Impulse Response 66
5.13 Normal Acceleration Singular Value Plot 67
5.14 Control Input Impulse Response 67
5.15 Control Input Singular Value Plot 68
5.16 Control Input Impulse Response 68
5.17 Control Input Impulse Response 69
5.18 Pitch Rate Comparison : Case 1 70
5.19 Control Input Comparison : Case 1 71
5.20 Structure Deformation Comparison : Case 1 72
5.21 Pitch Rate Comparison : Case 2 73
5.22 Control Input Comparison : Case 2 73
5.23 Structure Deformation Comparison : Case 2 74
5.24 Pitch Rate Comparison : Case 3 75
5.25 Control Input Comparison : Case 3 76
5.26 Structure Deformation Comparison : Case 3 77
5.27 Pitch Rate Comparison : Case 4 78
5.28 Control Input Comparison : Case 4 78
5.29 Structure Deformation Comparison : Case 4 79
5.30 Normal Acceleration Comparison : Open Loop 80
5.31 Structure Deformation Comparison : Open Loop 81
5.32 Normal Acceleration Comparison : Different Control Laws 82
5.33 Elevator Deflection Comparison : Different Control Laws 82
5.34 Structure Deformation Comparison : Different Control Laws 83
5.35 Comparison : Different Control Laws 83

List of Tables

3.1 Full-order Non-linear Model State Variables 32
3.2 Reduced-order Non-linear Model Trim Condition 33
3.3 Linear State-space Model State Variables 36
3.4 Longitudinal Linear State-space Model State Variables 37

List of Abbreviations

SATM	School of Aerospace, Technology and Manufacturing
MOGA	Multi-objective Genetic Algorithms
GAs	Genetic Algorithms
FCS	Flight Control System
LQR	Linearquadratic Regulator
CAP	Control Anticipation Parameter
HALE	High-Altitude Long-Endurance
MOI	Method of Inequalities
RCAH	Rate Command Attitude Hold

Acknowledgements

I would like to thank my supervisors Dr. James F Whidborne and Dr. Mudassir Lone for their advice, guidance, encouragement, and patience throughout the period of this research work.

It is really amazing to have them as my supervisors, especially Dr. Whidborne. At the beginning of the research, I understood nothing in this field. They are so patient to answer my stupid questions and always give me valuable advice. When I am writing the thesis, my bad English is always a problem. Thanks to Dr. Whidborne, he spent a lot of time on reading my bad writings. They are the best supervisors that I can ever imagine, I will not finish anything without them.

Thanks to Dr. Arturo M Cristóbal, for his expert advice in multi-objective optimal control, this work cannot be finished without him. Thanks to my colleges in Cranfield DSCG group for their support, advice and, discussions in related fields.

I would also like to thank my family. My parents who always support my dream and always encourage me when I am not confident. The deep thanks and love to my grandparents. This year is really tough for me because I lost my grandma. Although both of them cannot witness me to finish the degree, they are the main reason that I can overcome the difficulties during the research.

Chapter 1

Introduction

1.1 Motivation

Increasing demand for efficiency in the civil aerospace sector has resulted in manufacturers producing highly optimised aircraft with numerous features to reduce the airframe weight. The use of modern materials along with optimised structural designs has helped achieve incremental improvements in performance, but resulted in wings with increasing aspect ratios. This increase in the slenderness of wings has emphasised the importance of aeroservoelasticity where the interactions between the structures, aerodynamics and flight control cannot be neglected. Consequently, it is now critical that the flight control system not only provides good handling qualities but also ensures the aeroelastic effects do not have a negative impact on the overall aircraft flight dynamics and passenger comfort. Therefore, a multi-objective flight control system design problem for the flexible aircraft arises.

Multi-objective optimal control problems have been studied in detail in the control community ([Zadeh, 1963, Lin, 1976, Giesy, 1978, Tabak et al., 1979] and a review [Ng, 1989]). Normally some of these objectives are conflict (e.g. overshoot and rise time) and constrained (e.g. satisfied region for specific handling quality criterion). Therefore, a trade-off relationship exists, there is no single optimal solution

exists, rather a set of them known as Pareto optimal set. Therefore, suitable multi-objective searching method that is able to obtain a rich set of optimal solutions should be used in this study.

For multi-objective control problem, it is normal to translate different specifications and constraints of a different nature into a unique performance measure (e.g. H_2, H_∞) for measurement accuracy and computational ease. However, for flight control systems the handling quality is an important specification which is not easy to convert into a mathematical norm. Therefore, some time domain specifications should be included. To select a suitable handling quality criterion and measure the indices accurately in a computationally easy way is one of the most important objectives of this study.

To obtain the optimal controller, it is not enough just to use a multi-objective searching method (e.g. MOGA). Analytical optimal control method also should be used. A Combination of these two methods is called a 'Mixed Optimisation' approach. Selecting suitable methods of the study is another objective.

Normally, a good controller for the linear model will work well for the corresponding non-linear model under specific condition (e.g. flight condition for aircraft). But for a complex system, it is not safe to guarantee that. It is also important to investigate the relationship between the linear model and the non-linear model.

To address these problem, the aim and objectives of this study are listed next.

1.2 Aim and Objectives

The aim of this research is to develop an optimal flight control system for a flexible large aircraft and meet different design specifications simultaneously.

The objectives of this research are as follows:

a) Select suitable design specifications and translate them into appropriate mathematical expressions.

b) Select a suitable multi-objective optimisation method and analytical optimal controller design method.

c) Evaluate the performance of the designed controller in simulation using a non-linear model and and analyse the relationship between control gains and performance indices.

1.3 Outline of the Thesis

In summary, the thesis describes the development of multi-objective longitudinal flight control system (FCS) using a suitable multi-objective optimisation and optimal controller design method. The non-linear model test of the designed controller is also presented in this thesis.

Chapter 2 presents the literature review of this research. It includes the background of the model that is used in this research, the design specifications that the controller should meet, a review of multi-objective optimisation methods and a review of analytical optimal controller design methods.

Chapter 3 presents the details of the model. It includes the background of the non-linear model and the linearisation and decoupling process used in this study. Some assumptions and simplifications are also explained.

Chapter 4 describes the process of the optimal controller design. The controller structure, the objective functions and the non-linear constraints are also defined with mathematical expression in this chapter.

Chapter 5 is the results analysis chapter, which includes the linear and non-linear model test results of the designed controller and the analysis. The relationship between different objectives, gains and objectives and different solutions is analysed. A results comparison between the linear and non-linear models is also included.

Chapter 6 summarises the findings, concluding remarks and recommendations for future work.

1.4 Contributions

- The MOGA and LQR mixed optimization method, which is originally proposed by Baras et al. [1984] and developed by Liu et al. [2002] is proposed to design the longitudinal optimal flight control system along with the RCAH (Rate Command Attitude Hold) controller structure.

- Translated handling qualities in the form of Gibson drop back criteria as well as passengers comfort and control effort performance indices are proposed in computationally tractable forms.

- An analysis of the relationships between different objectives is provided. The relationship between different gains and objectives are also presented along with a comparison of the linear model results and non-linear model results of the same optimal solutions.

1.5 Dissemination of Results

Conference Paper

S. Song, J.F. Whidborne, M.M. Lone, A. Molina-Cristobal *Multi-objective Optimal Longitudinal Flight Control System Design for a Large Flexible Transport Aircraft*, 2018 UKACC 12th International Conference on Control (CONTROL), Year: 2018, Pages: 81 - 86, Adress: Sheffield, U.K.

Abstract: *This paper presents a multi-objective evolutionary algorithm design of a longitudinal optimal controller for a large flexible transport aircraft. The algorithm uses a mixed optimization approach based on a combination of Linear Quadratic Regulator(LQR) control and a Multi-Objective Genetic Algorithm (MOGA) to search over a set of possible weighting function structures and parameter values in order to satisfy a number of conflicting design criteria. The proposed approach offers a number of potential optimal solutions lying on or near the Pareto optimal front of*

competing objectives. The approach is explained in this paper and some results are presented.

Journal Paper

S. Song, J.F. Whidborne, M.M. Lone, A. Molina-Cristobal *Longitudinal Flight Control System Design for a Large Flexible Transport Aircraft using Mixed Optimization* (in preparation for submission to the Chinese Journal of Aeronautics)

Chapter 2

Literature Review

This study will focus on using the multi-objective optimal design for the longitudinal FCS design for large flexible aircraft. The literature review consists of four parts.

The review about modelling flexible aircraft comes first because the model will be the foundation of the rest of work. The modelling methods of previous flexible aircraft control law design works are reviewed. It also includes a review of flexible aircraft models that are used in this study. A brief introduction of the model used in this study is given and the reason is also explained.

After the modelling, the review of design specifications shows the possible criteria that could be used during the controller design process. The definition and the reason that why the chosen criteria are suitable for this study are also given.

The third and fourth parts are the reviews about optimisation methods, which includes both multi-objective optimisation methods and the mixed optimisation problem. The advantages and disadvantages of different methods are also listed. The reason for using MOGA and LQR in this project is also explained.

2.1 Aircraft Modelling

The flexible aircraft model is a foundation work of this study. Compared with rigid body aircraft models, a flexible aircraft model includes the coupling between aero-

dynamics, structural dynamics and inertial dynamics. Figure 2.1 shows Collar's Triangle, a well-known representation of the relationships among aerodynamics, elastic forces, inertial forces and control forces [Wright and Cooper, 2007]. Because of the coupling between these forces, the models have increased complexity which will be significant in the flight control design process.

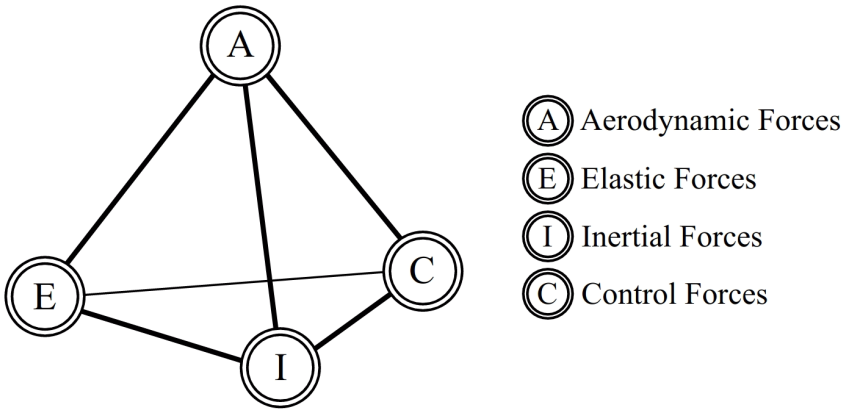

Figure 2.1: Collars Aeroelasticity Triangle [Wright and Cooper, 2007]

Over the years, there have been many models produced for flexible aircraft, but few of have been used as a target model for FCS design. Of those, Kubica and Livet [1994] and Ferreres and Puyou [2006] model the flexible aircraft in a simplified form by neglecting the couplings between the rigid body dynamics and the flexible dynamics. There also are some works about non-linear modelling of the flexible aircraft. Cesnik and Brown [2002] developed a non-linear, large deformation aeroelastic flexible aircraft model based on the High-Altitude Long-Endurance (HALE) aircraft. Kier and Looye [2009] and Palacios et al. [2010] [2010] also published their work about modelling flexible aircraft. These models could be used as target models in this study, but none of them is a transport aircraft model.

The CA^{2}LM framework has been developed by the Dynamics, Simulation and Control Group (DSCG) at Cranfield University [Andrews, 2010, Portapas et al., 2016, Dussart et al., 2017]. Considering the fidelity of the model and easy access to it, in this study, the CA^{2}LM framework is used as the working environment, and the AX-1 model the design target. The details of this model are presented in Chapter

3.

With increased complexity and coupling in the flexible aircraft model, the design specifications for an unaugmented aircraft are hard to meet. Thus an integral flight control system (FCS) that can meet the specifications is required.

2.2 Design Specifications

For large commercial aircraft, there is a set of design specifications that need to be met simultaneously. Good handling qualities will let the pilot fly this aircraft easier, less control effort during wind disturbance for the controller will extend the lifetime of the hardware of FCS, and most importantly, good comfort will be experienced by the passengers. Because the design target is a commercial transport aircraft, an ability to perform complex manoeuvres is not necessary, the longitudinal performance is more important. Thus this work is focused on designing a longitudinal FCS for AX-1 flexible aircraft.

2.2.1 Longitudinal Handling Qualities

From Cooper and Harper Jr. [1969], the definition of handling quality is "those qualities or characteristics of an aircraft that govern the ease and precision with which a pilot is able to perform the tasks required in support of an aircraft role." There are a number of specifications that are used to measure the longitudinal handling qualities. Of these criteria, there are four are widely used, the two that focus on time domain response are the C* Criterion and the Gibson Dropback Criterion, the frequency domain criteria are Bandwidth & Phase-delay Criterion and the CAP Criterion. Some details about these criteria are given below.

Bandwidth & Phase-delay Criterion

This criterion considers the bandwidth frequency (ω_{BW}) and phase delay (τ_p) of the pitch attitude response to a pilot control input to the aircraft. The ω_{BW} is the highest frequency at which the responses of aircraft pitch attitude to pilot control-force and control-deflection inputs have both 45 degrees or more of phase margin and 6 dB or more of gain margin. Figure. 2.2 shows the definition of ω_{BW}. The

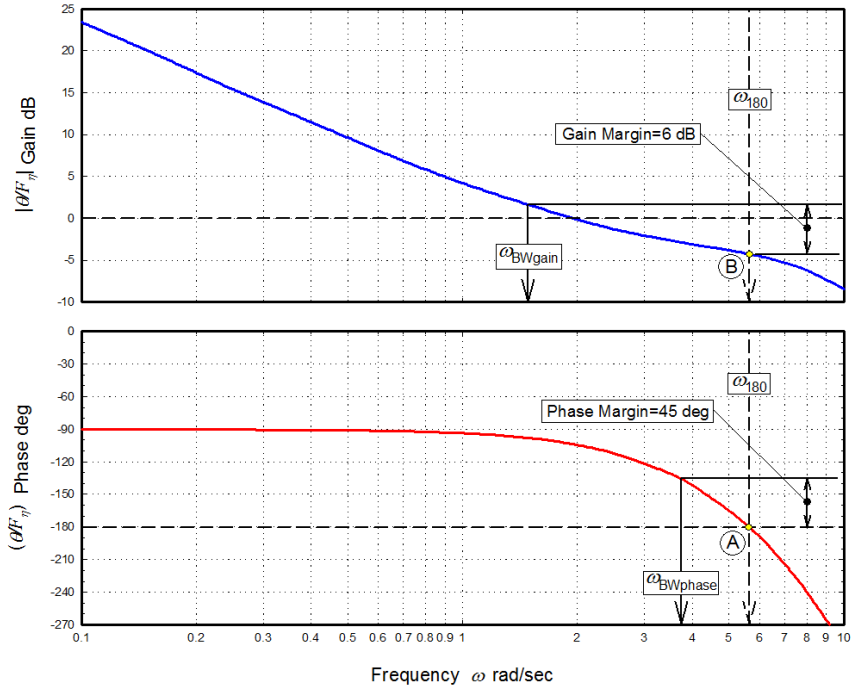

Figure 2.2: Bandwidth Definition [Cook, 2012]

phase delay τ_p is defined as:

$$\tau_p = \frac{-(\phi_{2\omega_{180}} + 180°)}{(57.3 \times 2\omega_{180})} \tag{2.1}$$

where ω_{180} is the frequency corresponding to -180 deg phase and $\phi_{2\omega_{180}}$ is the phase angle at twice that frequency [MIL-STD-1797A, 1997]. The two indices are located in Figure 2.3 to determine if the aircraft satisfies the criterion. This criterion can capture the aircraft capable of operating at a large enough value of bandwidth will have superior performance when regulating against disturbances. However, the bandwidth & phase-delay criterion is an evolutionary development of the Neal-Smith

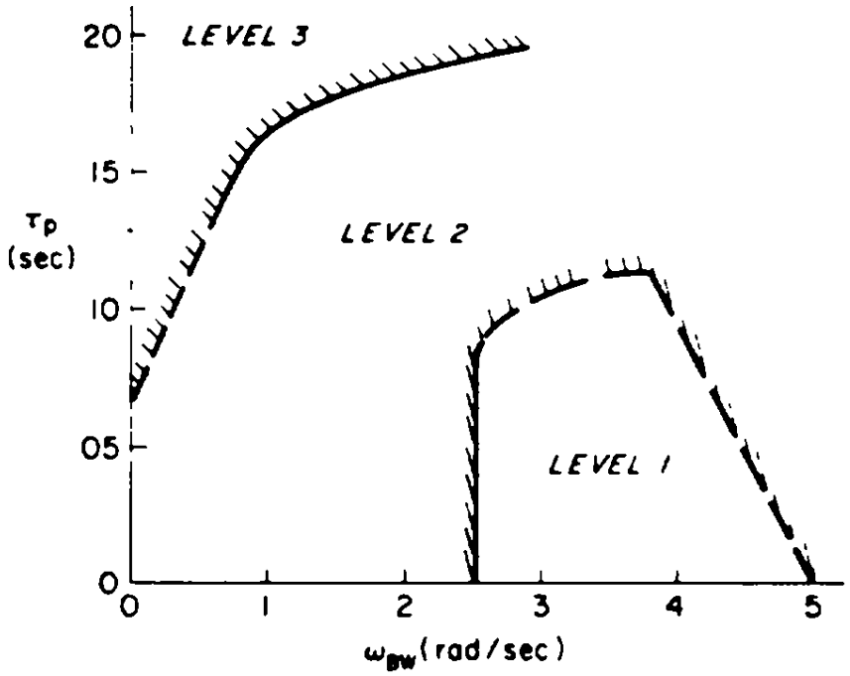

Figure 2.3: Bandwidth Requirements (Category C) [MIL-STD-1797A, 1997]

criterion, which includes an internal pilot model. Thus, the two indices that are used in this criterion are based on the transfer function describing pitch attitude response to pitch stick forces which also includes the pilot's dynamics. More details about this criterion can be found in MIL-STD-1797A [1997] and Cook [2012].

C* Criterion

The C* criterion considers a blend of normal load factor at the pilot's location and pitch rate as the feedback of the system. Its step response should lie within an acceptable envelope. The definition of C* is

$$C^* = k_{n_z} n_z + k_q q \tag{2.2}$$

where the k_{n_z} and k_q are the constant weighting terms that should be selected based on the flight condition. It has been argued that at high velocities the n_z would be dominant and at slower approach velocities q should dominate, the details can be found in Field [1993]. After the selection of k_{n_z} and k_q, the step response of C* should

lie in an acceptable envelope that is developed based on flight mission and flight condition. An example also can be seen in Field [1993]. In conclusion, C* criterion

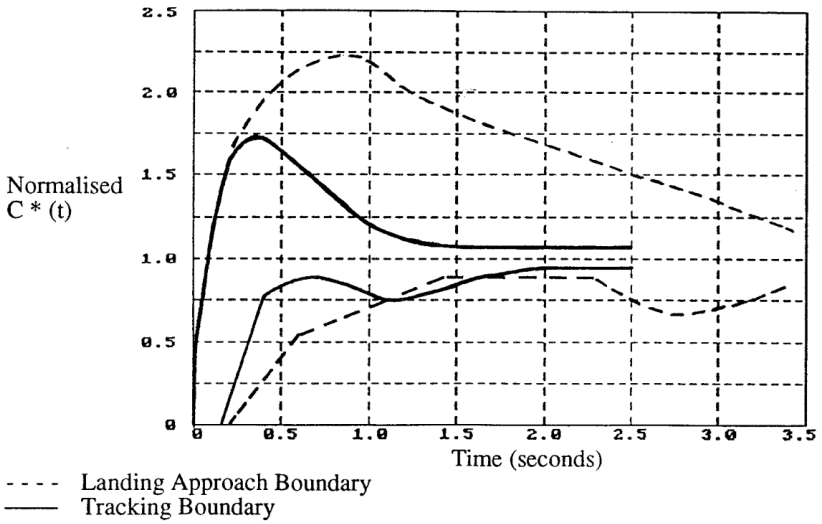

Figure 2.4: C* Time Response Envelopes [Field, 1993]

transfers the normal feedback signal (e.g. pitch rate and normal acceleration) into the C* signal which is the combination of n_z and q and if the normalised step response lies into the envelope, the longitudinal handling quality is satisfied.

CAP Criterion

The Control Anticipation Parameter (CAP) is another widely used criterion for longitudinal handling quality. The CAP is defined as,

$$CAP = \frac{\omega_{sp}^2}{n_z/\alpha} \tag{2.3}$$

where ω_{sp} is the short-period frequency, n_z is the normal acceleration of the pilot position and α is the angle of attack. This index gives a good indication about the pilot's perception of the pitch and vertical accelerations.

The criteria examine the relationship between CAP and the short-period damping ratio ζ_{sp}. Figure 2.5 shows the requirement of large aircraft in the military specifications [MIL-STD-1797A,1990]. With CAP on the y-axis and ζ_{sp} on the x-axis, locate the corresponding point. If the point is inside the satisfied region that

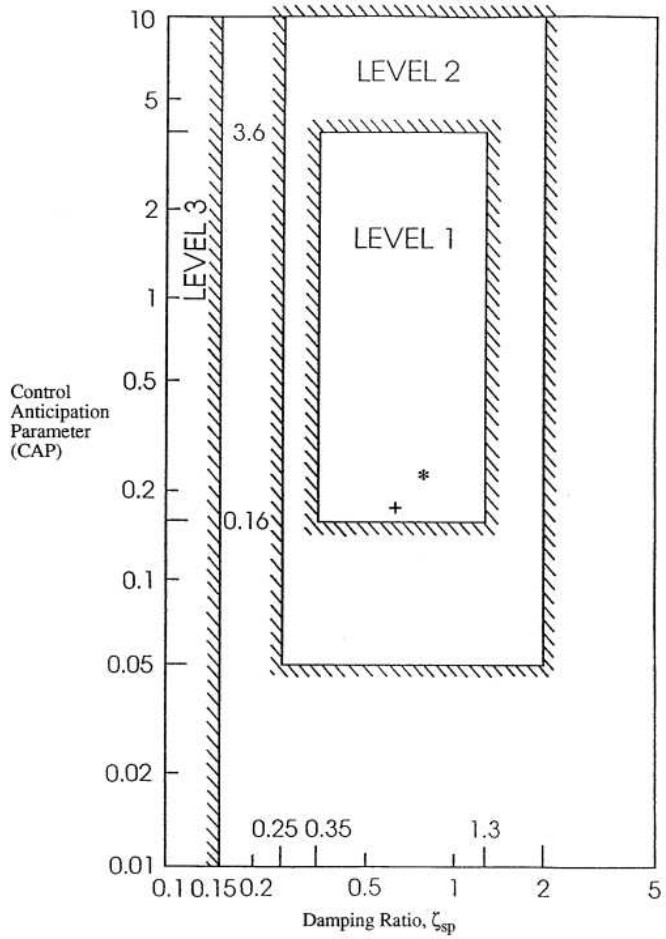

Figure 2.5: Short Period Dynamic Requirements of Large Aircraft [MIL-STD-1797A, 1997]

means the aircraft satisfies the criterion.

Gibson Dropback Criterion

The Gibson Dropback Criterion is another criterion that is widely considered. This criterion focuses on the pitch rate dynamics response and corresponding pitch angle response under a certain pulse input. Figure 2.6 shows the short period time response for a typical pulse input [Gibson, 1999]. It introduces the two performance indices of Gibson DropBack criterion, which are $q_{\max}/q_{\text{ss}}$ and DB/q_{ss} respectively. As shown in Figure 2.6, $q_{\max}$ is the maximum value of the pitch rate dynamic response under the pulse input, q_{ss} is its steady-state value. The drop back of pitch angle is denoted by DB in this criterion, which is the difference between the maximum pitch angle

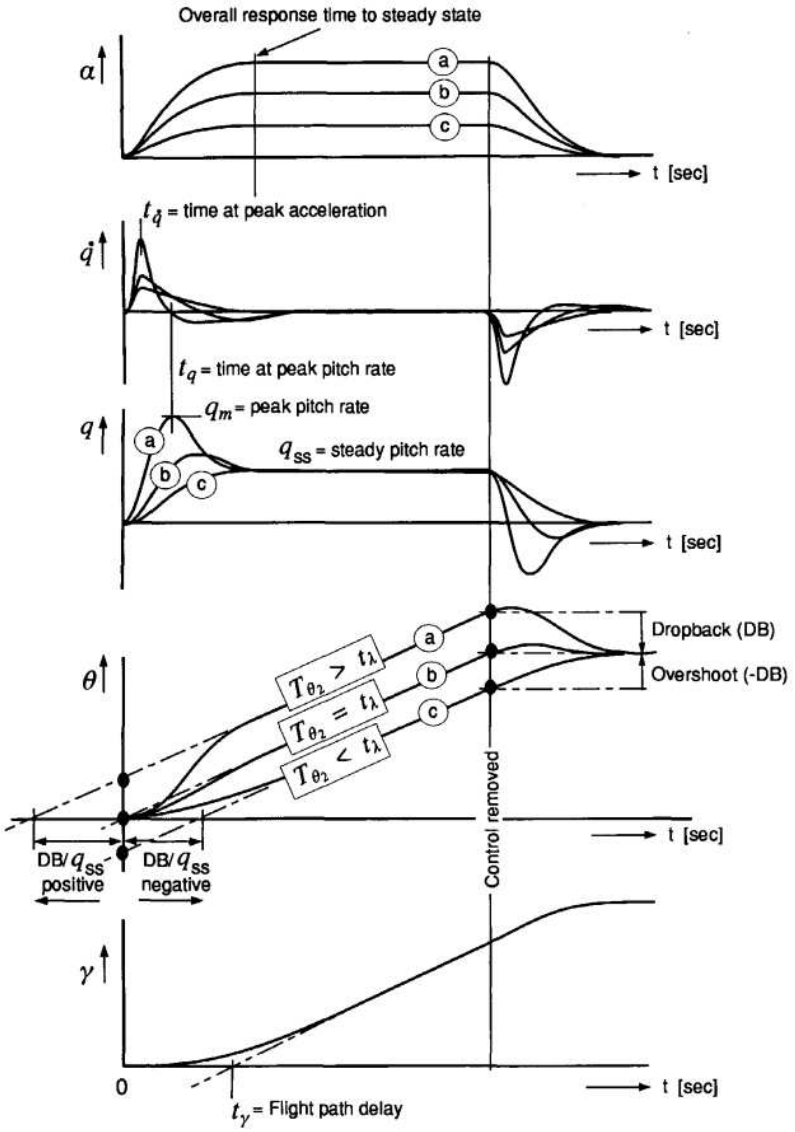

Figure 2.6: Generic Short Period Pitch Time Response [Gibson, 1999]

and the steady-state pitch angle. Thus the criterion can measure the longitudinal tracking performance of the aircraft, which is an important handling quality. The definition and details of these performance indices are given in Chapter 4.

This criterion is whether these two indices lie in the satisfied region. However, the original Gibson drop-back criterion is used for military combat aircraft. So the assessment of the Gibson criterion is unlikely to be satisfied for a large transport aircraft. Hence the original criterion has been modified. Figure 2.7 shows the modified assessment by Mooij [1985]. Further details of the criterion can be found

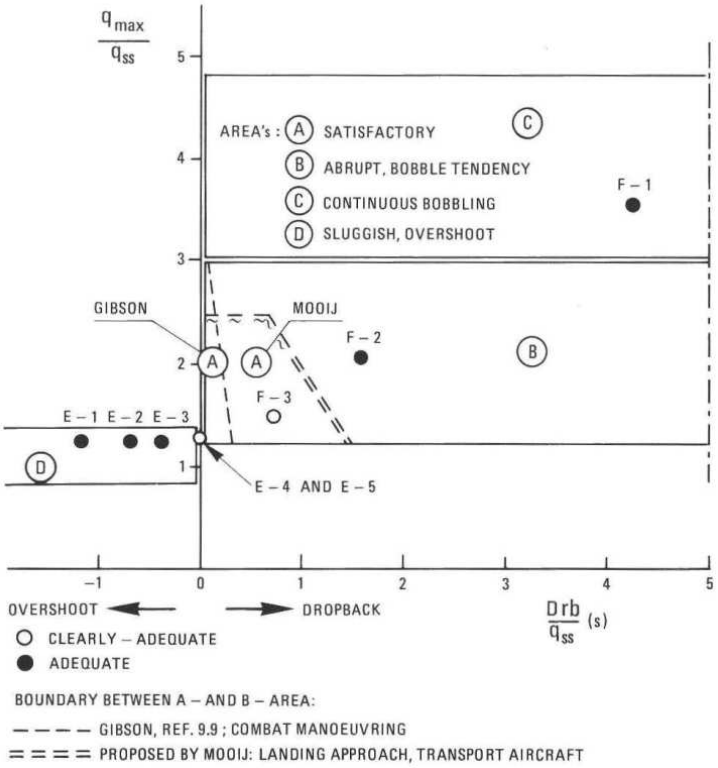

Figure 2.7: Dropback Criterion Assessment [Mooij, 1985]

in Moorhouse and Woodcock [1982].

Criterion Selection

The four criteria stated previously could be used for multi-objective control system design. However, generally, we do not want too many similar objective functions for the design because that will increase the complexity of the design process. Hence we need to establish the most appropriate criterion for the study.

Firstly, the bandwidth & phase-delay criterion includes a pilot dynamics model in the transfer function, which is not included in this study. So this criterion is not suitable.

The CAP criterion is not suitable, this is because this criterion is focused on the frequency domain analyses (ω_{sp} and ζ_{sp}). However, the flexible large aircraft model is a high order system which including several state variables which represent the structural deformations. So the analyses in the frequency domain may cause

the concern about neglecting the aeroservoelastic coupling during the FCS design process.

For time domain analyses, the C* criterion also has limitations for multi-objective optimisation approach. It is because that the envelope of acceptable responses is consist of infinite points in the time series. Thus it is a functional inequality rather than an algebraic inequality, that is

$$\underline{f}(t) \leq f(t) \leq \overline{f}(t) \tag{2.4}$$

This could be converted to an algebraic inequality, but generally functional inequalities are computationally expensive compared to algebraic inequalities.

Therefore, the Gibson Drop-back criterion is used in this study. It is more concerned about the signal tracking performance and the stabilised time of the large commercial aircraft and the performance indices are more easily presented in time domain analyses.

2.2.2 Comfort

Beside handling qualities, passenger's comfort is another critical factor in commercial aircraft design process. It is hard to define the comfort precisely because there are a lot of contributing elements (sound, temperature, smells, passenger activity, etc.).

For easy measurement and calculation in this project, the focus is on vibrational comfort, which is recognized to be preponderant for passenger comfort. The passenger comfort standard is defined by the ISO 2631-1 standard "Mechanical vibration and shock - Evaluation of human exposure to whole-body vibration." The standard proposes to compute a motion sickness index representative of the Percentage of Ill

Passengers (PIP) [ISO2631-1, 1997]

$$PIP = \frac{1}{3}\left[\int_0^T ({a_w}^2(t))dt\right]^{1/2} \tag{2.5}$$

where a_w is the measurement of vertical acceleration (m/s^2) during T seconds weighted by the sickness filtering. The specific mathematical definition of the objective function based on this specification is given in Section 4.2.2.

A related research has been presented by Kubica and Madelaine [1999]. The paper presents passengers comfort criteria based on ISO 2631-1 standard and shows how these criteria are applied to a large capacity civil aircraft for passenger comfort evaluation. Puyou et al. [2004a] also used this criterion in a multi-objective flight control law design process.

2.2.3 Control Effort

The control effort is also a well-known criterion in control system design. This index gives a good indication of the stability of the system under certain disturbance signals. There are two definitions of the control effort, either as the maximum control amplitude or as the integral of a certain function of the control, which is defined by Neustadt [1962]. Porter and Williams [1966] developed the minimum effort problem based on Neustadt's work . Ulsoy [1989] applied this theory on the linear controller design in 1989. Zakian and Al-Naib [1973] also mentioned the control effort in control system design by the method of inequalities (MOI).

In this study, the author decided to use the integral square of the control signal,

$$\int_0^\infty \mathbf{u}^2(t)dt \tag{2.6}$$

which can represent the control signal responding to a temporary disturbance [Maciejowski, 1989]. The integral square can be represented as H_2 norm that is easily computational in an algebraic calculation. The specific mathematical definition of

the objective function based on this specification is given in Section 4.2.2.

2.2.4 Conclusion

The problem considered here is the longitudinal handling quality for large flexible aircraft. Handling quality cannot be expressed by a simple criterion or single performance index. The details of the mathematical expression of different design specifications are shown in Chapter 4.

2.3 Multi-objective Optimisation

To meet the specifications simultaneously, the flight control system design problem can be posed as a multi-objective optimisation problem for FCS design arose. Therefore, the literature in this field is reviewed to support the method used in this work. The review in this section is largely drawn from the introduction in *Multi-objective Optimisation and Control* [Liu et al., 2002]

2.3.1 Problem Formulation

Objective Functions

The general muti-objective optimisation problem is the problem of simultaneously minimising the m objectives $\{f_i(\mathbf{p}) : i = 1 \dots m\}$ of a variable vector $\mathbf{p}$ in a set of possible design parameters $\mathcal{P}$, that is

$$\min_{\mathbf{p} \in \mathcal{P}} \{f_i(\mathbf{p}), \text{ for } i = 1 \dots m\} \tag{2.7}$$

In general, the problem (2.7) has no optimal solution that could optimise all objectives simultaneously. But there exist a set of solutions known as the Pareto-optimal set [Ben-Tal, 1980].

Constraint Functions

Practical problems are often constrained by a number of restrictions. These restrictions can provide a good region for design variable vector $\mathbf{p}$, and prevent the results from undesired performances.

Constraints can usually be described in terms of function inequalities of the form,

$$g_j(\mathbf{p}) \leq \epsilon_j, \quad j = 1 \ldots n \tag{2.8}$$

where $g_j(\mathbf{p})$ is generally a non-linear real-valued function of the design variable vector $\mathbf{p}$ and ϵ_j is a constant value. The inequalities may also be strict ($<$) rather than semi-strict ($\leq$). Equality constraints can be seen as particular cases of inequalities constraints.

2.3.2 Multi-objective Optimisation Method

After the formulation of the multi-objective problem, it is necessary to review the methods that can find the optimal design variable vector $\mathbf{p}$.

Pareto Optimality

In most cases, the objective functions are conflict, so the reduction of one objective function leads the increase in another. Subsequently, the result of the multi-objective optimisation is known as the Pareto-optimal solution. A Pareto-optimal solution has the property that it is not possible to reduce any of the objectives without increasing at least one of the other objective functions. A point $p^* \in \mathbf{p}$ is defined as being Pareto-optimal if and only if there exists no other point $p \in \mathbf{p}$ such that

a) $f_i(\mathbf{p}) \leq f_i(\mathbf{p}^*)$ for all $i = 1 \ldots m$ and

b) $f_j(\mathbf{p}) < f_j(\mathbf{p}^*)$ for at least one j

It is also known as non-dominated solution set. Figure 2.8 shows the Pareto-optimal

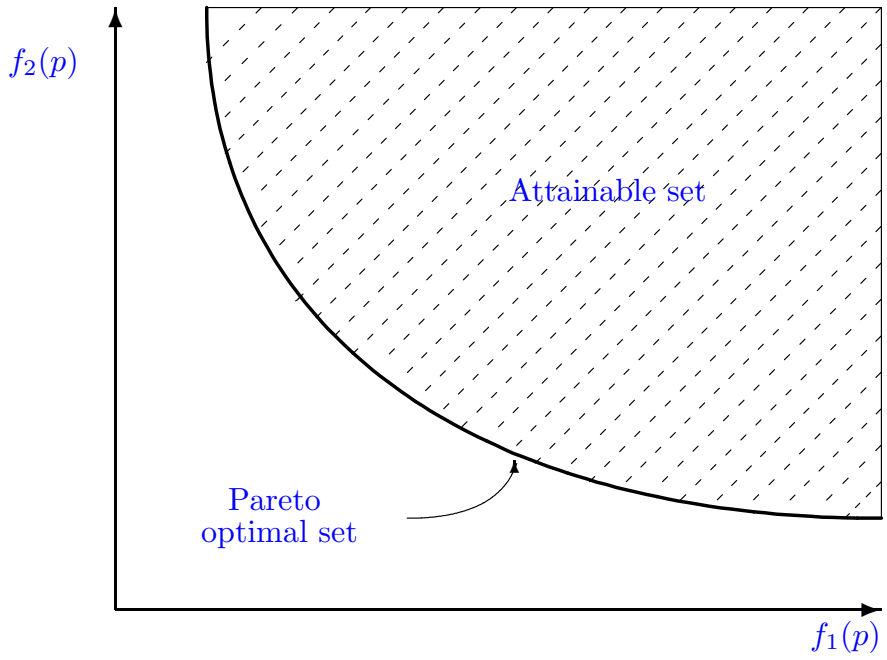

Figure 2.8: Pareto Front [Liu et al., 2002]

set for two conflicting objective functions.

Weighted Sum Method

The weighted sun method converts the multi-objective problem of minimising the objectives into a scalar one by constructing a weighted sum of all the objectives, that is

$$\min_{\mathbf{p}\in\mathcal{P}} \sum_{k=1}^{n} \omega_k f_i(\mathbf{p}) \tag{2.9}$$

where ω_k is the weighting coefficient. The problem can be solved as the single objective problem with a general optimisation method.

Goal Attainment Method

The goal attainment method involves expressing a set of design goals, which is associated with a set of objectives [Gembicki et al., 1975]. The problem formulation allows the objectives to be under- or over-achieved so that the initial design goals

can be set to be relatively imprecise by the designer. It can be formulated as,

$$\begin{aligned} &\min_{\lambda\in\mathbb{R},\mathbf{p}\in\mathcal{P}} \lambda \\ &f_i(\mathbf{p}) - \omega_k\lambda \leq f_i(\mathbf{p}^*), i = 1\ldots m \end{aligned} \tag{2.10}$$

where $f_i(\mathbf{p})$ is an objective, $f_i(\mathbf{p}^*)$ is a design goal, ω_k is the weighting coefficient and the λ is the parameter that should be minimized. [1] The method basically transfers the multi-objective problem into a single objective problem by just minimizing λ, so the solution that is found by this method is a feasible solution that satisfied all the constraints, but the found solution is not guaranteed to be an Pareto-optimal solution. Illustrative examples of control system design using goal attainment are given in Fleming and Pashkevich [1986].

Method of Inequalities (MOI)

It is difficult to determine a large set of Pareto-optimal solutions and choosing the solution which is the best design. To overcome this difficulty, the design problem can be formulated as the Method of Inequalities (MOI) problem. This formulation was proposed by Zakian and Al-Naib [1973], further details can be found in Patel and Munro [1982], Maciejowski [1989] and Whidborne and Liu [1993].

This method uses a set of algebraic inequalities which need to be satisfied during the design process to limit the solution search space. The problem can be formulated as: find $\mathbf{p}$ such that inequalities

$$f_i(\mathbf{p}) \leq \epsilon_i \quad \text{for} \quad i = 1, 2, \ldots m \tag{2.11}$$

are satisfied, where ϵ_i are real numbers, $\mathbf{p} \in \mathcal{P}$ is a real vector chosen from a set of possible design parameters and $f_i(\mathbf{p})$ are real functions of $\mathbf{p}$. This method indeed reduces the workload by searching for a feasible solution, but the solution is generally

[1] Note that there is a typographical error in this equation in *Multi-objective Optimisation and Control* ([Liu et al., 2002]).

not a Pareto-optimal solution.

Q-parametrization

Q-parametrization (sometimes referred to as "Youla Parameterization") is recognised by Boyd and Barratt [1991]. This method is proposed to solve the convex optimisation problems, many multi-objective control problems can be posed as convex optimisation problems. Ahmed and Whidborne [2007] used this method to solve H_∞ and time domain specifications problem. Puyou et al. [2004b] used this method to design the initial controller for the multi-objective problem of flexible aircraft flight control law problem.

However, Q-parametrization did not use in this study. This is because this method will normally give a high-order optimal controller. As considering the coupling between rigid body dynamics and flexible dynamics in the aircraft model (which did not consider in Puyou et al. [2004b]), the model that used in this study is a high-order system (detail in Chapter 3). It will be really complicated to design a high-order optimal controller for this system.

Nonsmooth Optimisation

Apkarian and Noll [2006] developed nonsmooth optimazations techniques to solve H_∞ synthesis problems under additional structural constraints on the controller. The approach avoids the use of Lyapunov variables and therefore leads to moderate size optimazation programs even for very large systems. Burke et al. [2006] developed a new MATLAB package called HIFOO, which aimed at solving fixed-order stabilization and local optimization problems based on the research. Gumussoy et al. and Arzelier et al. updated the HIFOO toolbox into version 2.0 and 3.0, and the toolbox is capable to solve H_2/H_∞ mixed problems.

This method is efficient to design a H_∞ controller for linear system when the order of the controller is fixed to be less than that of the open-loop plant, a typical

requirement is embedded aerospace control systems. However, this method is easily to find the local minima instead of the globe one. So this method did not use in this study.

2.3.3 Multi Objective Genetic Algorithms (MOGA)

Method Selection

Comparing the three main optimisation methods, some conclusions can be made,

1. The weighted sum method can only produce one optimal solution when the problem is convex.

2. The weighted sum method will miss some local minimum because of the constant slope in Pareto front which is decided by the constant weighting coefficients.

3. As explained in Section 2.3.2, the goal attainment method can find a feasible solution to the problem but it cannot be guaranteed as an optimal solution.

Therefore, the Pareto optimal solution is the ideal result of the problem. In this study, the author is looking for a method which can satisfy these terms.

1. Can find a set of Pareto-optimal solutions.

2. Will not miss local minimum solutions in a non-convex problem because of the complexity of previous set time domain specifications.

3. Can show the conflicts among different objectives.

Thus, a method named Multi-objective Genetic Algorithms (MOGA) is used in this work.

Theory

Genetic Algorithms (GAs) are searching procedures based on the evolutionary process in nature. Mostly they are used for solving single objective problems like the other search algorithms. However, there are also some multi-objective schemes proposed by Schaffer, Wienke et al. [1992]. Fonseca and Fleming [1995] have proposed an approach named Multi-objective Genetic Algorithms (MOGA) , which is an extension of an idea of Goldberg [1989].

The philosophy of MOGA is to find a set of simultaneous solutions and the designer can select the most suitable one from the set. The idea behind MOGA is to develop a population of Pareto-optimal or near Parato-optimal solutions which are non-dominated and which satisfy a set of inequalities. An individual j with a set of objective functions $f^j = (f_1^j, \ldots, f_n^j)$ is said to be *non-dominated* if for a population of N individuals, there are no other individuals $k = 1, \ldots, N, k \neq j$ such that,

a) $f_i^k \leq f_i^j$ for all $i = 1 \ldots m$ and

b) $f_i^k < f_i^j$ for at least one i

Combined with the constraints, the problem can be stated as: find a set of M admissible points $\mathbf{p}^j, j = 1 \ldots M$ such that

$$f_i^j \leq \epsilon_i, j = 1 \ldots M, i = 1, \ldots, n \tag{2.12}$$

and such that $f^j (j = 1 \ldots M)$ are non-dominated.

Further detail of MOGA can be found in Fonseca and Fleming [1993b,a, 1994].

MATLAB Toolbox

In MATLAB Global Optimization Toolbox, there is a function named `gamultiobj`, which can find a set of non-dominated solutions which may be close to the Pareto

front of multiple fitness functions using the genetic algorithm(GA). It allows the user to define the fitness functions and linear and non-linear constraints, the searching space of the design parameters. It will find a set of non-dominated solutions which may be close to the Pareto front based on these settings. Thus, this function is used in this work.

This algorithm is based on the work of Deb [2001]. It should be mentioned that this algorithm is using NSGA-II procedure [Deb et al., 2002] to sort the non-dominated solutions, which considered the crowding distance of these non-dominated solutions.

2.3.4 Application to Flight Control

There have been a number of other multi-objective optimization based flight control studies. For example, Tabak et al. [1979] designed a multi-objective lateral FCS based on both fighter aircraft and large manned lifting re-entry vehicle models. The Method of Inequalities (MOI) [Zakian and Al-Naib, 1973] has been used to design a longitudinal FCS focused on the ride qualities of a Short Take Off and Landing (STOL) aircraft [Crossley and Dahshan, 1982]. More specifically, there have been several multi-objective optimization approaches applied to flexible aircraft. These include a multi-objective method based on eigenstructure assignment [Livet et al., 1995] and Q-parameterization closed-loop shaping approaches [Ferreres and Puyou, 2006, Puyou et al., 2004a].

2.4 Mixed Optimisation Problem

Traditionally, controller designers using design methods based on either analytical optimisation or parameter optimisation. Both of them have advantages and disadvantages.

Generally, the analytical optimisation method (*e.g.* $\mathcal{H}_\infty$, LQR) are robustly

stable, provide a global optimum and can deal with relatively large multi-variable problems. However, usually they are single objective, not very flexible, provide high order controllers and the closed loop performance is non-explicit.

In the other hand, the parameter optimisation methods are generally multi-objective (*e.g. MOGA*) and flexible, provide simple controllers and have explicitly closed-loop performance. However, they are often non-convex resulting in local minima, not implicitly robustly stable, can only deal with small problems and may have difficulty in stabilising the system.

Therefore, a combination of analytical optimisation methods and the parameter optimisation methods is proposed, called *mixed optimisation* which is able to overcome some limitations of using just one approach [Whidborne et al., 1995b].

2.4.1 Previous Work

Many of the methods proposed for multi-objective control design rely either on a direct search of the controller parameters [Kreisselmeier and Steinhauser, 1983, Tabak et al., 1979, Zakian and Al-Naib, 1973] or a Q-parametrization of the controller [Boyd et al., 1990, Ferreres and Puyou, 2006, Puyou et al., 2004a] that maintains convexity of the system performance indices. The former suffers from the problem of multiple local minima and a high dimension search space (except for simple SISO controllers), whilst the latter results in high dimension, complex controllers. An alternative approach, dubbed *mixed optimization* [Whidborne et al., 1996] overcomes some of these limitations by using a numerical method to search for the parameters of the weighting functions required by analytical approaches such as LQR and $\mathcal{H}_\infty$-optimal control. The earliest mixed optimization appears to be Baras et al. [1984] who developed a Computer-Aided Control Systems Design (CACSD) package, DELIGHT.LQG, that used tuning algorithms for the weights of an LQG problem to satisfy a number of engineering specifications. Other early efforts for linear quadratic control include [Haessig, 1995, Paddison et al., 1994, Whidborne et al., 1995a]. An

$\mathcal{H}_\infty$-based approach using the MOI has been proposed by Postlethwaite et al. [1994], Whidborne et al. [1994]; this was extended to utilize the MOGA as the searching algorithm [Dakev et al., 1997]. The MOGA has also been combined with LMIs for mixed optimization [Molina-Cristóbal et al., 2006] and applied for robust controller design for aircraft lateral dynamics [Giacomán-Zarzar et al., 2008].

2.4.2 Analytical Control Method Selection

For flexible aircraft model, an important characteristic of it is the linear model will be high order because it includes not only rigid body dynamics but also the aero-structural dynamics (details in Chapter 3). Therefore the Linear Quadratic Regulator (LQR) theory is selected as the analytical optimisation method in this work. This is because of the simple structure of LQR controllers (full-state feedback controller) and their relatively simple computation make them a good candidate for high order system control (see McKernan et al. [2007] for example). Furthermore, for an ℓ-input, n-state system model with the $\mathbf{Q}$ and $\mathbf{R}$ weighting matrices set to be diagonal, the number of tuning parameters is $\ell + n - 1$, where as direct tuning of the feedback gain matrix will hence $\ell \times n$ parameters.

2.4.3 Linear Quadratic Regulator(LQR) Problem

For a linear state-space system:

$$\dot{\mathbf{x}}(t) = \mathbf{A}\mathbf{x}(t) + \mathbf{B}\mathbf{u}(t) \tag{2.13}$$

To get an optimal controller, the quadratic cost function that should be minimized is

$$J = \int_0^\infty (\mathbf{x}(t)^T \mathbf{Q}\mathbf{x}(t) + \mathbf{u}(t)^T \mathbf{R}\mathbf{u}(t))dt \tag{2.14}$$

using a state feedback controller $\mathbf{K}$ such that

$$\mathbf{u}(t) = -\mathbf{K}\mathbf{x}(t) \tag{2.15}$$

where $\mathbf{Q}$ is positive semi-definite and $\mathbf{R}$ is positive define control weighting matrices, normally chosen to be diagonal. Thus the problem is to find an optimal constant feedback controller $\mathbf{K}_0$ such that (2.14) is minimized.

The controller $\mathbf{K}_0$ that minimizes J is well-known and is given by

$$\mathbf{K}_0 = \mathbf{R}^{-1}\mathbf{B}^T\mathbf{P} \tag{2.16}$$

where $\mathbf{P} = \mathbf{P}^T > 0$ is found by solving

$$\mathbf{A}^T\mathbf{P} + \mathbf{P}\mathbf{A} - \mathbf{P}\mathbf{B}\mathbf{R}^{-1}\mathbf{B}^T\mathbf{P} + \mathbf{Q} = 0. \tag{2.17}$$

In this study, the $\mathbf{Q}$ and $\mathbf{R}$ matrices are constrained to be diagonal positive matrices

$$\mathbf{Q} = \text{diag}(q_1, \ldots, q_n) \qquad \text{and} \qquad \mathbf{R} = \text{diag}(1, r_1, \ldots, r_{\ell-1}). \tag{2.18}$$

The matrix $\mathbf{P}$ is an $n \times n$ symmetric matrix (n is the number of state variables) and is positive semi-definite (*i.e.* $\mathbf{x}^T\mathbf{P}\mathbf{x} \geq 0$ for all $\mathbf{x} \neq 0$). A positive definite (or semi-definite) matrix has all eigenvalues positive (non-negative). Equations of the form (2.17) are known as Algebraic Riccati Equations (ARE) and can be solved using numerical methods [Macirjowski, 1989].

If $\mathbf{p}$ parameterizes the weighting matrices $\mathbf{Q}$ and $\mathbf{R}$, then (2.7) represents a mixed optimization problem which overcomes some of the limitations of the direct approach (see Whidborne et al. [1994]). It also should be mentioned that Boyd and Barratt [1991] proposed a method to solve the multi-criterion LQR problem based

on weighted sum method.

2.5 Conclusion

In conclusion, in this work, it is proposed that MOGA is mixed with LQR control to solve the design problem of a multi-objective optimal controller for the longitudinal dynamics of a large flexible transport aircraft with the respect of the design specifications.

Chapter 3

System Modelling

In this study, the AX-1 model is used as the target design model. This model is under the CA^{2}LM framework, a simulation environment for coupled aerodynamics and structural dynamics analysis. Developed as a Simulink tool, it is versatile and suited for the analysis of flight dynamics, flight loads and handling qualities. This framework has been developed by the Dynamics Simulation & Control group in Cranfield University [Portapas et al., 2016, 2017].

3.1 AX-1 model

The AX-1 model is a non-linear generic large flexible transport aircraft model based on the CA^{2}LM framework. This model was initially developed for the evaluation of handling qualities of large flexible aircraft [Andrews, 2010]. It also provides the capability for flight control law design of user-defined airframe configurations. The AX-1 configuration is shown in Figure 3.1. This CA^{2}LM non-linear framework provides a simulation environment for time domain simulation based on large flexible transport aircraft. The user can define time domain signals to represent inputs such as elevator deflections. The outputs of the AX-1 model are aircraft rigid body state variables such as aircraft position in the Earth axis, its angular and translational velocities and attitude in the body axis. The Simulink environment and the developer

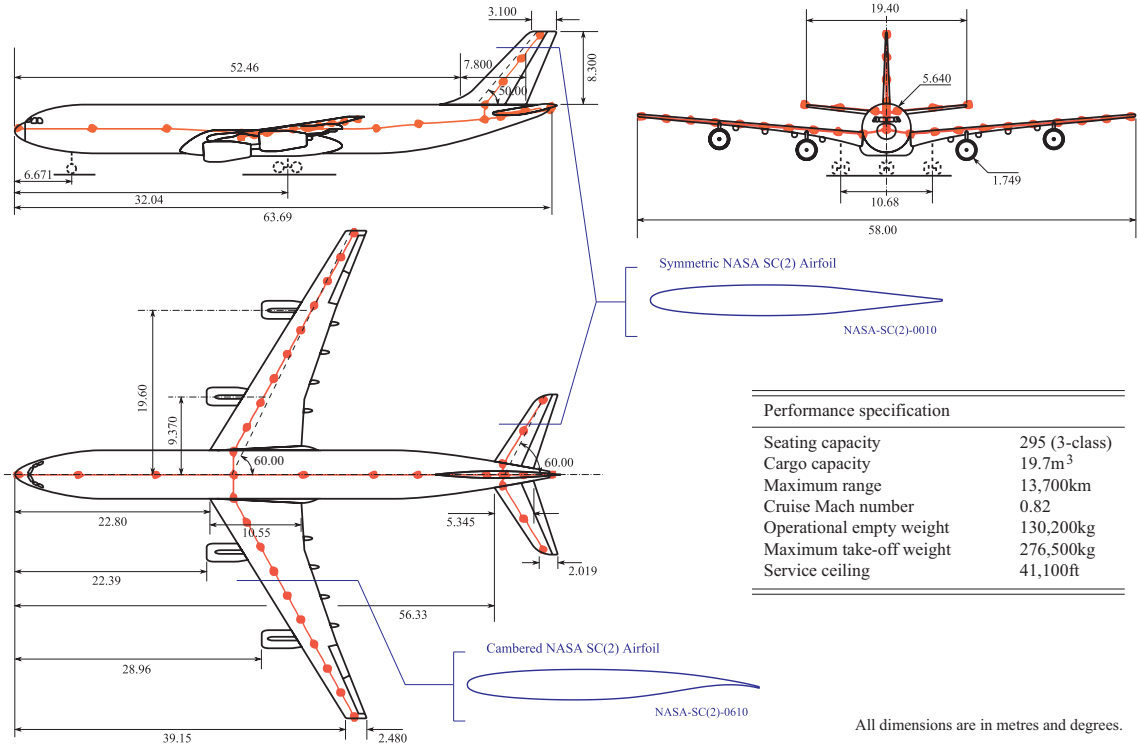

Figure 3.1: AX-1 Aircraft Model [Portapas et al., 2017]

of the model also enable users to select their own desired output. Internal structural loads such as bending moments and torsion, the forces acting on the aircraft and the acceleration in body axis can also be output. The core of the framework consists of the aerodynamics, structural dynamics, gravity and equations of motion blocks.

The gust/turbulence block provides an environment for modelling atmospheric disturbances and allows the implementation of continuous turbulence and discrete gusts. The non-aerodynamic loading block allows the specification of additional mass properties. Fuel, cargo and passenger loadings can be specified in detail and this information is used to calculate aircraft mass, inertia and centre of gravity. The overall structure of the CA^{2}LM framework is shown in Figure 3.2.

3.2 Trim and Linearisation

Most FCSs consist of a set of flight control laws for different flight conditions and flight missions. In this study, the aircraft is considered at the cruise flight condition

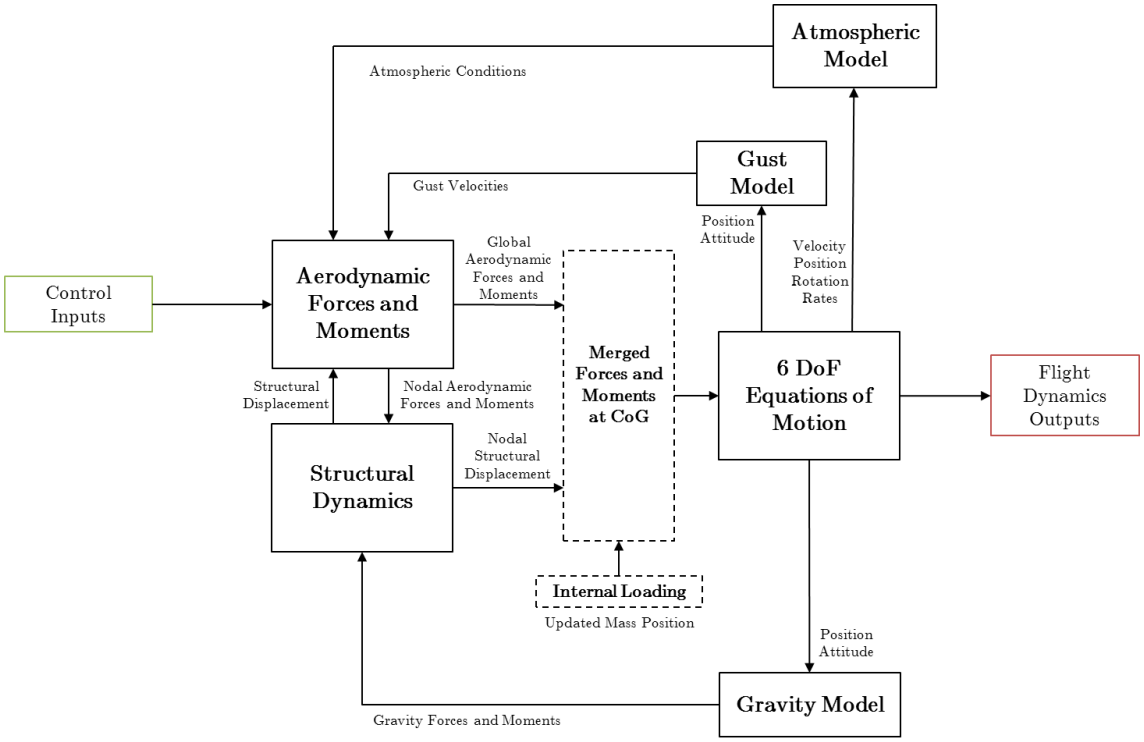

Figure 3.2: CA^{2}LM framework Structure [Portapas et al., 2017]

with an airspeed of 180 m/s and altitude of 6069m (20,000ft). The MATLAB `trim` command is used to trim the model in this flight condition.

The CA^{2}LM framework provides a non-linear model in the Simulink environment. To design flight control laws, it is necessary to linearise the non-linear model at a chosen flight condition. In this study, the MATLAB `linmod` routine is used to linearise the model.

Before designing control law based on the linear model, it is necessary to test if the linear model has a similar dynamic response as the non-linear model.

3.2.1 Reduced Order Non-linear Model

The original AX-1 model includes unsteady aerodynamics, actuator dynamics, and some integrator blocks, these blocks increase the number of state variables. The state variables number of the original AX-1 model is 1662, which makes the trim condition a large vector and hard to find a precise trim point. Furthermore, full

state feedback is used for the control (LQR). This means that it would be very hard to measure or estimate such a high order state for the controller implementation. In addition, designing the gains/weighting function parameters is difficult for such a high order. Therefore, a reduced-order non-linear model is required for the trim and linearisation process.

To obtain a proper trim model (reduced-order model), the full-order model should reduce more than 1600 undesired statevaribles (transport delay, actuator dynamics, integrator etc) in the Simulink model. This process affects the simulation modelling accuracy of the reduced-order model.

Table 3.1: Full-order Non-linear Model State Variables

Category	Amount
Rigid Body State Variables	12
Structural Displacements	12
Structural Velocities	12
Wind Model State Variables	16
Actuator Dynamics	18
Gust Model Integrator	116
Turbulence Time Delay	192
Indicial Downwash State Variables	414
Unsteady Aerodynamics Integrator	870
Total State Variables	1662

Table 3.1 shows the full-order non-linear model state variables. The reduced order model just keeps the rigid body state variables, the structural displacements and the structural velocities, giving 36 state variables in total.

3.2.2 Trim and Linearisation

The trim condition is found using the `trim` command in MATLAB and the linear model is obtained by the `linmod` routine at flight condition 180m/s and 6069m (20,000ft) altitude based on the trim model (reduced-order model).

The trim condition is shown in Table 3.2 and is validated in the reduced-order model by simulating the model with zero inputs and examining the state variables

Table 3.2: Reduced-order Non-linear Model Trim Condition

Category	State Variables/Trim Value			
Velocities	u	v	w	units
	179.9026	-0.0374	5.9262	(m/s)
Angular Velocities	p	q	r	units
	0	0	0	(rad/s)
Euler angles	ϕ	θ	ψ	units
	0	0.0329	0	(rad)
Structural Displacements	η_1	η_2	η_3	η_4
	0	3.4905	-3.5811	0
	η_5	η_6	η_7	η_8
	0	0.4812	-0.7858	0
	η_9	η_{10}	η_{11}	η_{12}
	0.7953	0	-0.0764	0
Structural Velocities	$\dot{\eta}_1$	$\dot{\eta}_2$	$\dot{\eta}_3$	$\dot{\eta}_4$
	0	0	0	0
	$\dot{\eta}_5$	$\dot{\eta}_6$	$\dot{\eta}_7$	$\dot{\eta}_8$
	0	0	0	0
	$\dot{\eta}_9$	$\dot{\eta}_{10}$	$\dot{\eta}_{11}$	$\dot{\eta}_{12}$
	0	0	0	0

responses. The linearised model is obtained by the `linmod` routine shown in the next section.

3.2.3 Linear State-Space Model

The linearised state-space model is a 33rd order system. There are 9 state variables that are the same as a rigid body aircraft, velocities (u, v, w), angular velocities (p, q, r) and Euler angles (ϕ, θ, ψ). The displacement state variables (X, Y, Z) are not included because they do not have a strong link to the flight dynamics. The remaining 24 state variables capture 12 different aeroelastic modes with state variables consisting of the structural displacements and corresponding velocities.

The linearised model is constructed in the state-space form as:

$$\begin{bmatrix} \dot{\mathbf{x}}_\mathrm{r} \\ \dot{\mathbf{x}}_\mathrm{e} \end{bmatrix} = \begin{bmatrix} \mathbf{A}_\mathrm{r} & \mathbf{A}_\mathrm{er} \\ \mathbf{A}_\mathrm{re} & \mathbf{A}_\mathrm{e} \end{bmatrix} \begin{bmatrix} \mathbf{x}_\mathrm{r} \\ \mathbf{x}_\mathrm{e} \end{bmatrix} + \begin{bmatrix} \mathbf{B}_\mathrm{r} \\ \mathbf{B}_\mathrm{e} \end{bmatrix} \mathbf{u} \tag{3.1}$$

where $\mathbf{A}_\mathrm{r}$ and $\mathbf{A}_\mathrm{e}$ are the rigid body and aeroelastic modes motion matrices respectively, $\mathbf{A}_\mathrm{er}$ and $\mathbf{A}_\mathrm{re}$ represent the coupling characteristics between them, $\mathbf{B}_\mathrm{r}$ and $\mathbf{B}_\mathrm{e}$ matrices are the contribution of control input to rigid body and aeroelastic modes. The rigid body state variables and aeroelastic state variables are also partitioned into two vectors named $\mathbf{x}_\mathrm{r}$ and $\mathbf{x}_\mathrm{e}$.

The rigid body state vector consists of the classical flight dynamics state variables as:

$$\mathbf{x}_r = [q, \theta, u, w, v, p, r, \phi, \psi]. \tag{3.2}$$

The flexible modes are represented by generalized modal deflections vector ($\boldsymbol{\eta}$) and modal velocities vector ($\dot{\boldsymbol{\eta}}$). There are 12 different modes in total, and are shown in Figure 3.3. The critical part in representing the areoelastic component of the system is to specify generalized coordinates [Yusuf et al., 2017]. In this study, the elastic deformation is obtained from the known mode shapes, that can be validated from Ground Vibration Tests (GVT). Therefore, the function of deformation of structure about time can be obtained as:

$$\mathbf{d}(x, y, z, t) = \Phi(x, y, z)\boldsymbol{\eta}(t) \tag{3.3}$$

where Φ is mode shape matrix, which can transit mode displacement ($\boldsymbol{\eta}$) to structural deformation ($\mathbf{d}$).

The generalised modal deflection vector is hence calculated from:

$$\boldsymbol{\eta}(t) = \Phi^{-1}(x, y, z)\mathbf{d}(x, y, z, t) \tag{3.4}$$

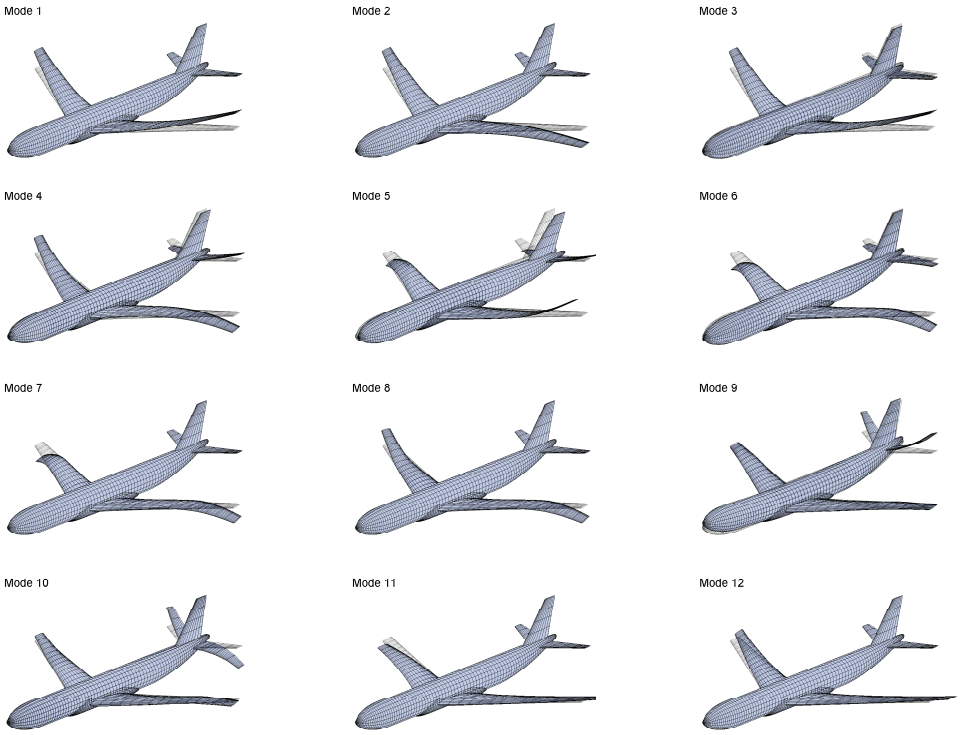

Figure 3.3: Mode Shapes

Furthermore, the mode shape matrix Φ is a transition matrix rather than a function of time. So the structure velocity and acceleration can also be defined as:

$$\begin{aligned} \dot{\mathbf{d}}(x,y,z,t) &= \Phi(x,y,z)\dot{\boldsymbol{\eta}}(t) \\ \ddot{\mathbf{d}}(x,y,z,t) &= \Phi(x,y,z)\ddot{\boldsymbol{\eta}}(t) \end{aligned} \tag{3.5}$$

Therefore, the aeroelastic state vector can be represented as:

$$\mathbf{x}_e = [\eta_1, \ldots, \eta_{12}, \dot{\eta}_1, \ldots, \dot{\eta}_{12}]. \tag{3.6}$$

Thus, in the state-space model, the structural deformation, velocity and acceleration can be represented. The linear model state variables are summarised in Table 3.3.

Table 3.3: Linear State-space Model State Variables

Category	State Variables
Rigid Body State Variables	$q, \theta, u, w, v, p, r, \phi, \psi$
Structural Displacements	$\eta_1, \ldots, \eta_{12}$
Structural Velocities	$\dot{\eta}_1, \ldots, \dot{\eta}_{12}$

3.2.4 Longitudinal/Lateral Mode Decoupling

In common with most classical fixed wing aircraft, the lateral and longitudinal dynamics can be decoupled and the flight control laws designed separately. In this work, the focus is the longitudinal flight dynamics. So it is necessary to decouple the linear model to longitudinal linear model.

For the rigid body state variables, there are four longitudinal state variables in classical flight dynamics (q, θ, u, w) [Cook, 2007], so

$$\mathbf{x}_{\text{rlong}} = [q, \theta, u, w]. \tag{3.7}$$

For the aeroelastic state vector, the aeroelastic modes can be divided into symmetric and asymmetric sets. Only the symmetric aeroelastic modes affect the longitudinal responses of the aircraft. So the longitudinal model state vector should contain just these symmetric aeroelastic modes.

From Figure 3.3, the symmetric modes are modes 1,3,6,7,9,12. So the symmetric aeroelastic mode structural displacements are $\eta_1, \eta_3, \eta_6, \eta_7, \eta_9$ and η_{12} and the corresponding structural velocities are $\dot{\eta}_1, \dot{\eta}_3, \dot{\eta}_6, \dot{\eta}_7, \dot{\eta}_9$ and $\dot{\eta}_{12}$. Denoting them as,

$$\boldsymbol{\eta}_{\text{long}} = [\eta_1, \eta_3, \eta_6, \eta_7, \eta_9, \eta_{12}] \tag{3.8}$$

$$\dot{\boldsymbol{\eta}}_{\text{long}} = [\dot{\eta}_1, \dot{\eta}_3, \dot{\eta}_6, \dot{\eta}_7, \dot{\eta}_9, \dot{\eta}_{12}] \tag{3.9}$$

$$\mathbf{x}_{\text{elong}} = [\boldsymbol{\eta}_{\text{long}}, \dot{\boldsymbol{\eta}}_{\text{long}}] \tag{3.10}$$

We define the state-space longitudinal dynamics model as

$$\begin{bmatrix} \dot{\mathbf{x}}_{\text{rlong}} \\ \dot{\mathbf{x}}_{\text{elong}} \end{bmatrix} = \begin{bmatrix} \mathbf{A}_{\text{rlong}} & \mathbf{A}_{\text{erlong}} \\ \mathbf{A}_{\text{relong}} & \mathbf{A}_{\text{elong}} \end{bmatrix} \begin{bmatrix} \mathbf{x}_{\text{rlong}} \\ \mathbf{x}_{\text{elong}} \end{bmatrix} + \begin{bmatrix} \mathbf{B}_{\text{rlong}} \\ \mathbf{B}_{\text{elong}} \end{bmatrix} \delta_e \tag{3.11}$$

where δ_e is the longitudinal model input,this being the deflection of the elevator.

The decoupled state variables are listed in Table 3.4. There are 16 state variables in this model in total. The details of this decoupled linear model are given in Appendix A.

Table 3.4: Longitudinal Linear State-space Model State Variables

Category	State Variables
Rigid Body State Variables	q, θ, u, w
Structural Displacements	$\eta_1, \eta_3, \eta_6, \eta_7, \eta_9, \eta_{12}$
Structural Velocities	$\dot{\eta}_1, \dot{\eta}_3, \dot{\eta}_6, \dot{\eta}_7, \dot{\eta}_9, \dot{\eta}_{12}$

3.2.5 Comparison between Linear and Non-linear Model

The purpose of linearising the model is to simplify the complex model to a similar performance simple model by using small perturbation theory. Therefore, it is important to examine that if the simplified model and original model have similar performance under same flight condition and same input.

Additionally, as explained previously in Section 2.2, for longitudinal FCS, the pilot will more concentrate on short period performance which can be captured by the pitch rate ($q(deg/s)$) and normal acceleration ($a_w(m/s^2)$) responses.

Pitch Rate Response

Figure 3.4 shows the comparison of $1°/3°/5°$ elevator deflection input pitch rate dynamics response between original AX-1 model (full-order non-linear model), trim model (reduced-order non-linear model) and the linearised longitudinal model.

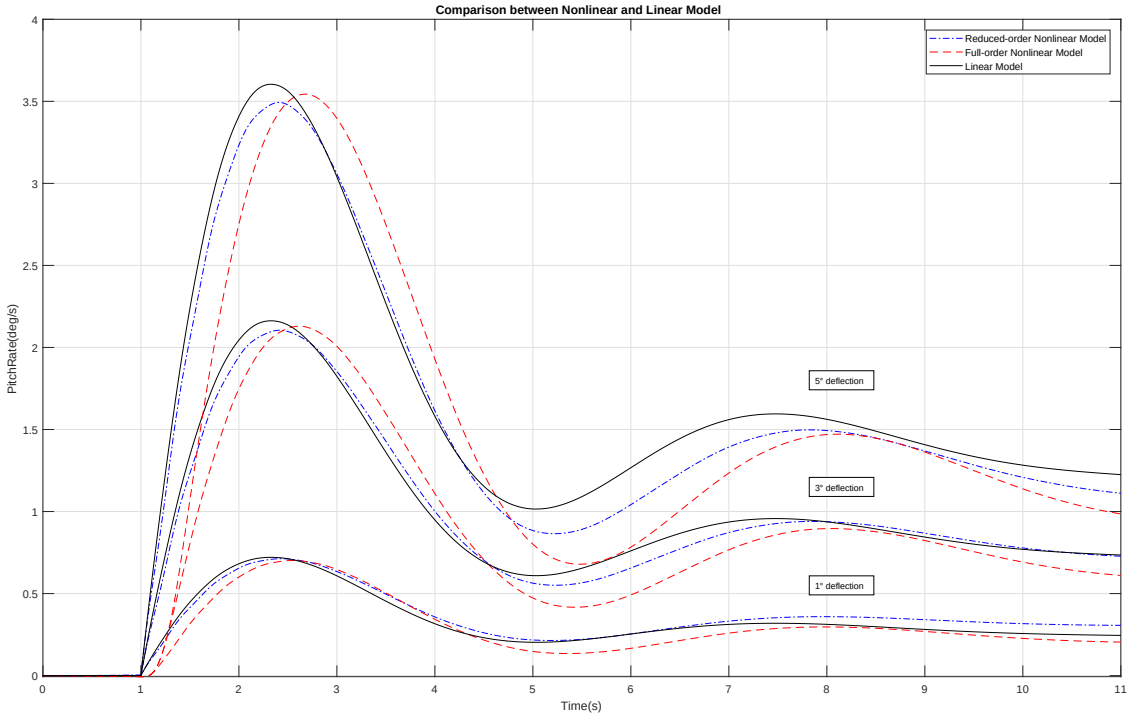

Figure 3.4: Pitch Rate Responses Comparison

It can be seen that the responses do not perfectly match. The full-order non-linear model response has a lag and larger undershoot compared with the linear model and reduced-order non-linear model. With larger deflection, the difference between them will also be larger.

Figure 3.5 and Figure 3.6 shows the difference between them. It can be seen that the difference between reduced-order non-linear model and the linear model is less than the differences between the full-order model and the others. The maximum error exists about 0.5 second after the input because of the lag of the full-order non-linear model.

As explained in Table 3.1, for trim flight condition, the state variables of wind, gust, and turbulence should be zero. So the difference is basically caused by indicial downwash state variables and unsteady aerodynamics integrators. The lag between full-order model and the others is mainly because of the unsteady aerodynamics integrators. The actuator dynamics do not affect the responses very much.

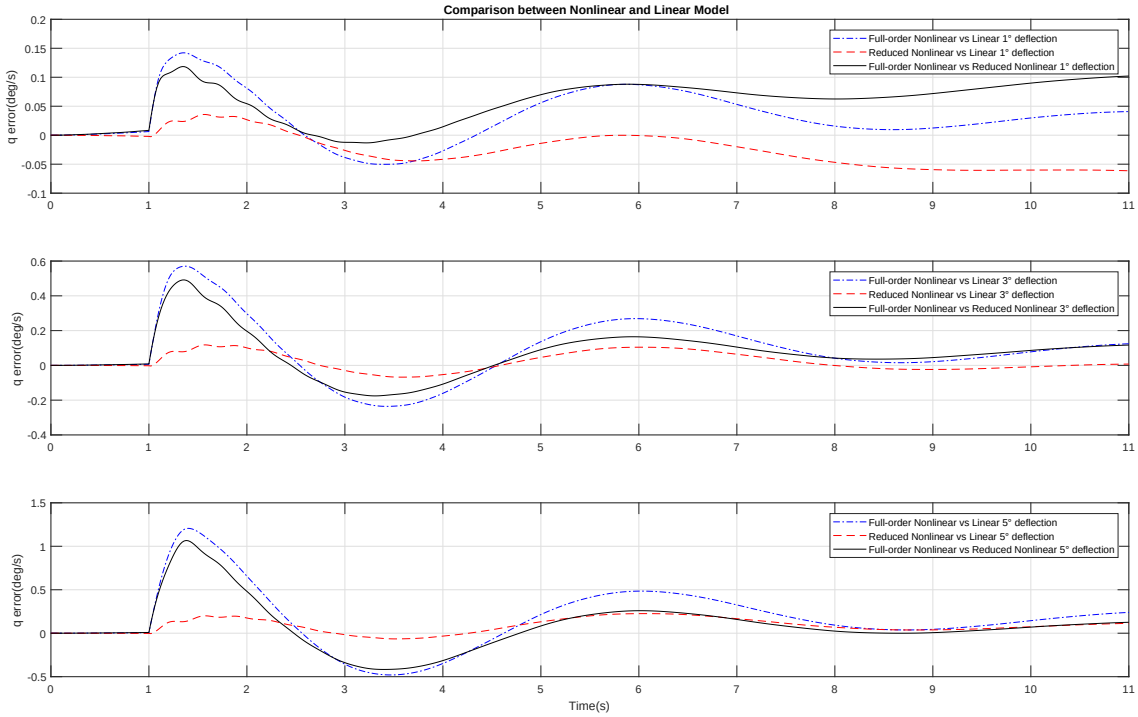

Figure 3.5: Pitch Rate Error between Different Model

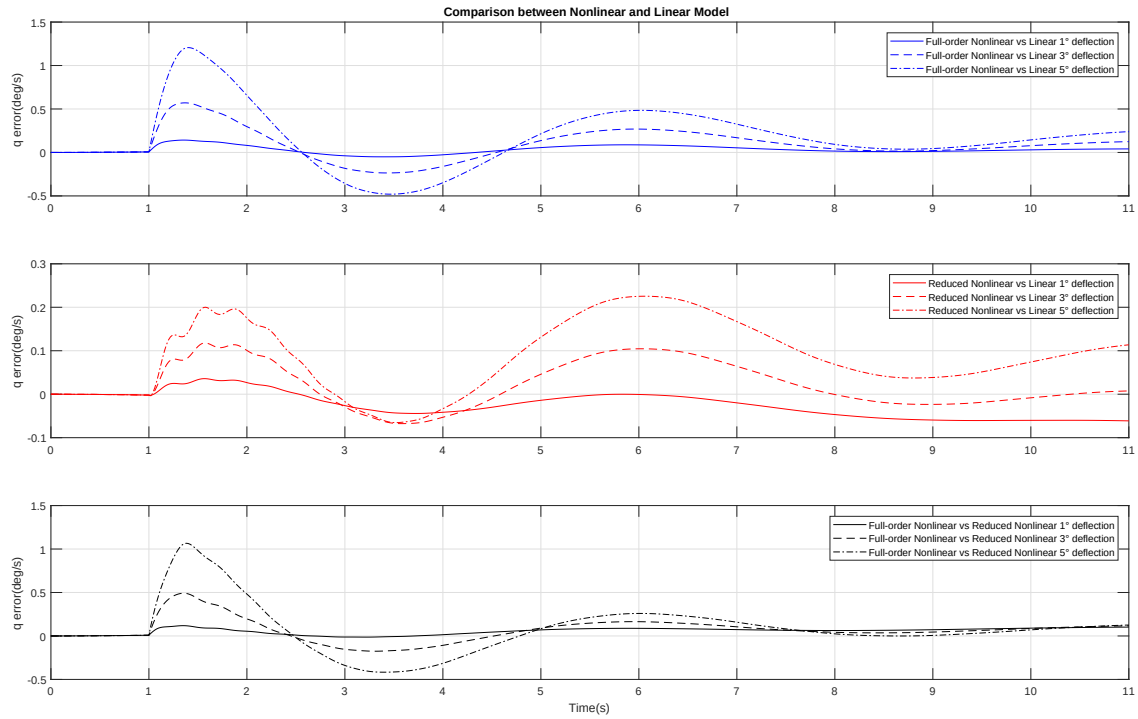

Figure 3.6: Pitch Rate Error between Different Input

Normal Acceleration Response

Figure 3.7 shows the comparison of 1°/3°/5° elevator deflection input normal acceleration dynamics response between original AX-1 model(full-order non-linear model),

trim model (reduced-order non-linear model) and the linearised model.

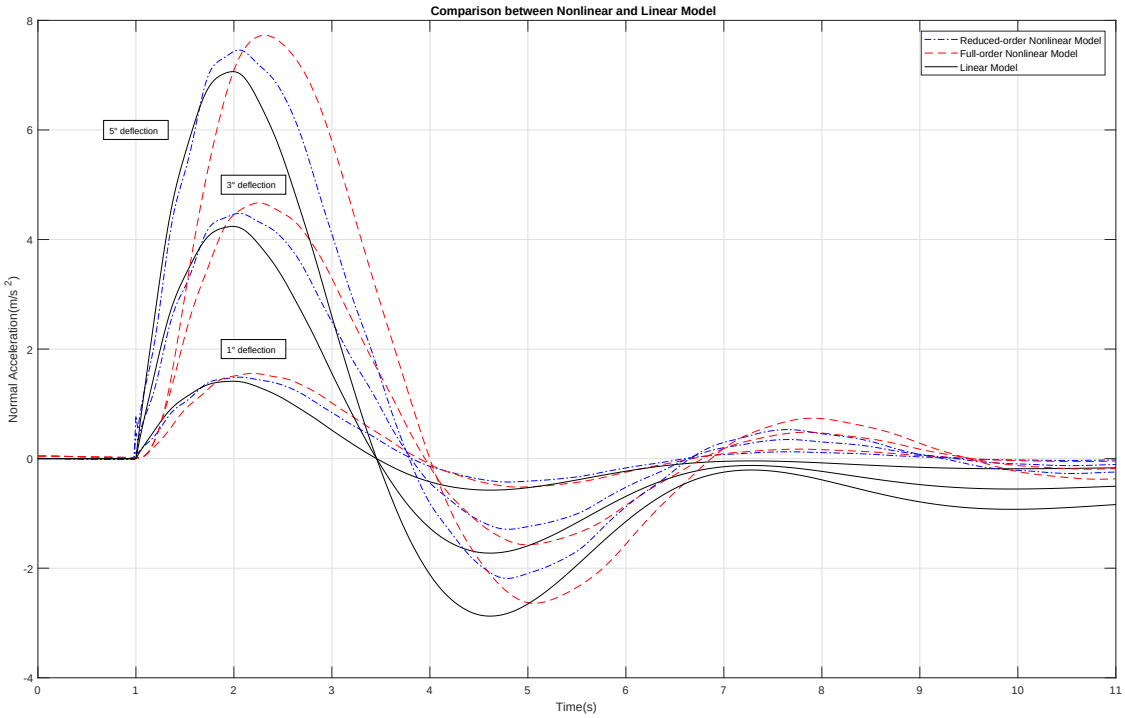

Figure 3.7: Normal Acceleration Responses Comparison

The normal acceleration responses also do not perfectly match. The full-order non-linear model responses still have a lag and larger overshoot compared with the linear model and the reduced-order non-linear model. The linear model has a larger undershoot. The steady-state values have relatively large differences between the linear and two non-linear models. This is because the input is a step input, the non-linear models included the non-linearities that can trim again at the new flight condition (zero pitch rate), which the linear model cannot. With larger deflection, the difference between them will also be larger.

Figures 3.8 and 3.9 show the difference between them. It can be seen that the maximum error of normal acceleration also existed at the beginning because of the lag in the full-order non-linear model. The difference between the linear model and the reduced order non-linear model is much smaller than the error between them and the full-order non-linear model.

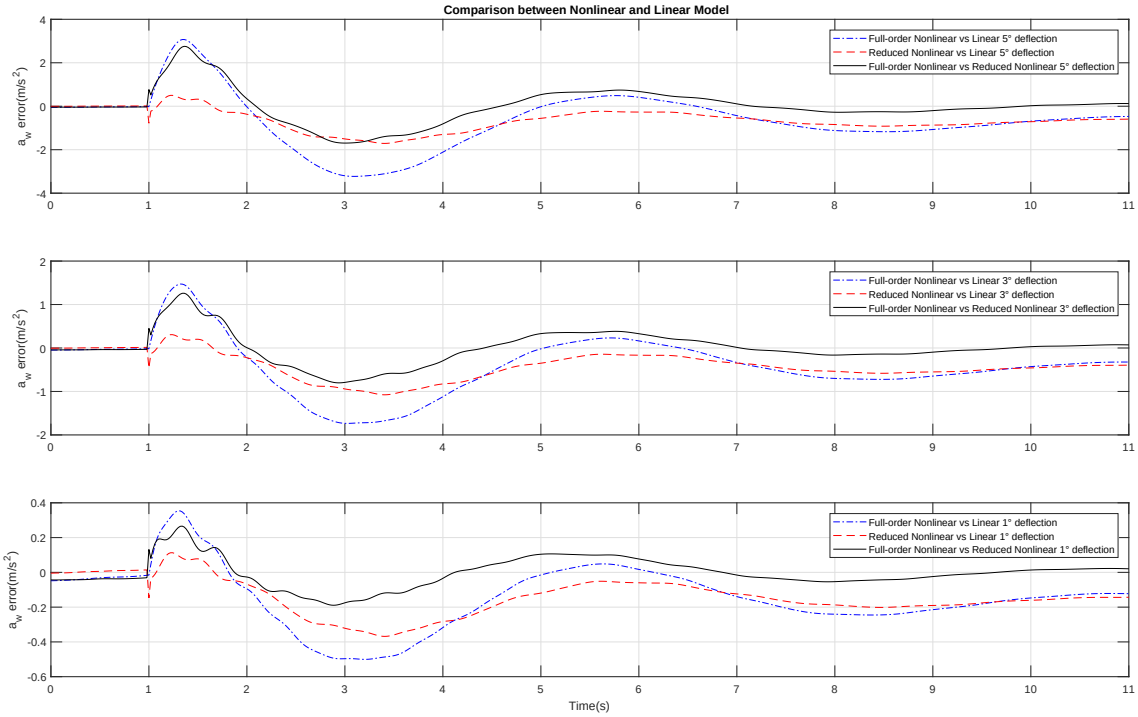

Figure 3.8: Normal Acceleration Error between Different Model

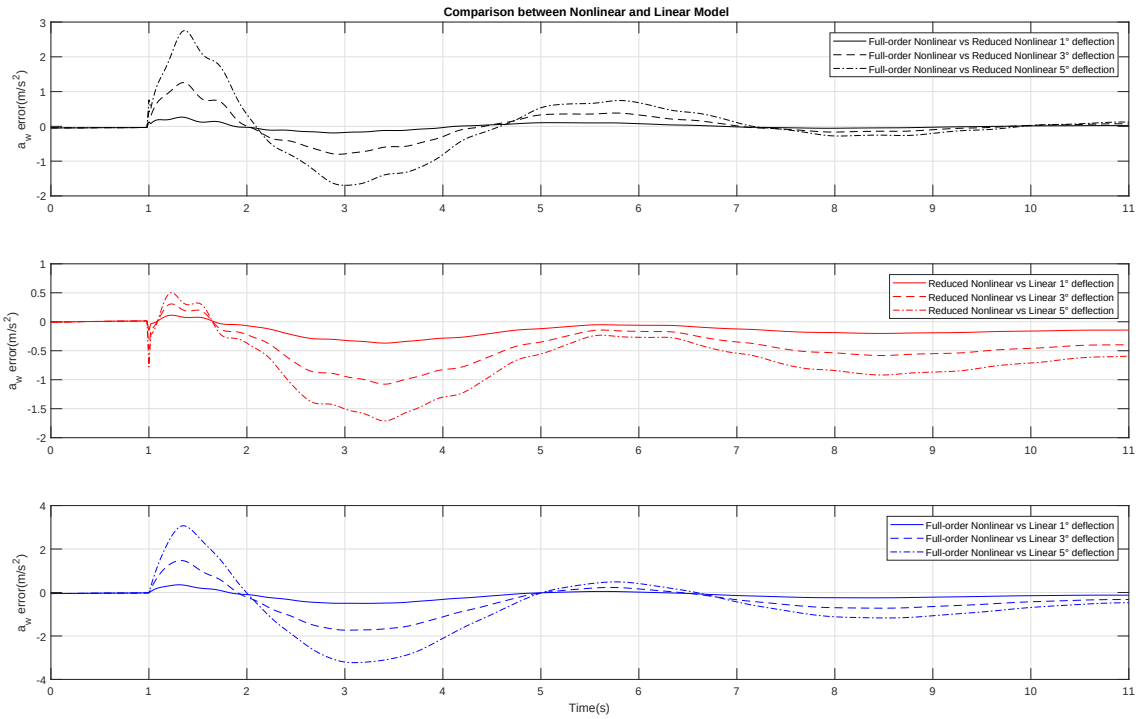

Figure 3.9: Normal Acceleration Error between Different Input

Summary

In conclusion, the difference between the original AX-1 model(full-order non-linear) and the simplified model (linearised model) that is used to design the control law is

mainly caused by the reduced order non-linear model for trim. The `linmod` routine is relatively accurate.

However, even the linear model and the full-order non-linear model cannot perfectly match each other, it still the most accurate linear model that the author can find so far. So the control law design is based on this linearised model.

3.2.6 Wind Disturbance Modelling

In this study, two design criteria related to the wind disturbance during flight (i.e. passenger comfort and control effort). Modelling the relationship between wind disturbance and output is hence important for this work.

From Nelson [1998], the original rigid body longitudinal linear model with wind disturbance can be represented as:

$$\begin{bmatrix} \Delta\dot{q} \\ \Delta\dot{\theta} \\ \Delta\dot{u} \\ \Delta\dot{w} \end{bmatrix} = \begin{bmatrix} M_q & 0 & M_u & M_w \\ 1 & 0 & 0 & 0 \\ 0 & -g & X_u & X_w \\ u_0 & 0 & Z_u & Z_w \end{bmatrix} \begin{bmatrix} \Delta q \\ \Delta\theta \\ \Delta u \\ \Delta w \end{bmatrix} + \begin{bmatrix} M_\delta & M_{\delta_T} \\ 0 & 0 \\ X_\delta & X_{\delta_T} \\ Z_\delta & Z_{\delta_T} \end{bmatrix} \begin{bmatrix} \Delta\delta_e \\ \Delta\delta_T \end{bmatrix} + \begin{bmatrix} -M_u & -M_w & -M_q \\ 0 & 0 & 0 \\ -X_u & -X_w & 0 \\ -Z_u & -Z_w & 0 \end{bmatrix} \begin{bmatrix} u_t \\ w_t \\ q_t \end{bmatrix} \tag{3.12}$$

which can be written as

$$\dot{\mathbf{x}} = \mathbf{A}\mathbf{x} + \mathbf{B}\mathbf{u} + \mathbf{F}\mathbf{w} \tag{3.13}$$

where the $\mathbf{F}$ is wind dynamics matrix and $\mathbf{w}$ is the wind disturbance vector. It is can be seen that $\mathbf{F}$ is essential $-\mathbf{A}$ excluding the θ row because this model does not include θ in wind disturbance input.

Because this work is focused on the short period dynamics response, the wind

disturbance vector just included the wind velocity component in the z-direction and vorticity about the y-axis, and the AX-1 non-linear model does not have an input for vorticity disturbance, thus $\mathbf{w} = (w_t)$, the control input is $\mathbf{u} = \delta_e$. The state variable vector is $\mathbf{x} = (q, \theta, u, w, \eta_1, \eta_3, \eta_6, \eta_7, \eta_9, \eta_{12}, \dot{\eta}_1, \dot{\eta}_3, \dot{\eta}_6, \dot{\eta}_7, \dot{\eta}_9, \dot{\eta}_{12})^T$.

As denoting the longitudinal structural displacement as $\boldsymbol{\eta}_{\text{long}}$ and the structural velocities as $\dot{\boldsymbol{\eta}}_{\text{long}}$ previously, and $\mathbf{A}$ matrix wind disturbance corresponding columns (w) are $\mathbf{A}_{\text{wr}}$ and $\mathbf{A}_{\text{wre}}$ (rigid part and rigid elastic coupling part respectively). Thus the wind disturbance model can be formulated as,

$$\begin{bmatrix} \dot{\mathbf{x}}_{\text{rlong}} \\ \dot{\boldsymbol{\eta}}_{\text{long}} \\ \ddot{\boldsymbol{\eta}}_{\text{long}} \end{bmatrix} = \left[\begin{array}{c|c} \mathbf{A}_{\text{rlong}} & \mathbf{A}_{\text{erlong}} \\ \hline \mathbf{A}_{\text{relong}} & \mathbf{A}_{\text{elong}} \end{array}\right] \begin{bmatrix} \mathbf{x}_{\text{rlong}} \\ \boldsymbol{\eta}_{\text{long}} \\ \dot{\boldsymbol{\eta}}_{\text{long}} \end{bmatrix} + \begin{bmatrix} \mathbf{B}_{\text{r}} \\ \mathbf{B}_{\text{e}} \end{bmatrix} \delta_e + \begin{bmatrix} -\mathbf{A}_{\text{wr}} \\ -\mathbf{A}_{\text{wre}} \end{bmatrix} w_t \quad (3.14)$$

Chapter 4

Controller Design Process

After modelling the system, the controller can be designed. Zakian's [1986] paper about performance criteria is used as the theory reference in this chapter. A satisfactory design requires consideration of a set of performance indices that are required to meet a set of certification specifications. Thus it is natural to place the problem in a multi-objective setting. The chosen design approach is a mixed optimization consisting of LQR control synthesis combined with a MOGA that searches for the weighting matrix parameters. In this chapter, the mixed optimization process is described. The details of the controller structure, performance objective functions and non-linear constraints are also formulated.

4.1 Controller Structure

As explained in Section 2.4, the LQR is selected as the analytical optimisation design method in this study. According to the LQR theory, the original controller structure should be the full-state feedback controller structure.

However, the original LQR controller structure will bring undesired response because of the feedback of θ, which will not eliminate to zero during the Gibson Drop-Back test. From a handling qualities perspective, pilots prefer pitch command. However, feedback of θ can increase the stability of the control system.

Therefore, a Rate Command Attitude Hold (RCAH) [McCuish and Caldwell, 1996] flight control system is used in this study. This kind of structure is designed because transport aircraft pilots prefer command of pitch rate, so it is used with a structure shown in Figure 4.1.

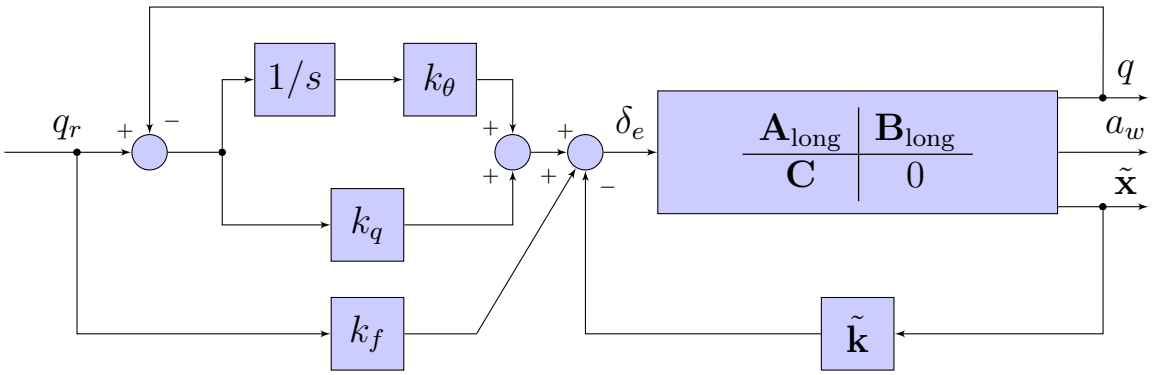

Figure 4.1: Controller Structure

The plant is represented by the longitudinal state-space model that is defined in Chapter 3, where $\mathbf{A}_{\text{long}}$ and $\mathbf{B}_{\text{long}}$ are defined in (3.11) and are,

$$\mathbf{A}_{long} = \begin{bmatrix} \mathbf{A}_{\text{rlong}} & \mathbf{A}_{\text{erlong}} \\ \mathbf{A}_{\text{relong}} & \mathbf{A}_{\text{elong}} \end{bmatrix} \qquad \mathbf{B}_{long} = \begin{bmatrix} \mathbf{B}_{\text{rlong}} \\ \mathbf{B}_{\text{elong}} \end{bmatrix}. \tag{4.1}$$

Because LQR does not explicitly include input and output behaviour, we have to adopt the controller structure that will give proper input/output behaviours for different performance indices measurement. The RCAH controller structure provides a structure that with the input as pitch rate reference. The outputs are determined by different output matrices. In this study, the LQR theory requires full-state feedback and the comfort criterion requires the normal acceleration output. However, as explained previously, θ cannot be feedback directly for the RCAH controller structure. Rather than feedback θ directly, feedback pitch rate, q, is fed back with integral action as part of a PI controller, since $\dot{\theta} = q$, the stabilizing effect of θ feedback from

the LQR is maintained. The corresponding output matrix then can be defined as

$$\mathbf{C} = \begin{bmatrix} \mathbf{c}_q \\ \mathbf{a}_w \\ \mathbf{C}_{\tilde{\mathbf{x}}} \end{bmatrix} \tag{4.2}$$

where $\mathbf{c}_q = [1, 0, \ldots, 0]$, the $\mathbf{a}_w$ is the normal velocity corresponding row of the open loop A matrix, and $\mathbf{C}_{\tilde{\mathbf{x}}} = [\mathbf{0}, \mathbf{0}, \mathbf{I}_{14}]$.

Thus the LQR optimal controller, $\mathbf{K}$, is partitioned so that $\mathbf{K} = [k_q, k_\theta, \tilde{\mathbf{k}}]$ with k_q acting on the pitch rate error signal and k_θ on the pitch rate error integral signal as the PI controller. The remaining state variables, $\tilde{\mathbf{x}} = (u, w, \boldsymbol{\eta}_{\text{long}}, \dot{\boldsymbol{\eta}}_{\text{long}})^T$, are fed back through $\tilde{\mathbf{k}}$.

A feed-forward gain, k_f, is included in the controller structure. This gain corrects the reference input, q_r, so that the output equals the reference input at steady state but only in the short term. Thus the pitch, θ, is removed from the state variables to give a reduced order model with state $\hat{\mathbf{x}} = (q, \tilde{\mathbf{x}})^T$ and controller $\hat{\mathbf{k}} = [k_q, \tilde{\mathbf{k}}]$. If $(\hat{\mathbf{A}}, \hat{\mathbf{B}})$ represents the reduced order model matrix pair, then $k_f = k_q(k_m - 1)$ where

$$k_m = \left(\hat{\mathbf{c}_q} (\hat{\mathbf{A}} - \hat{\mathbf{B}}\hat{\mathbf{k}})^{-1} \hat{\mathbf{B}} \right)^{-1} \tag{4.3}$$

and $\hat{\mathbf{c}}_q = [1, 0, \ldots, 0]$.

The longitudinal dynamics system is single input, hence $\mathbf{R}$ is a scalar and is set to 10000. Hence, from (2.18), the vector of design parameters is

$$\mathbf{p} = (q_1, \ldots, q_n)^T \tag{4.4}$$

A good choice of the design objective functions, f_i, is critical to allow the correct trade-offs between competing criteria. The performance indices used are defined next.

4.2 Performance Objective Functions

4.2.1 Gibson Drop-Back Criterion

Definition

As explained in Section 2.2, one of the main objective is satisfactory longitudinal handling qualities. Here, two objective functions based on the Gibson Drop-Back criterion [Gibson, 1982] are used. Gibson Drop-Back is based on the response of a low order model that excludes the phugoid mode to a pulse elevator input [Field et al., 2000]. Figure 4.2 shows a typical Gibson drop-back response along with the terms of the Gibson drop-back criteria.

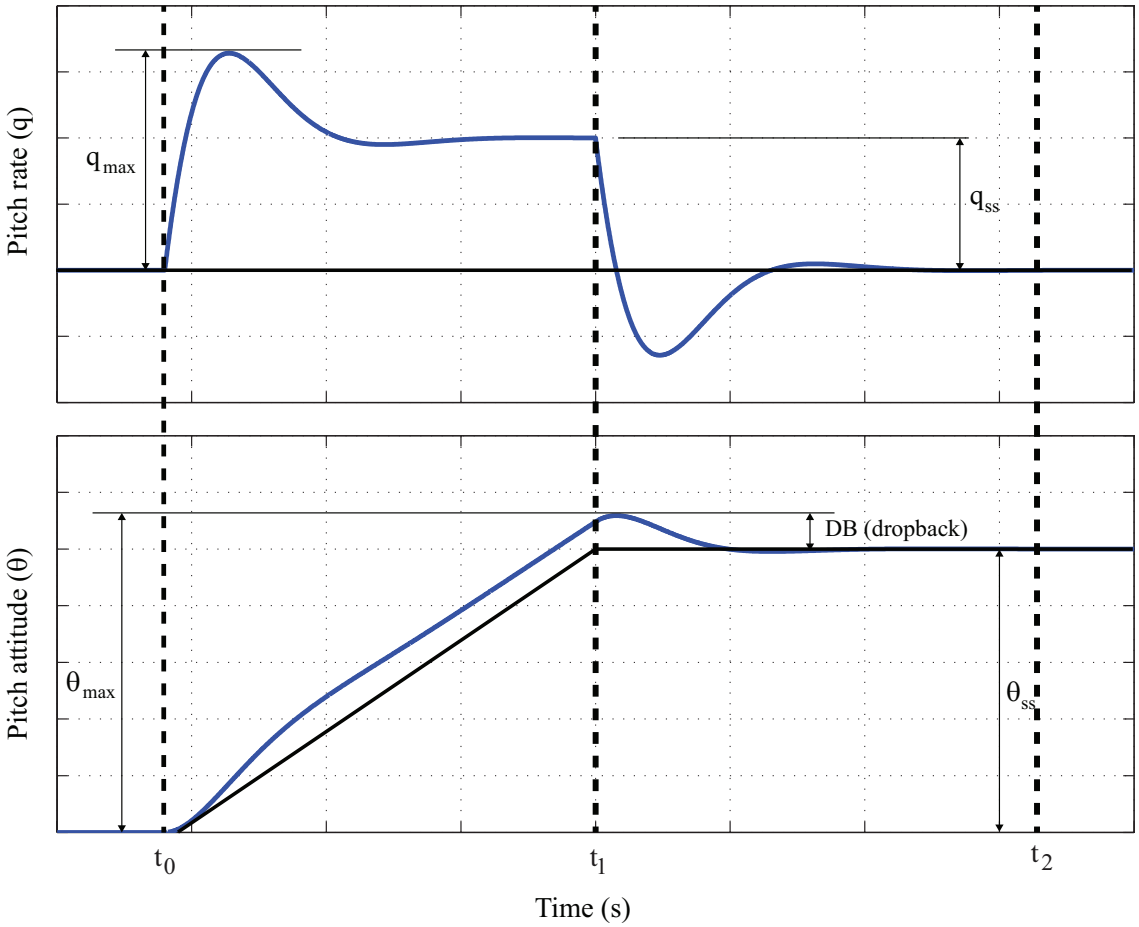

Figure 4.2: Definition of $q_{\max}$, q_{ss} and DB terms

The open-loop test uses a 5° elevator deflection pulse input as the test input which is typical for flight test. The closed-loop reference is pitch rate command, q_r,

and the response is obtained from the system model with a reduced order model that has the phugoid mode removed. This is done by removing the lowest frequency complex mode pair from the Jordan canonical form of the closed-loop system.

Satisfactory handling qualities based on Gibson drop-back can be assessed by two terms, $q_{\max}/q_{\text{ss}}$ and DB/q_{ss}, where the $q_{\max}$ is the maximum value of pitch rate, q_{ss} is the steady state value of pitch rate for the certain elevator input and DB is the drop-back of the pitch altitude θ, between the maximum value and the steady state value of θ [Gibson, 1982]. The model is linear, hence the input magnitude is unity and the Gibson Drop-back input is

$$q_r(t) = \begin{cases} 1 & \text{for } t \in [t_0, t_1), \\ 0 & \text{for } t \text{ elsewhere.} \end{cases} \tag{4.5}$$

To evaluate $q_{\max}$, q_{ss} and DB, we take $t_0 = 0$ and we need to calculate t_1 and t_2. This is done based on the convergence of the modal responses.

Let $\lambda_1, \ldots, \lambda_n$ be the eigenvalues of the closed-loop system, then if α is the spectral abscissa defined by

$$\alpha = \max_i \{Re(\lambda_i)\} \tag{4.6}$$

then let $t_{\text{ss}} = -10/\alpha$ be the time such that the modal responses have decayed to nearly zero. Then $t_1 = t_{\text{ss}}$ and $t_2 = 2t_{\text{ss}}$.

Because of the requirement of the measurement of Gibson Drop-Back criterion, the longitudinal phugoid mode should be removed during the measuring process of the performance indices. This is done by removing the lowest frequency complex mode pair from the Jordan canonical form of the closed-loop system.

Maximum Pitch Rate

This is the first Gibson criterion index, to measure the ratio between the maximum pitch rate and the state pitch rate. This index can display the overshoot of the pitch rate response and measure the signal tracking performance of the system.

The formulation of this objective is,

$$f_1 = q_{\max}/q_{\text{ss}}, \tag{4.7}$$

where the maximum pitch rate is the maximum value of the pitch rate response,

$$q_{\max} = \max_t q(t) \tag{4.8}$$

and the q_{ss} is the steady state value of pitch rate response,

$$q_{\text{ss}} = q(t_1) \tag{4.9}$$

where t_1 is the steady state time of pitch rate, which shown in Figure 4.2.

Drop Back

The second index of the Gibson Drop-back criterion is the ratio between the pitch angle drop-back and the steady state pitch rate,

$$f_2 = DB/q_{\text{ss}} \tag{4.10}$$

This index shows the integral of the negative pitch rate, which is the combination of overshoot and convergence time. Additionally, the overshoot is also incorporated in the previous objective, so with the same value of f_1, the less value of f_2 means the system has shorter convergence time. The pitch angle drop-back is the difference

between θ_{max} and θ_{ss},

$$DB = \theta_{\max} - \theta_{\mathrm{ss}} \tag{4.11}$$

with the maximum value of θ for the Gibson drop-back response

$$\theta_{\max} = \max_{t} \theta(t) \tag{4.12}$$

and θ_{ss} is the steady-state value of θ,

$$\theta_{\mathrm{ss}} = \theta(t_2) \tag{4.13}$$

where t_2 is two times the steady state time of pitch rate, which is shown in Figure 4.2.

Rise Time

This objective function measures the response speed of the system and ensures the bandwidth is maintained and the system is not over-damped. The rise time is the time ittakes for the response to rise from 10% to 90% of the steady-state response, which is defined as

$$f_3 = t_r = t_{0.9q_{\mathrm{ss}}} - t_{0.1q_{\mathrm{ss}}}. \tag{4.14}$$

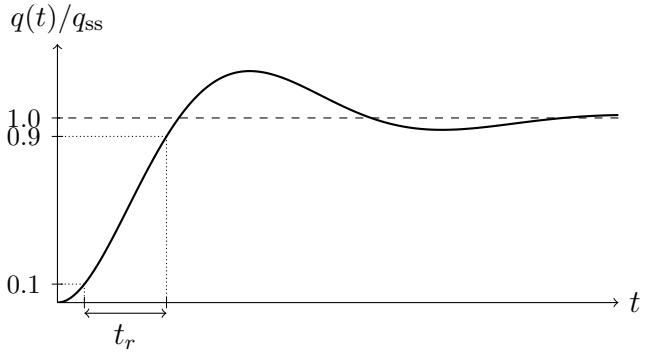

Figure 4.3: Definition of Rise Time

where, $t_{0.1q_{\mathrm{ss}}} = \min t$ such that $q(t) = 0.1q_{ss}$, $t_{0.9q_{\mathrm{ss}}} = \min t$ such that $q(t) =$

$0.9q_{ss}$, and the q_{ss} is the steady state value of pitch rate, as shown in Figure 4.3, the rise time thus shows the response speed of the closed loop system.

4.2.2 Wind Disturbance Criteria

Controller Structure

Besides the handling qualities, the performance of the aircraft under wind disturbance is also considered in this study. Because these performance indices are measured under the wind disturbance, the reference input of pitch rate should be zero. The closed loop system is an LQR full-state feedback system. The equivalent controller structure of Figure 4.1 is shown in Figure 4.4, where

$$\mathbf{B}_{\text{tur}} = \begin{bmatrix} \mathbf{F} & \mathbf{B}_{\text{long}} \end{bmatrix} \qquad \mathbf{C}_{\text{tur}} = \begin{bmatrix} \mathbf{a}_w \\ \mathbf{I}_{16} \end{bmatrix} \tag{4.15}$$

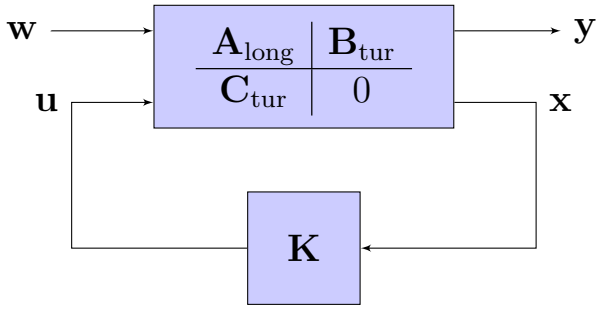

Figure 4.4: Equivalent Controller Structure (Wind Disturbance)

Control Effort

However, with different wind disturbance input, the control effort will be different in each case. It is hard to find a typical input of wind disturbance to represent this set of input. Therefore, it is reasonable to measure the system characteristic rather than the dynamics response. Control effort means the effort of the controller to keep the aircraft stable when the aircraft hits wind disturbance. This can be measured

by

$$\int_0^\infty \mathbf{u}^2(t)dt \tag{4.16}$$

in the time domain, where $\mathbf{u}$ is the feedback control signal of the LQR closed loop system in (2.15). For computational ease, (4.16) is replaced by the norm.

$$\|\mathbf{u}\|_2 = \sqrt{\int_0^\infty \mathbf{u}^2(t)dt} \tag{4.17}$$

For computational efficiency, rather than calculating the norm of the specific time response, the H_2 norm of the SISO system is calculated with $\mathbf{w}$ as input and control signal $\mathbf{u}$ as output.

From (3.12) and (3.13), the linear system can be represented as:

$$\begin{aligned} \dot{\mathbf{x}} &= \mathbf{A_{cl}}\mathbf{x} + \mathbf{F}\mathbf{w}, \\ \mathbf{y} &= \mathbf{u} = -\mathbf{K}\mathbf{x} \end{aligned} \tag{4.18}$$

where

$$\mathbf{A_{cl}} = \mathbf{A} - \mathbf{B}\mathbf{K} \tag{4.19}$$

This linear system is named $\mathbf{T_u}$. So this index measures the H_2 norm of the system because the output of this system is the control effort,

$$f_4 = \|\mathbf{T_u}\|_2 \tag{4.20}$$

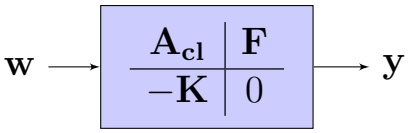

Figure 4.5: Equivalent Controller Structure (Control Effort)

Thus the equivalent controller structure is shown in Figure 4.5. After defining the two corresponding closed loop SISO systems, this norm can be calculated by

MATLAB command `norm` for H_2 norm, the command will convert system into state-space form and then uses the same algorithm as `covar`.

For a general state-space model, **H**, given by

$$\begin{aligned} \dot{\mathbf{x}} &= \mathbf{A}\mathbf{x} + \mathbf{B}\mathbf{u}, \\ \mathbf{y} &= \mathbf{C}\mathbf{x} \end{aligned} \tag{4.21}$$

the controllability Gramian **S** is obtained by solving the Lyapunov equation,

$$\mathbf{A}\mathbf{S} + \mathbf{S}\mathbf{A}^T + \mathbf{B}\mathbf{B}^T = 0. \tag{4.22}$$

The index can be calculated as,

$$\|\mathbf{H}\|_2 = \mathbf{C}\mathbf{S}\mathbf{C}^T. \tag{4.23}$$

The detail of the algorithm can be seen in Varga [1992].

Comfort

Passenger comfort during wind disturbance is also important for a transport aircraft. The following comfort criteria based on the ISO 2631-1 standard

$$PIP = \frac{1}{3}\left[\int_0^T ({a_w}^2(t))dt\right]^{1/2} \tag{4.24}$$

where PIP means Percentage of Ill Passengers. For computational speed consideration, here we define the comfort measure using H_2 norm as,

$$\|a_w\|_2 = \left[\int_0^\infty ({a_w}^2(t))dt\right]^{1/2} \tag{4.25}$$

Similar to control effort, this criterion is also needed to be measured under wind disturbance input. Thus the equivalent controller structure in Figure 4.4 also can

be used in this case.

To measure the comfort characteristic of the system, the corresponding state-space linear system have the same equations of motion as control effort measuring linear system (4.18). But the output should be changed to normal acceleration a_w.

The state-space system $\mathbf{T_{a_w}}$ is,

$$\begin{aligned} \dot{\mathbf{x}} &= \mathbf{A_{cl}}\mathbf{x} + \mathbf{F}\mathbf{w}, \\ \mathbf{y} &= a_w = \dot{w} = \mathbf{a}_{\mathrm{cw}}\mathbf{x} \end{aligned} \tag{4.26}$$

where the $\mathbf{a}_{\mathrm{cw}}$ is the normal velocity corresponding row of closed loop $\mathbf{A_{cl}}$ matrix.

Therefore, this index is determined from the H_2 norm of $\mathbf{T_{a_w}}$.

$$f_5 = \|\mathbf{T_{a_w}}\|_2 \tag{4.27}$$

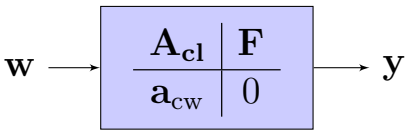

Figure 4.6: Equivalent Controller Structure (Comfort)

The system can be represented as in Figure 4.6. The calculation process is the same as Control Effort performance index.

4.3 Non-linear Constraints

Because MOGA is a numerical searching algorithm, it will search for optimal numerical solutions based on the objective functions included previously. To avoid undesired results, some constraints that the system needs to meet should also be defined. These non-linear constraints will narrow the MOGA algorithm search space to get more reasonable solutions.

In particular, a constraint on the maximum controller gain to prevent actuator saturation should be defined. In addition, the flight control law should not overly alter the phugoid mode as this may cause problems with the outer loop autopilot control loops and the calculation of the low-order model required for the calculation of f_1 and f_2.

4.3.1 Gain Constraint

It is important to limit the gains to a reasonable region so the controller can be implemented in practice. In this case, the gains are limited in $[-1, 1]$. This gives the constraint

$$\|\mathbf{K}\|_\infty < 1. \tag{4.28}$$

4.3.2 Phugoid Mode Constraint

The phugoid mode is the lowest frequency complex mode pair obtained from the Jordan canonical form of the closed-loop system. For handling quality evaluation, the phugoid mode response is not important. This is because it is comparatively slow compared to the short period mode and does not affect the handling quality. Here, the phugoid mode damping ratio, ζ_{phu}, is constrained

$$\zeta_{(\text{phu})} \leq 0.5 \tag{4.29}$$

In addition, the phugoid closed-loop poles should not move too far from the open-loop poles, so the mode natural frequency change is also constrained as,

$$\delta\omega_{n(\text{phu})} \leq 0.01. \tag{4.30}$$

where $\delta\omega_{n(\text{phu})}$ is the change of the phugoid mode frequency.

The frequency can be obtained from the closed loop system by transforming the

system into Jordan canonical form. The lowest frequency complex mode pair is the phugoid mode, and the corresponding frequency is the closed loop phugoid mode frequency $\omega_{n(\mathrm{phu_c})}$. The open loop phugoid mode frequency is $\omega_{n(\mathrm{phu_o})}$

The change is absolute difference between open loop phugoid mode frequency and closed loop phugoid mode frequency, which can be defined as

$$\delta\omega_{n(\mathrm{phu})} = |\omega_{n(\mathrm{phu_c})} - \omega_{n(\mathrm{phu_o})}|. \tag{4.31}$$

4.4 Conclusion

This chapter formulated the mixed optimization procedure. The corresponding controller structure, objective functions and non-linear searching constraints are also defined. The control problem solution procedure in this study is working based on these. The result analyses are shown in next chapter.

Chapter 5

Results Analysis

5.1 Linear Results

The `gamultiobj` MOGA from the MATLAB Global Optimization Toolbox was used to search for possible solutions of the LQR control weighting. Note that to get a rich enough set of results, the algorithm cannot be run just a single time. The algorithm will find more non-dominated solutions by starting the algorithm run with the non-dominated solutions found by the previous run as the seed. The size of the population will also affect the region of non-dominated solutions. In this chapter, the final presented result is obtained after 7 runs of the algorithm, the seed of the last 6 runs is the non-dominated solutions found by the previous run.

Figure 5.1 shows the progress of the optimal solution searching process. It shows the non-dominated solutions' trade-off relationship between f_1 ($q_{\max}/q_{\text{ss}}$) and f_5 (Rise Time) after the 1st, 3rd, 5th and 7th runs. It should be mentioned after the 5th run, the population size is increased from 200 to 500, so the corresponding non-dominated solutions number also increased from 70 to 175.

From the figure, it is clear that with the increasing number of runs, the non-dominated solutions set becomes richer, both increasing in size and range and converges towards the Pareto-optimal front.

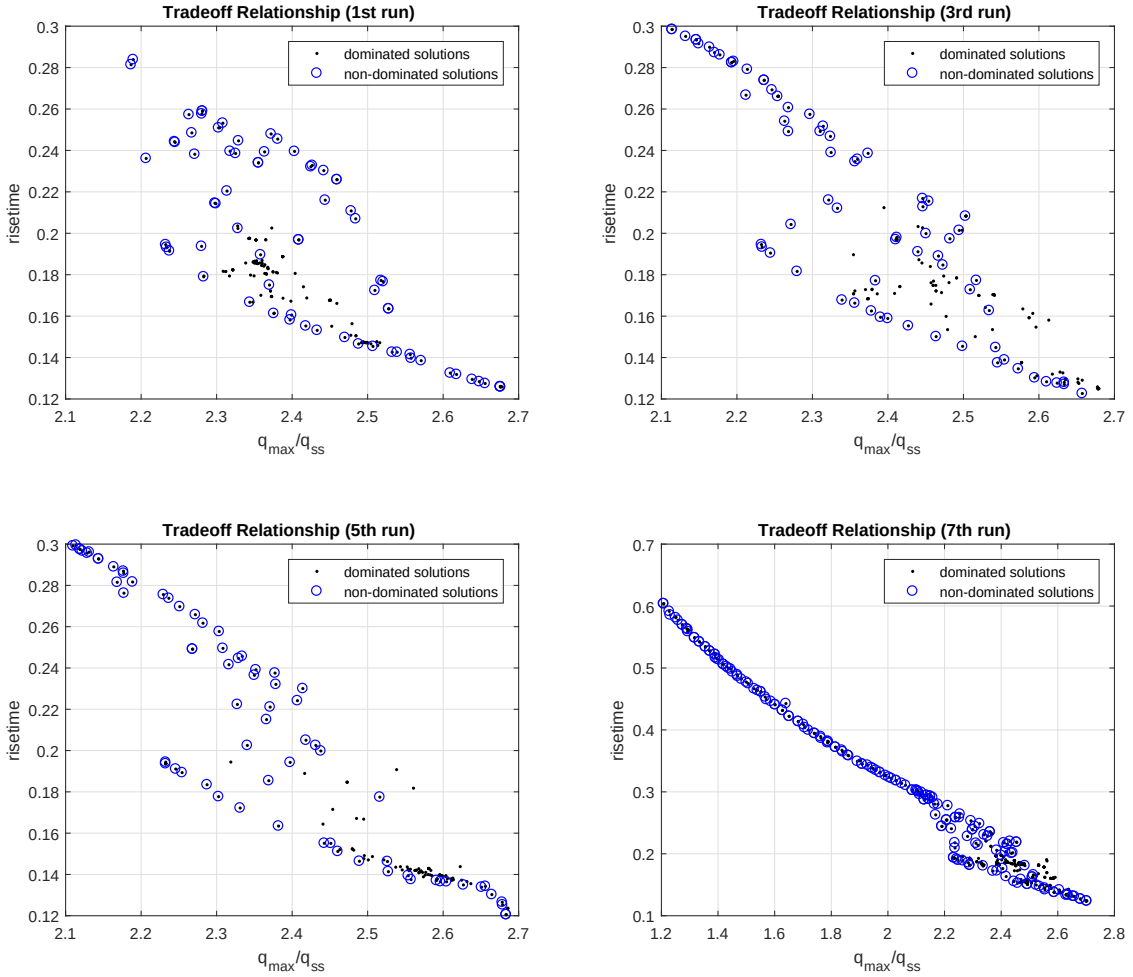

Figure 5.1: Tradeoff between f_1 ($q_{\max}/q_{\text{ss}}$) and f_5 (Rise Time)

The algorithm took approximately 45 minutes to evaluate 102 generations for the 7th run. The final generation's population size is 500 and has 175 non-dominated members. The set of solutions that found by the algorithm is denoted as $\mathcal{S}$, where $\mathcal{S} \subset \mathcal{P}$, where $\mathcal{P}$ is the set of all possible solutions defined in Chapter 3. The cardinality of $\mathcal{S}$ is 500.

Figure 5.2 is a trade-off diagram that shows the relations between the different objectives. The set of non-dominated solutions is represented by the blue lines and the dominated set of solutions by the grey. In this case, the non-dominated set of solutions is denoted by $\mathcal{S}_n$, the cardinality of this set is 175, and the dominated set of solutions is denoted by $\mathcal{S}_d$, the cardinality of this set is 325. Note that $\mathcal{S}_d \cup \mathcal{S}_n = \mathcal{S}$.

From the figure, it is clear that the entire set of non-dominated solutions $\mathcal{S}_n$ can

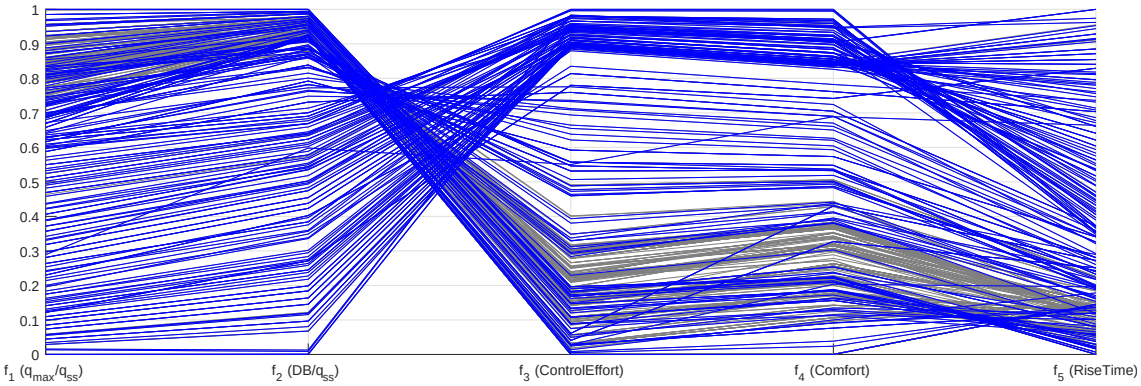

Figure 5.2: Multi-objective Trade-off Diagram

be divided into 3 subsets, denoting them as $\mathcal{S}_1$, $\mathcal{S}_2$ and $\mathcal{S}_3$, where $\mathcal{S}_1 \cup \mathcal{S}_2 \cup \mathcal{S}_3 = \mathcal{S}_n$.

Figure 5.3 shows the subsets of non-dominated solutions in different colours, where the blue lines represents $\mathcal{S}_1$, green lines $\mathcal{S}_2$ and red lines $\mathcal{S}_3$.

The conflict between $f_2(\mathrm{DB}/q_{\mathrm{ss}})$ and f_3 (Control Effort) are basically between $\mathcal{S}_1$ and $\mathcal{S}_3$. However within all the subsets, f_1 $(q_{\mathrm{max}}/q_{\mathrm{ss}})$, f_2 $(\mathrm{DB}/q_{\mathrm{ss}})$, f_3 (Control Effort) and f_4 (Comfort) have strong links, and inside subsets $\mathcal{S}_1$ and $\mathcal{S}_3$, all of the other objectives are competing with f_5 (Rise Time). However, the subset $\mathcal{S}_2$ does not have strong competition between f_5 and the other objectives.

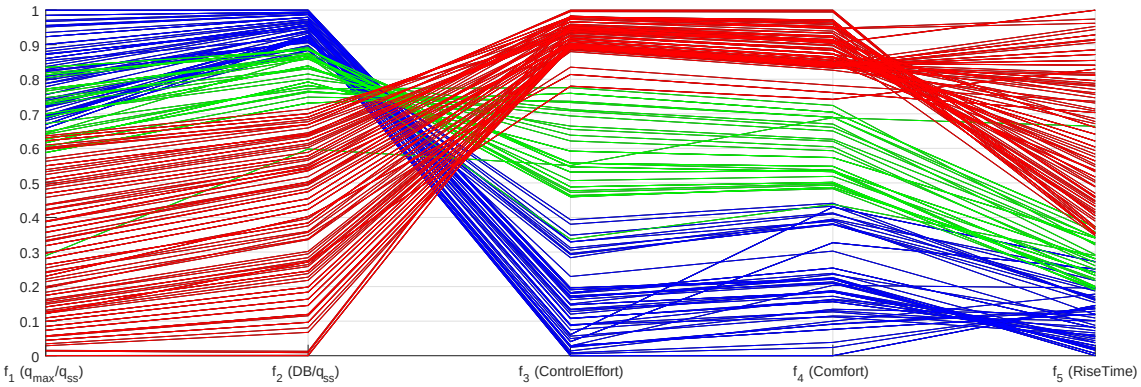

Figure 5.3: Multi-objective Trade-off Diagram (non-diminated solutions)

The near-Pareto front between f_1 and f_5 is shown in Figure 5.4. The black points represent all the found solutions in $\mathcal{S}$, and the blue circles are the non-dominated members, $\mathcal{S}_n$.

The trade-off relationship between overshoot and rise time is a typical conflict relationship in control systems design. The trade-off between them should be a

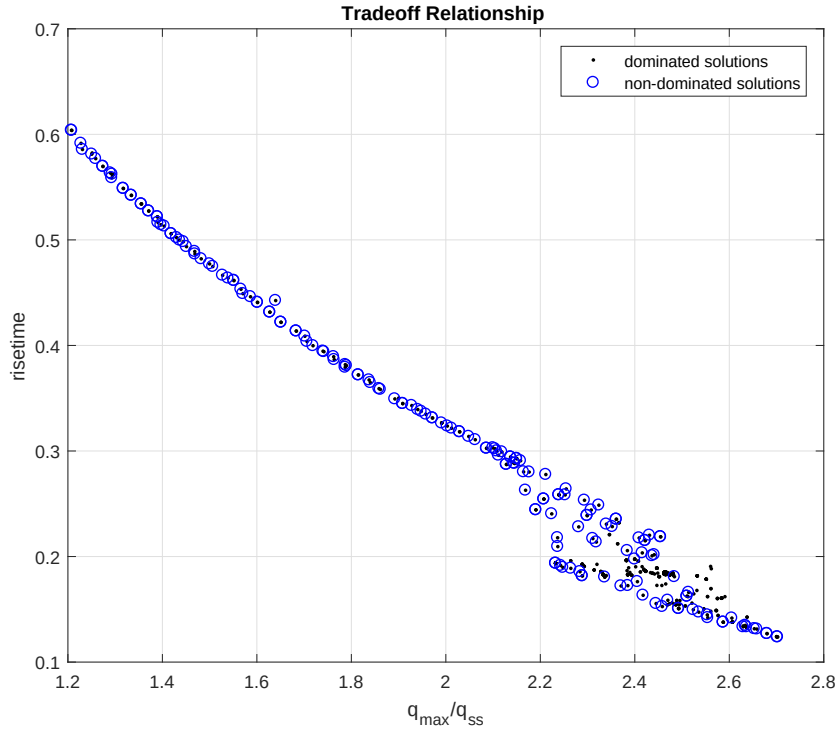

Figure 5.4: Tradeoff between f_1 ($q_{\max}/q_{\text{ss}}$) and f_5 (Rise Time)

Pareto-front. However, in Figure 5.4, the trade-off plot shows two different 'slope'

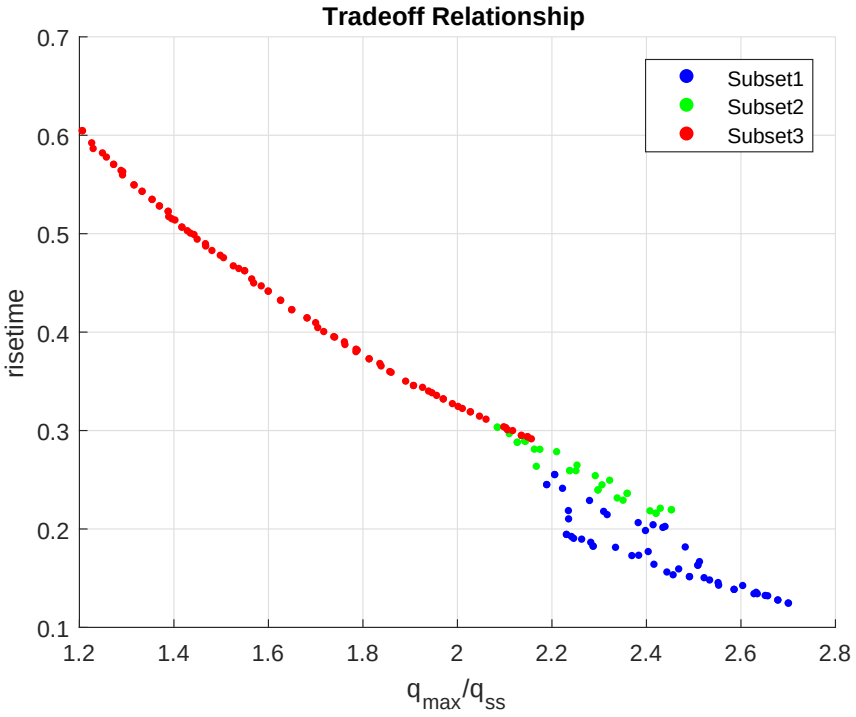

Figure 5.5: Tradeoff between f_1 and f_5

relationships, which represent the two subsets of solutions that mentioned previously, $\mathcal{S}_1$ and $\mathcal{S}_3$. There also is a transition region which is the other subset $\mathcal{S}_2$. Figure 5.5 shows the link between different subsets and the trade-off between f_1 and f_5.

It is necessary to investigate the reason for this 'separation'. As explained in Chapter 4, the controller used in this study is based on LQR theory and RCAH controller structure. Therefore, although the other gains are also important, the k_q is still the dominant one in this structure. Figure 5.6 shows the variation of k_q in the trade-off relationship in non-dominated solutions between f_1 and f_5. The dark blue represents higher values of k_q and light blue represents the lower ones.

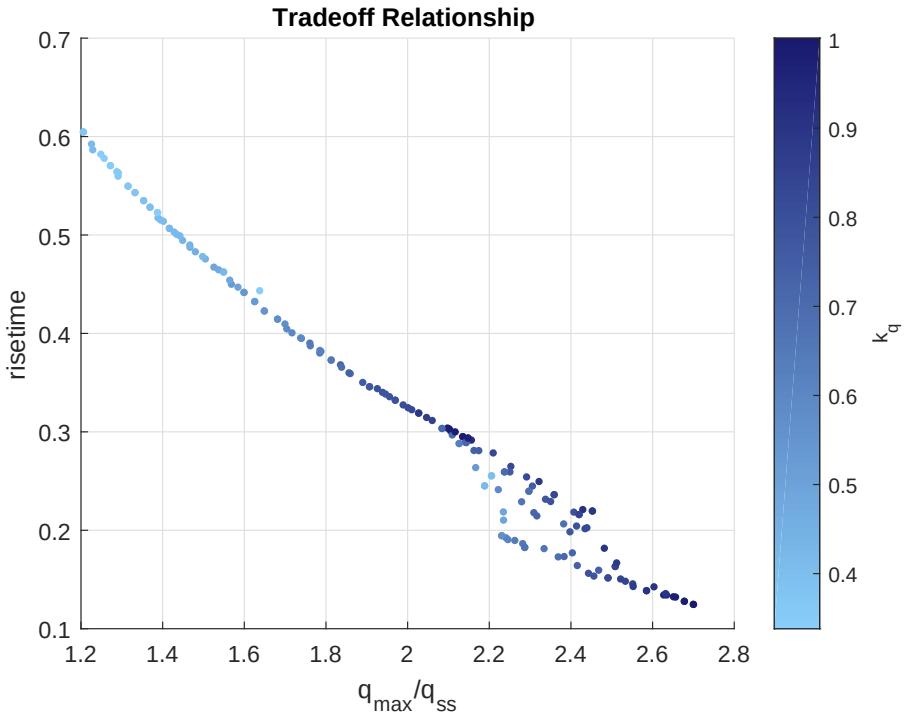

Figure 5.6: Tradeoff between f_1 and f_5

Figure 5.7 displays the detailed region $f_1 \in [1.8, 2.8]$, $f_5 \in [0.1, 0.4]$, which shows the relationships among f_1, f_5 and k_q are more clearly. The tradeoff plot actually consists of two different 'slope' relationships. The gain k_q is decreasing with the increase of rise time and the decrease of $q_{\max}/q_{\text{ss}}$ in each subset of solutions. Therefore, k_q is not the reason that caused the 'separation'. Apart from k_q, the other gains also influence the performance of the closed-loop system.

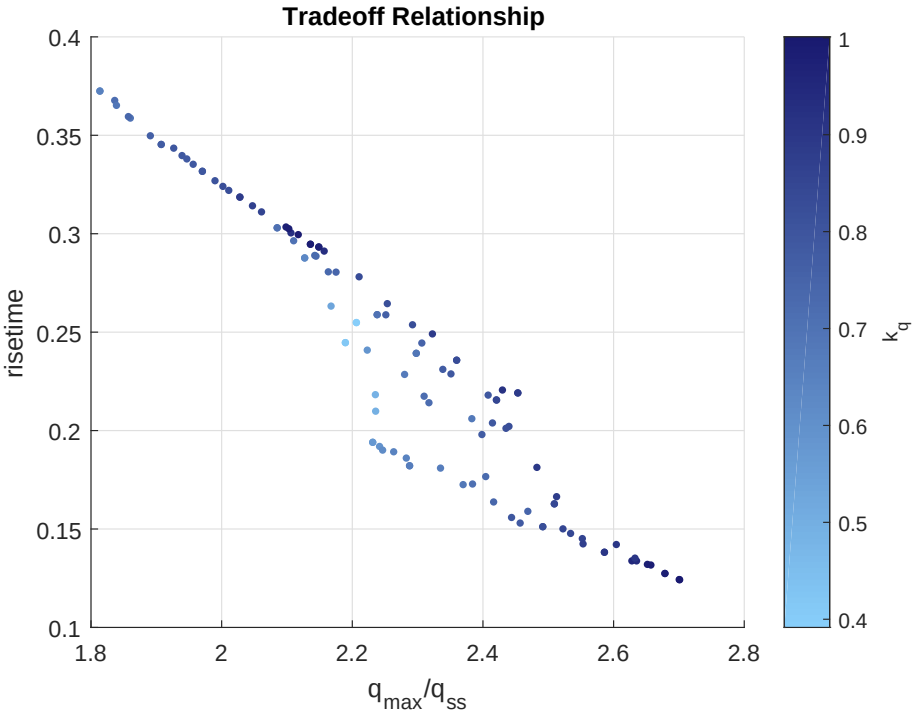

Figure 5.7: Tradeoff between f_1 and f_5 (detail)

After examination, the reason is due to the gains on the structure deformation feedback. Figure 5.8 shows the variation of k_η in the trade-off relationship in non-

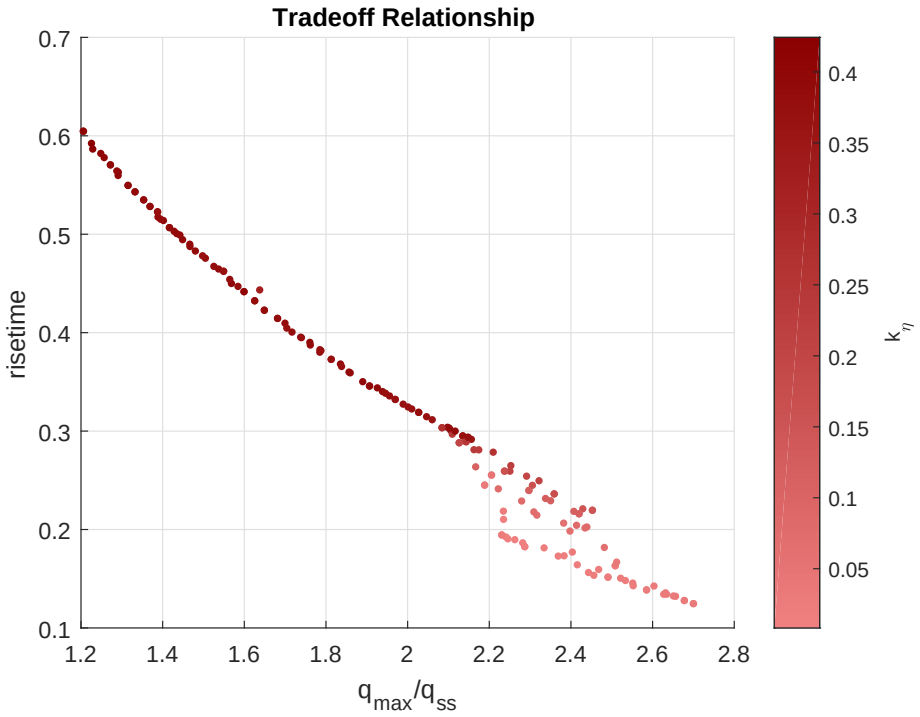

Figure 5.8: Tradeoff between f_1 and f_5

dominated solutions between f_1 and f_5, where $\mathbf{k_\eta} = [k_{\eta_1}, k_{\eta_3}, k_{\eta_6}, k_{\eta_7}, k_{\eta_9}, k_{\eta_{12}}]$ is the gain vector about the structure deformation feedbacks ($\boldsymbol{\eta}$) and $k_\eta = ||\mathbf{k_\eta}||_1$.

Thus considering both Figures 5.8 and 5.5, the conclusion is clear, the variation of the gains for structure deformation ($\mathbf{k_\eta}$) caused the 'separation', and the gains improved the system performance in handling quality.

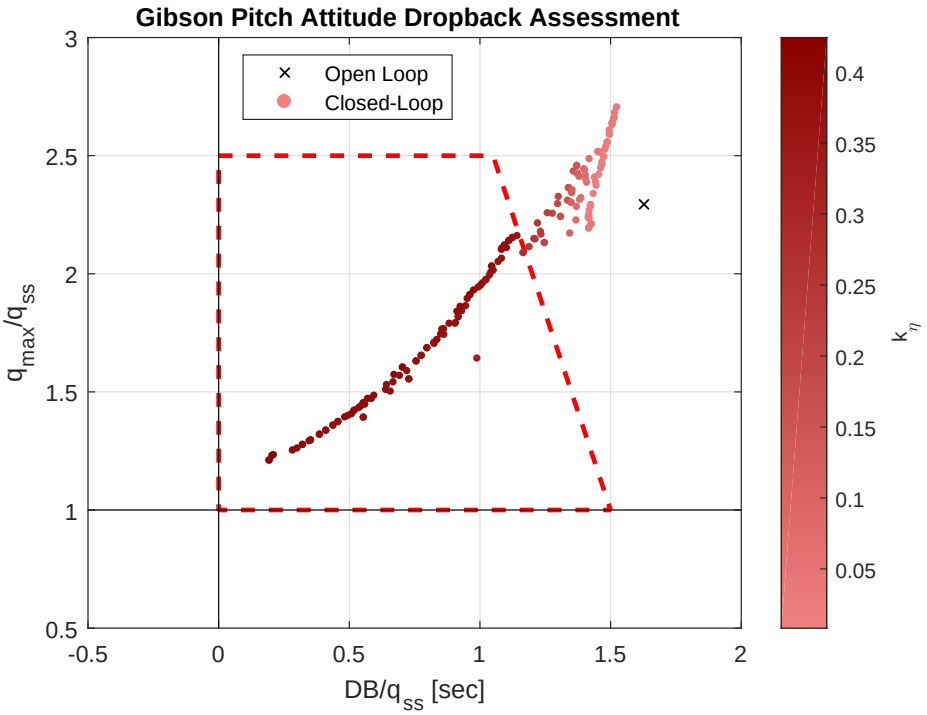

Figure 5.9: Gibson Pitch Attitude Dropback Assessment

Figures 5.9 and 5.10 show the Gibson drop back criterion in a Gibson Drop-back assessment diagram [Mooij, 1985] for the non-dominated solutions. The open-loop system ($\times$) is also shown in the figures. Based on these two plots, two conclusions can be made. First, with increasing the gains for structure deformation, the closed-loop system can obtain much better performance in Gibson drop-back criterion. Second, with similar k_η, lower k_q can improve the performance in Gibson drop-back criterion. In summary, this controller can 'use' the deformation of the structure to obtain better handling qualities by feeding back the structure deformations ($\boldsymbol{\eta}$) in the linear model.

Figure 5.11 shows the Gibson drop-back criteria pitch rate responses for three

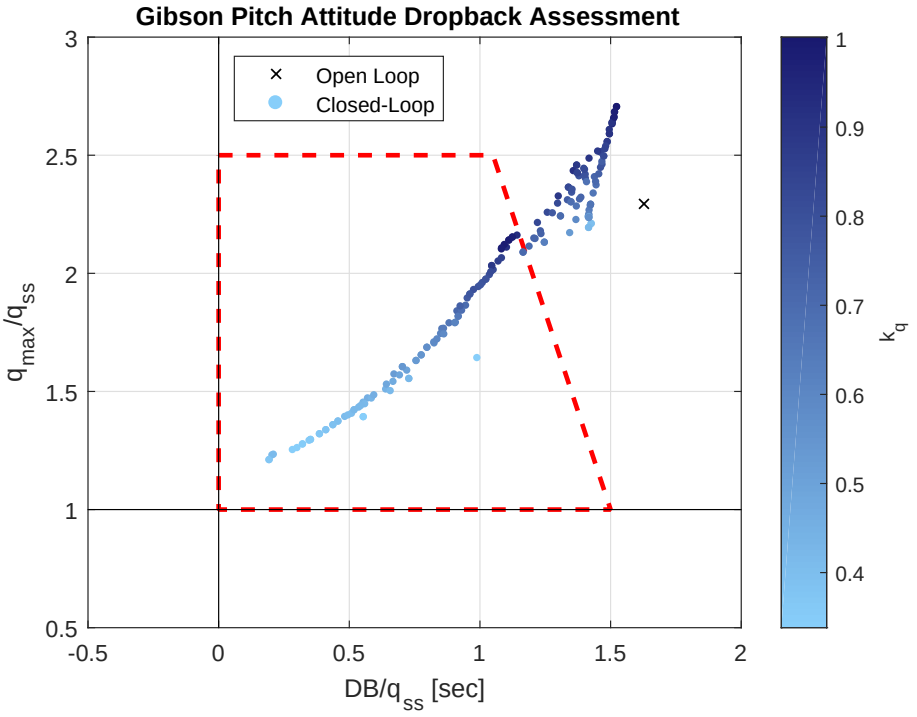

Figure 5.10: Gibson Pitch Attitude Dropback Assessment

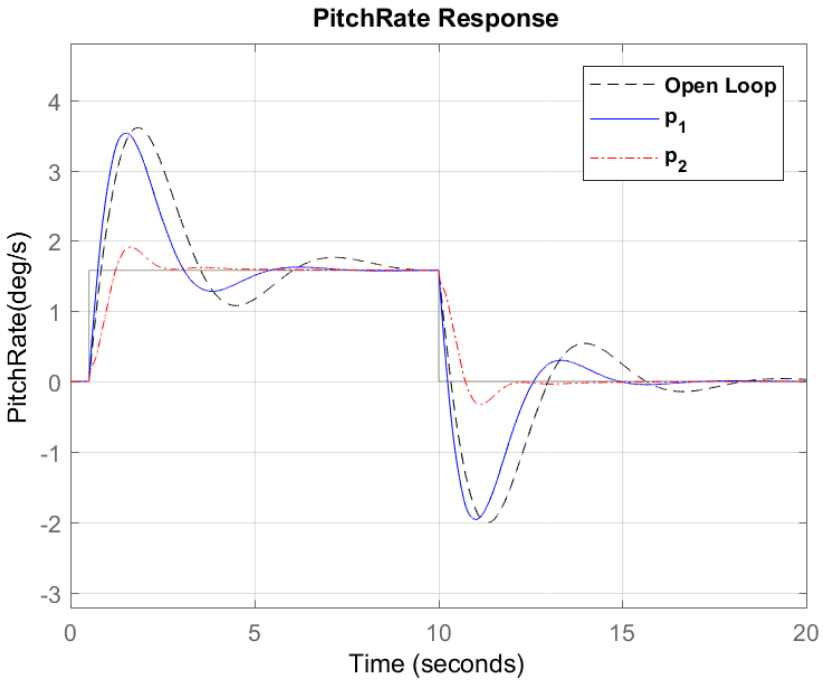

Figure 5.11: Gibson Criteria Pitch Rate Response

solutions: the open loop response (—), the solution $\mathbf{p}_1 \in \mathcal{S}_1$ (- - -) which has a low value of the k_η, and solution $\mathbf{p}_2 \in \mathcal{S}_3$ ($- \cdot -\cdot$) which has relatively high value of k_η.

Both of $\mathbf{p}_1$ and $\mathbf{p}_2$ have the lowest k_q from their subset. Solution $\mathbf{p}_1$ (- - -) has a better rise time than the open loop and the other closed loop solutions. It also

decreased the overshoot and undershoot compared with the open loop system.

The corresponding $\mathbf{Q}$ value of solution $\mathbf{p}_1$ is given by

$$\mathbf{Q}_1 = \text{diag}([0.0122, 0.8839, 1.1651, 0.1500, 0.0779, 1.4083, 0.2588, 0.1661, 6.8086, 0.4926, 0.0620, 30.6912, 0.9043, 0.7295, 0.2446, 0.0451]^T).$$

The control vector is

$$\mathbf{K} = [k_q, k_\theta, k_u, k_w, k_{\eta_1}, k_{\dot{\eta}_1}, k_{\eta_2}, k_{\dot{\eta}_2}, k_{\eta_3}, k_{\dot{\eta}_3}, k_{\eta_4}, k_{\dot{\eta}_4}, k_{\eta_5}, k_{\dot{\eta}_5}, k_{\eta_6}, k_{\dot{\eta}_6}, k_f] \tag{5.1}$$

with the value

$$\mathbf{K}_1 = [-0.5915, -0.1515, 0.0005, -0.0020, 0.0006, -0.0005, 0.0016, 0.0010, 0.0010, -0.0050, 0, 0, 0, 0, 0, 0, 7.8534]$$

corresponding to the performance vector

$$\mathbf{f} = \begin{bmatrix} f_1(q_{\max}/q_{\text{ss}}) & f_2(DB/q_{\text{ss}}) & f_3(\text{Control Effort}) & f_4(\text{Comfort}) & f_5(\text{RiseTime}) \end{bmatrix}^T$$

with the value

$$\mathbf{f}_1 = \begin{bmatrix} 2.2431 & 1.4198 & 0.9002 & 0.5069 & 0.1915 \end{bmatrix}^T$$

For the solution $\mathbf{p}_2$ $(-\cdot-\cdot)$, the overshoot and undershoot are significantly smaller than the open loop response and the other closed loop responses. The settling time is much shorter than the other two responses, but the rise time is larger.

Solution $\mathbf{p}_2$ has $\mathbf{Q}$ value

$$\mathbf{Q}_2 = \text{diag}([0.0189, 0.0408, 1.7576, 1.1817, 76.6584, 0.4051, 1.4938, 0.7815,$$

$$7.4946, 0.1538, 0.5072, 0.8937, 40.1041, 0.4792, 20.2176, 2.3372]^T).$$

and control vector

$$\mathbf{K}_2 = [-0.3659, -0.2043, -0.0038, -0.0357, 0.0747, -0.1492, 0.0121,$$
$$0.1668, 0.0006, -0.0090, 0, 0, 0, -0.0006, 0, -0.0007, 9.0059]$$

corresponding to the performance vector

$$\mathbf{f}_2 = \begin{bmatrix} 1.2076 & 0.1955 & 3.5647 & 5.5287 & 0.6039 \end{bmatrix}^T$$

Next, the objectives f_3 and f_4 are investigated.

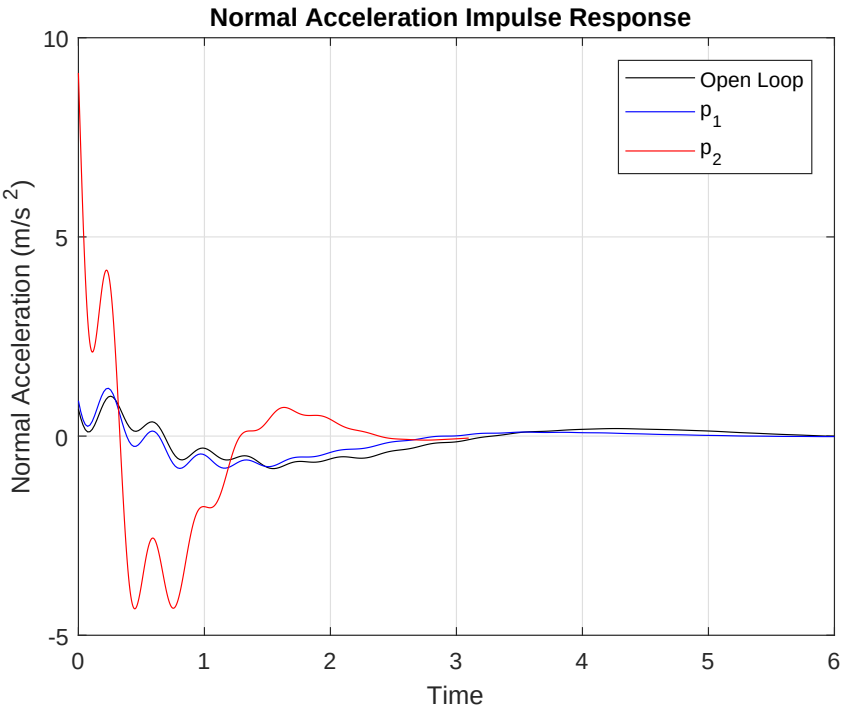

Figure 5.12: Normal Acceleration Impulse Response

Figure 5.12 shows the normal acceleration responses of the open loop and solutions $\mathbf{p}_1$ and $\mathbf{p}_2$ with impulse input of w_t (defined in Section 3.2.6) disturbance. Solution $\mathbf{p}_1$ has a similar response to the open loop, but the initial value and undershoot are much less than the response of solution $\mathbf{p}_2$. This is because when the

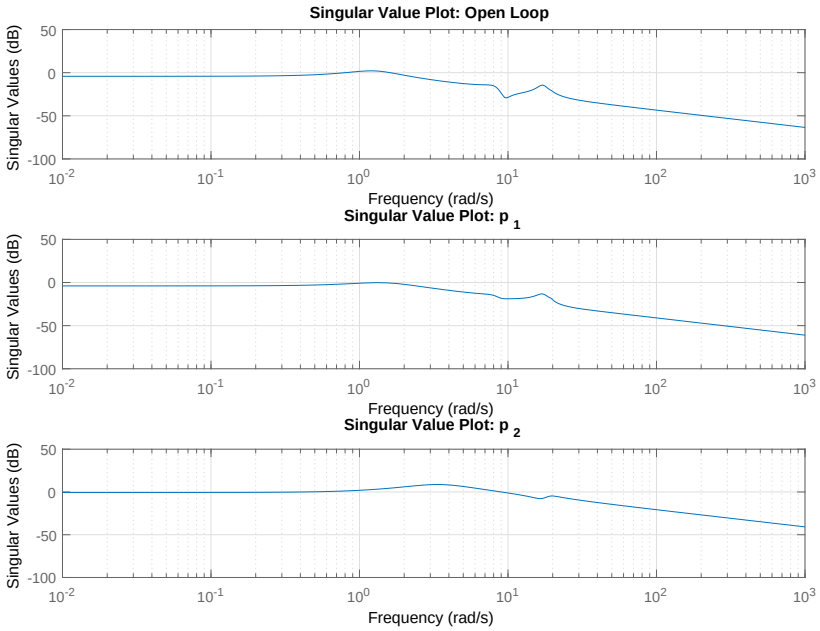

Figure 5.13: Normal Acceleration Singular Value Plot

aircraft hits wind disturbance, the structure will deform because of the flexibility, with high value of k_η, the control system will be more 'sensitive' to the deformations. However, a 'sensitive' FCS will bring aggressive input and that will decrease the value of passengers' comfort.

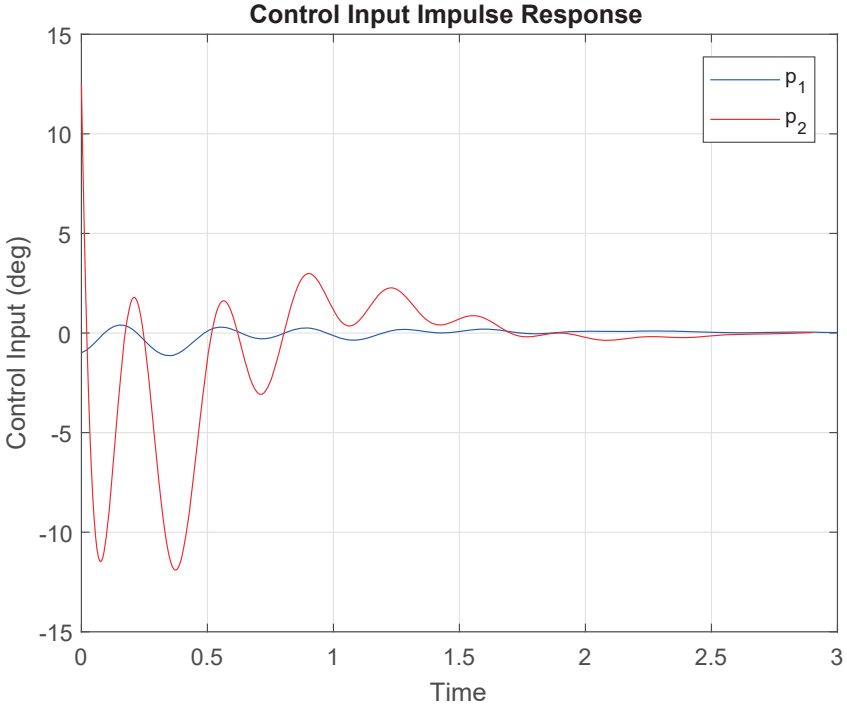

Figure 5.14: Control Input Impulse Response

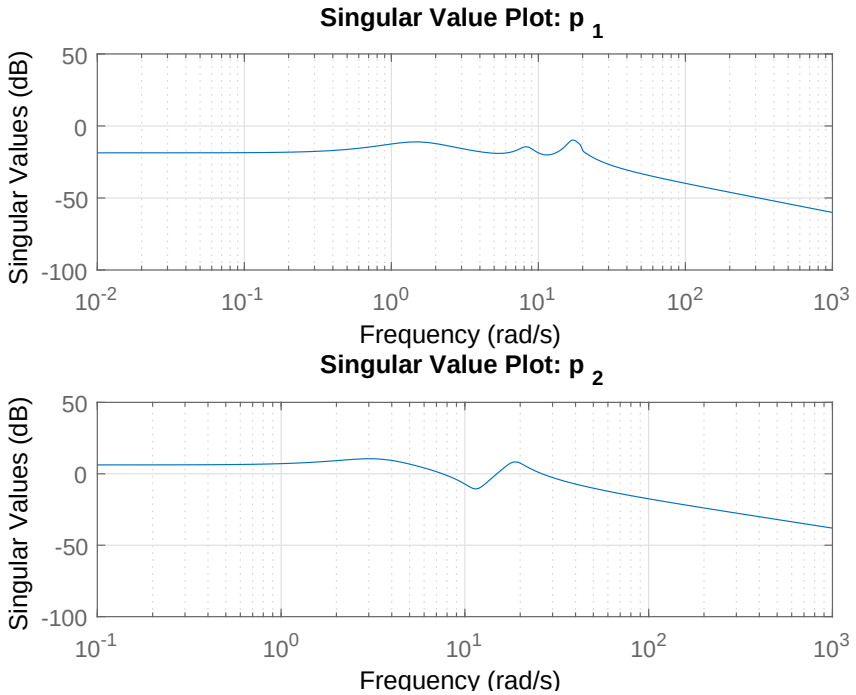

Figure 5.15: Control Input Singular Value Plot

Figure 5.13 shows the singular value plots about the normal acceleration response under w_t input of the three different systems. It is clear that larger k_η will give larger amplitude. Figure 5.14 shows the corresponding control input with the same

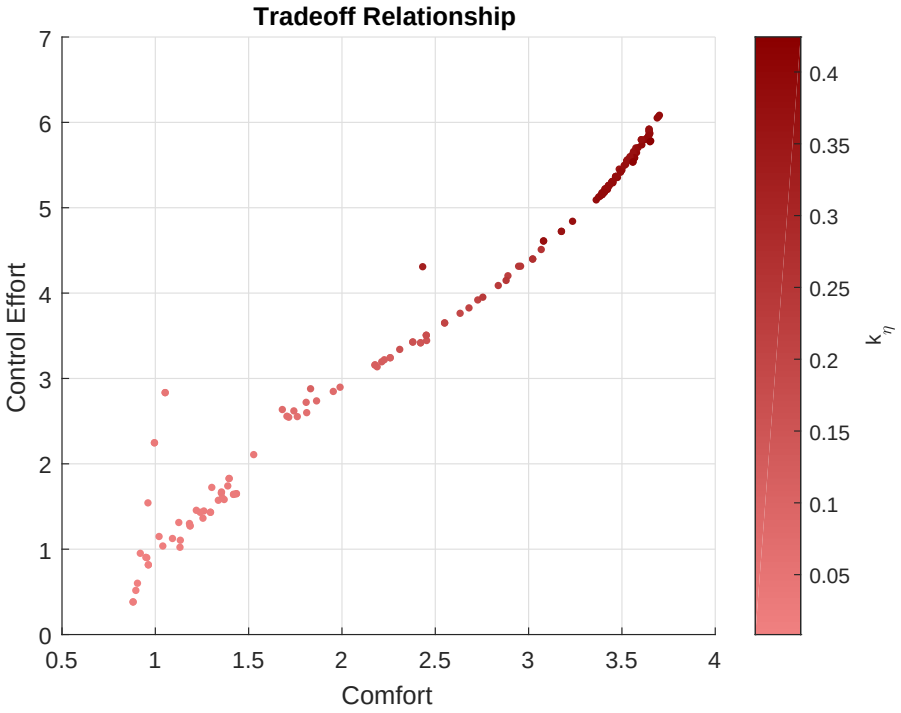

Figure 5.16: Control Input Impulse Response

w_t impulse disturbance. The 'sensitive' FCS $\mathbf{p}_2$ gives much larger control effort than $\mathbf{p}_1$. Figure 5.15 shows the singular value plots about the closed-loop elevator deflection responses under w_t input of the two closed loop systems. It also shows that larger k_η will give a larger amplitude of the singular values.

To investigate the relationships among f_3, f_4, k_q and k_η, scatter plots about them should be displayed.

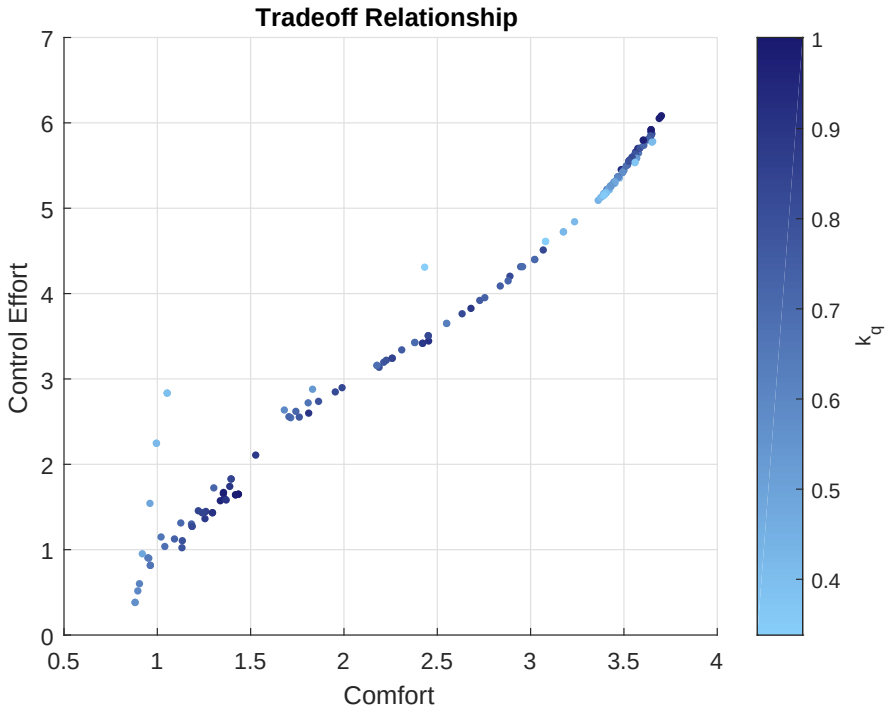

Figure 5.17: Control Input Impulse Response

From Figures 5.16 and 5.17, it is clear that with lower k_η, the closed loop system can achieve better comfort and low control effort, and with similar k_η, lower k_q will provide better performance for the closed loop in f_3 and f_4.

5.2 Non-linear Simulation Results

Because the linear model is an approximation of the simplified non-linear model trimmed at a certain flight condition using small perturbation theory, the dynamic responses will be different between them. More importantly, in this study the model

is a flexible model, which will have a more significant difference between the linear and non-linear models (see Section 3.2.5). So it is necessary to test the designed control law in the non-linear model with same flight condition.

5.2.1 Pitch Rate Response

Solution $\mathbf{p}_1$

The first test is using the control law of solution $\mathbf{p}_1$, which has a low $k_\eta = 0.0097$.

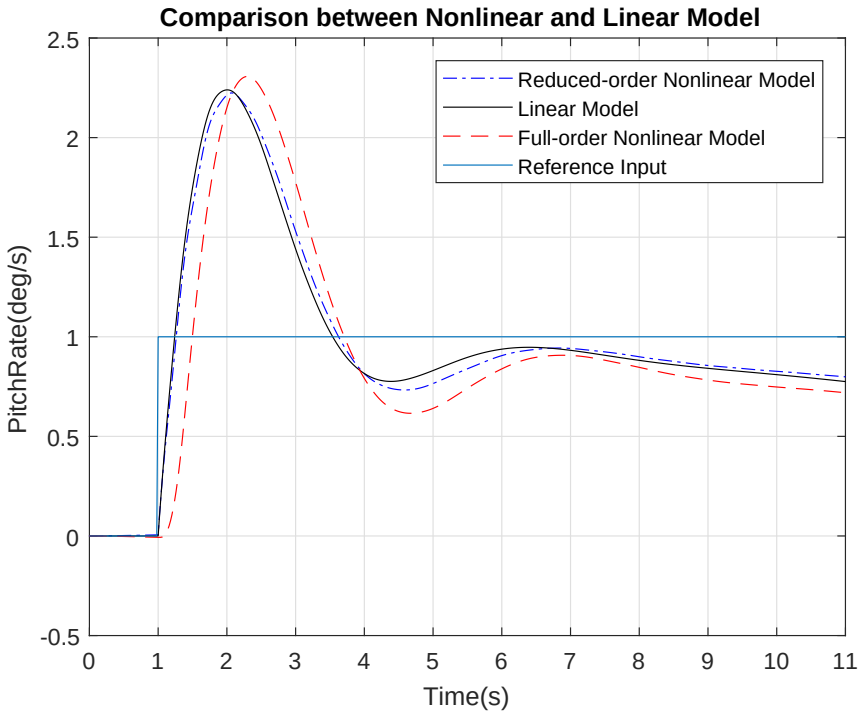

Figure 5.18: Pitch Rate Comparison : Case 1

Figure 5.18 shows the comparison between the linear model, reduced-order non-linear model and full-order non-linear model with the same unit step input. The difference between the linear and non-linear responses are not significant. The full-order non-linear model has a lag and slightly larger overshoot and undershoot. This is because of the effect for the reduced state variables in non-linear model, which is explained in Section 3.2.5.

Figure 5.19 shows the corresponding control signal input(elevator deflection) time

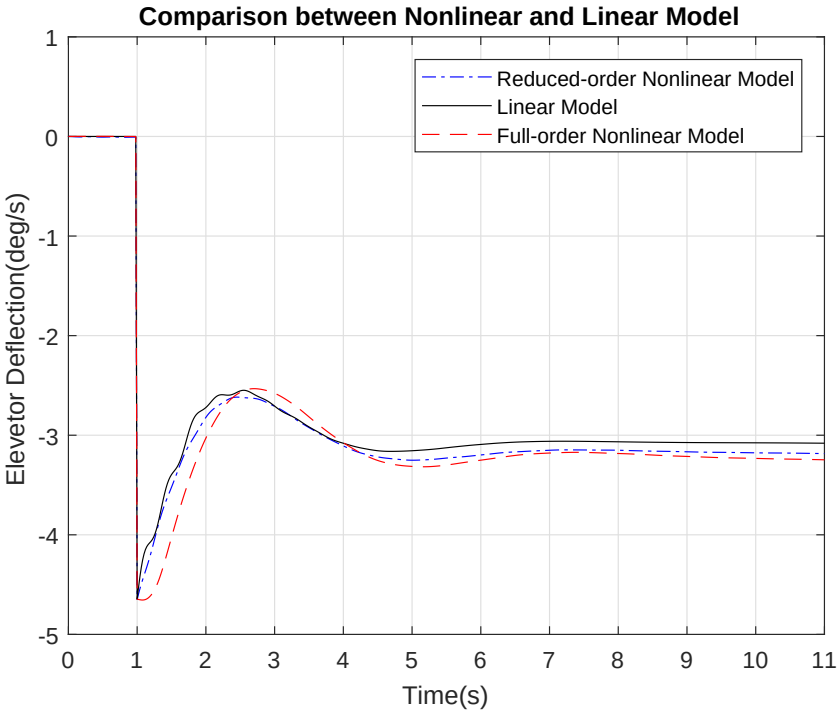

Figure 5.19: Control Input Comparison : Case 1

series for different models. It is clear that the full-order non-linear model's deflection has a lag compared with the other two for the same reason as pitch rate response that was explained previously.

The elevator deflections for reduced-order non-linear and linear model have small differences, resulting from the differences between the structure deformation modal state variables, $\boldsymbol{\eta}_{\text{long}}$, is shown in Figure 5.20, which is defined in (3.8). However, the difference of control input in Figure 5.19 is small because k_η is small in $\mathbf{p}_1$. It should be mentioned that the responses of $\boldsymbol{\eta}_{\text{long}}$ for non-linear models are close.

However, in Figure 5.20 the differences between the linear model and non-linear models are very large. This is because the linear model is linearised at a specific flight condition using small perturbation theory (see Section 3.2). It is fairly accurate for the rigid body flight dynamics parameters (i.e. u, w, q, θ). However, for the flexibility state variables, $\boldsymbol{\eta}_{\text{long}}$, the dynamic relationship among themselves and between them and rigid body flight dynamics parameters will change a lot when the structure deformation changes. Thus the flexible parts of state-space model (3.11)

is not accurate when the aircraft doing continuously pitch.

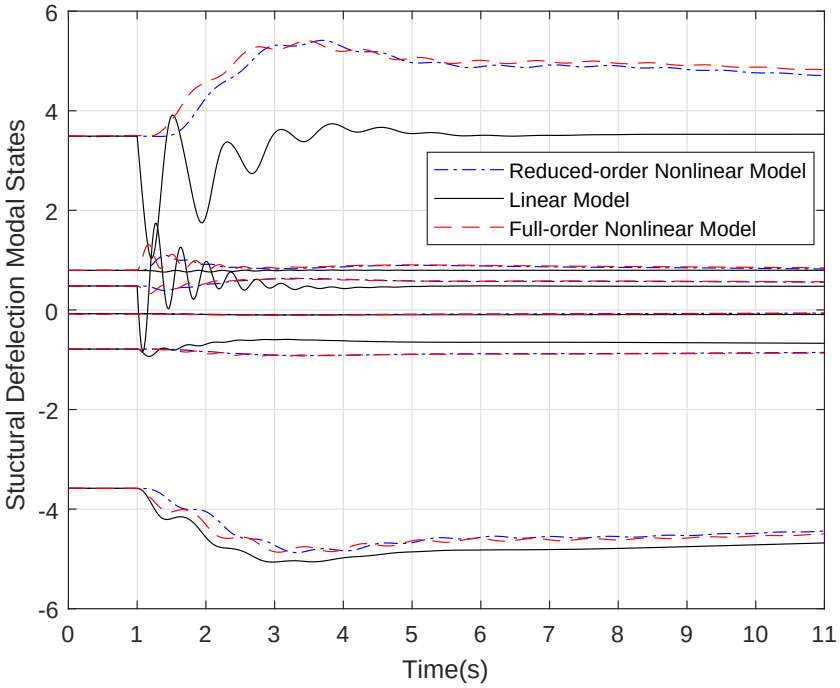

Figure 5.20: Structure Deformation Comparison : Case 1

Solution $\mathbf{p}_2$

As solution $\mathbf{p}_1$ works well in the non-linear model, solution $\mathbf{p}_2$ with high value of k_η should also be tested, the corresponding $k_\eta = 1.0847$.

Figure 5.21 shows the comparison between the linear and non-linear models with the same unit step reference input in the previous section. It can be seen that the non-linear model responses have much larger overshoot and undershoot than the linear model response. The full-order non-linear model response still has a lag compared with the others.

In Figure 5.21, it is clear that the full-order non-linear model has a small response with zero reference input. This is because the full-order non-linear model did not actually 'trim' at the trim point as explained in Section 3.2.5 and the high value of k_η magnified the after-trim oscillation of the non-linear model. So the elevator deflection is not actually zero for 'zero reference input'. It is more clear in Figure

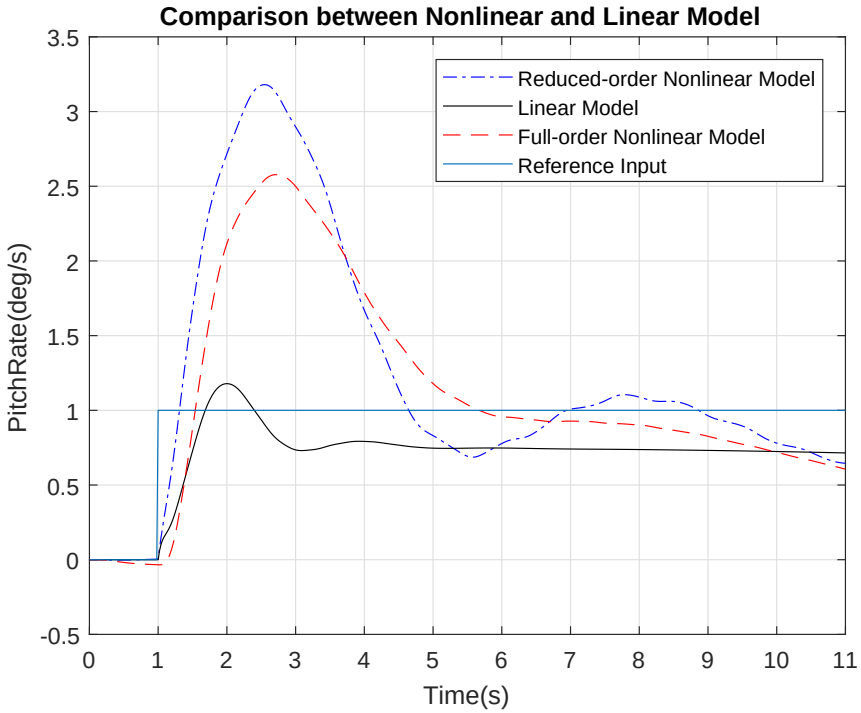

Figure 5.21: Pitch Rate Comparison : Case 2

5.22, which shows the differences of control input among different models. From

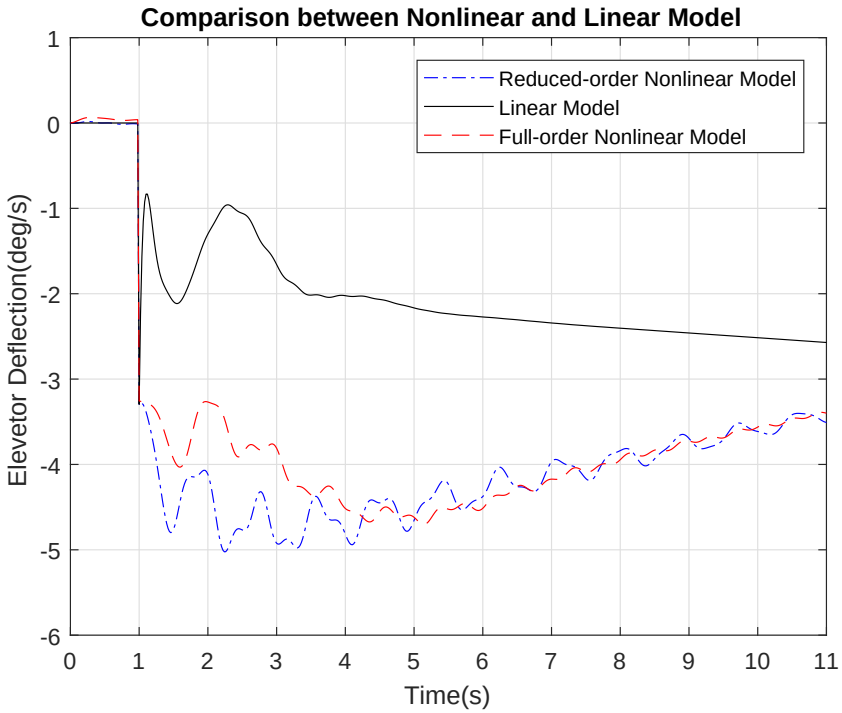

Figure 5.22: Control Input Comparison : Case 2

Figure 5.22, it can be seen that the differences between the linear and non-linear

model responses are large. This is just because of the high value of k_η. As explained

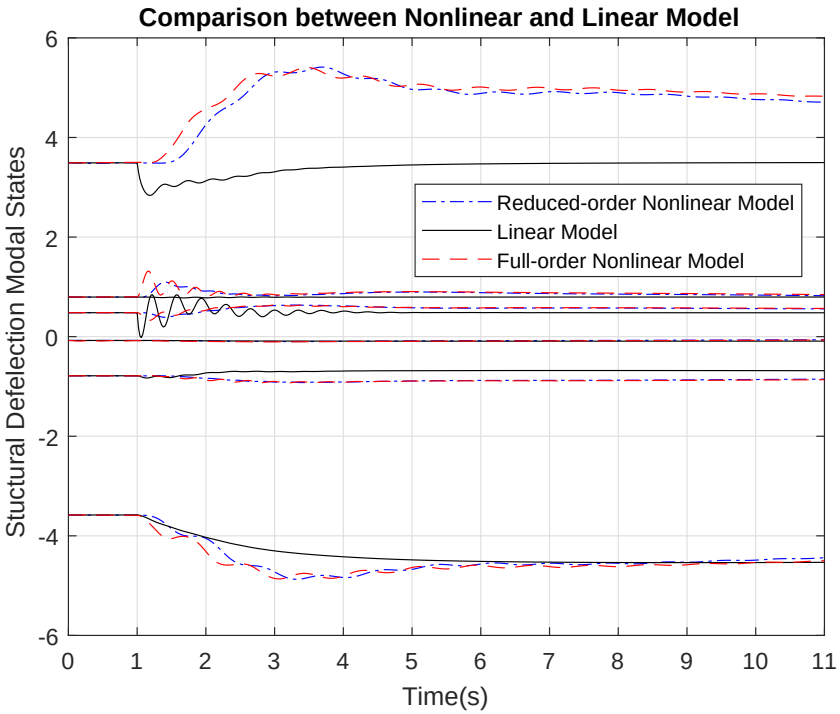

Figure 5.23: Structure Deformation Comparison : Case 2

previously, the $\boldsymbol{\eta}_{\text{long}}$ responses have enormous differences between linear and non-linear models (Figure 5.23). Thus with the high value of k_η, $\boldsymbol{\eta}_{\text{long}}$ the control input will have a large magnified difference between them.

But on the other hand, high k_η also provided high damping for $\boldsymbol{\eta}_{\text{long}}$. Thus the oscillation of $\boldsymbol{\eta}_{\text{long}}$ in solution $\mathbf{p}_2$ is smaller than solution $\mathbf{p}_1$. Therefore, the good matching between linear and non-linear models and the damping of $\boldsymbol{\eta}_{\text{long}}$ is another pair of trade-off indices. It is worth finding a solution that can give the system a good balance between them.

Solution $\mathbf{p}_3$

From Figure 5.9, it can be seen that the solutions that satisfied the Gibson Drop-back criterion always have a high value of k_η. The light red solutions that are far away from the satisfied region have low values of k_η. The solutions between these two groups of solutions are named as 'transfer solutions' which belongs to $\mathcal{S}_2$. To

avoid the bad effect from high k_η, we use the solution $\mathbf{p}_3$ for case 3, where the $k_\eta = 0.1191$. The corresponding $\mathbf{Q}$ values are

$$\mathbf{Q}_3 = \text{diag}([0.0386, 2.7875, 4.9276, 3.0350, 11.8728, 1.0355, 0.5411, 3.2366, 4.5060, 0.1754, 2.6874, 0.7662, 17.7977, 0.4439, 10.3163, 0.5921]^T).$$

The control vector is

$$\mathbf{K}_3 = [-0.7859, -0.2650, 0, -0.0144, -0.274, 0.0259, 0.0078, 0.0536, 0.0004, -0.0038, 0, 0, 0, 0, 0, 0, 0, 8.5599]$$

corresponding to the performance vector

$$\mathbf{f}_3 = \begin{bmatrix} 2.3523 & 1.3558 & 2.2315 & 3.2090 & 0.2283 \end{bmatrix}^T$$

Figure 5.24 shows the comparison between the linear and non-linear models with

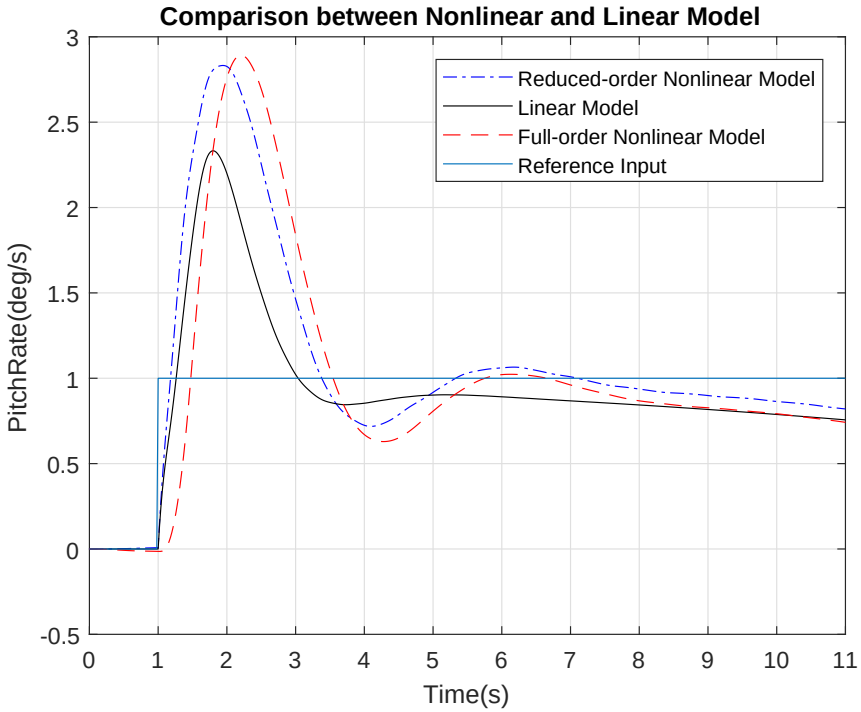

Figure 5.24: Pitch Rate Comparison : Case 3

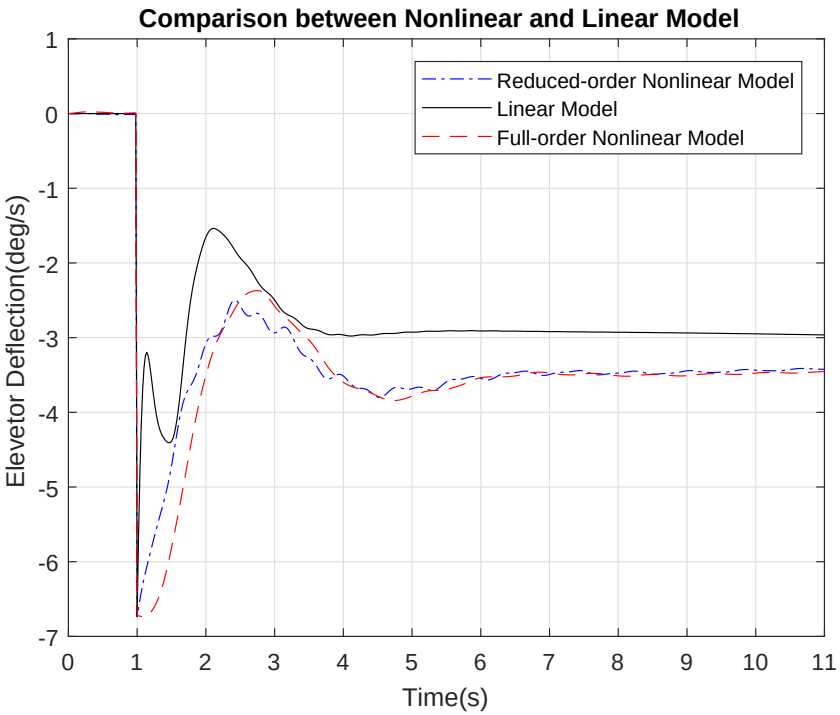

Figure 5.25: Control Input Comparison : Case 3

the same unit step reference input in solution $\mathbf{p}_3$. The corresponding control inputs and the structure state variables, $\boldsymbol{\eta}_{\text{long}}$, response are shown in Figure 5.25 and Figure 5.26 respectively. It shown that the matching between different models is not good enough for the solution that is $k_\eta = 0.1191$. Thus a lower k_η solution should be tested.

Solution $\mathbf{p}_4$

In case 4, k_η is selected as a quite small number which equals to 0.0121, $\mathbf{p}_4$ also belongs to $\mathcal{S}_2$. Figure 5.27 shows the comparison between the linear and non-linear model with same unit step input in solution $\mathbf{p}_4$. The $\mathbf{Q}$ values of $\mathbf{p}_4$ are

$$\mathbf{Q}_4 = \text{diag}([0.0286, 0.5158, 7.0612, 3.8083, 0.3672, 5.7773, 0.4607, 1.4920,$$
$$6.3461, 1.0830, 0.6380, 2.2306, 0.6256, 0.4098, 26.3464, 0.4438]^T).$$

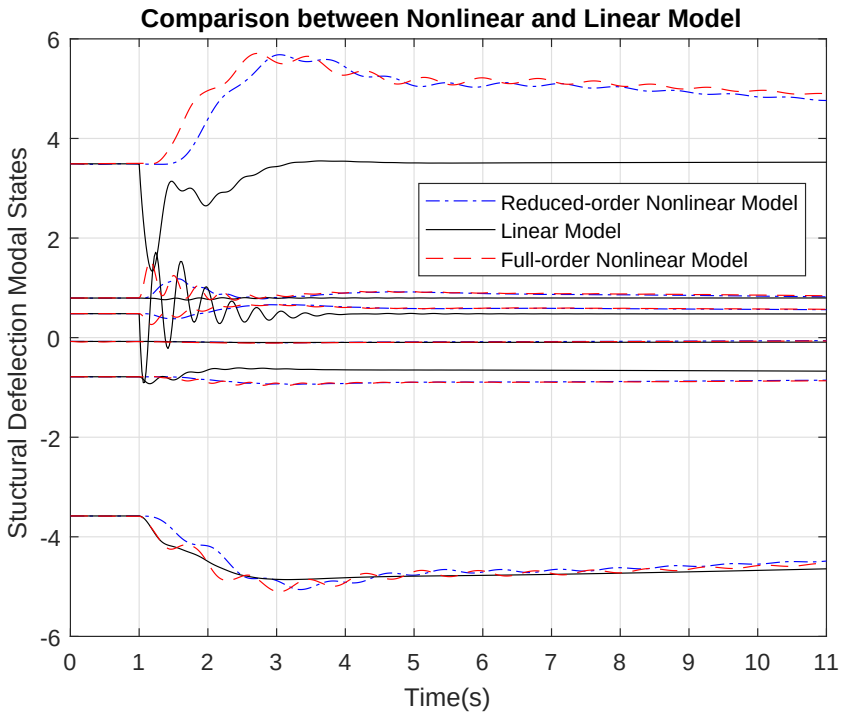

Figure 5.26: Structure Deformation Comparison : Case 3

The control vector

$$\mathbf{K}_4 = [-0.4898, -0.2400, 0.0007, -0.0015, 0.0023, -0.0002,$$
$$0.0031, 0.0026, 0.0007, -0.0031, 0, 0, 0, 0, 0, 0, 0, 9.0060]$$

corresponding to the performance vector is

$$\mathbf{f}_4 = \begin{bmatrix} 2.2371 & 1.4171 & 0.9242 & 0.9416 & 0.2094 \end{bmatrix}^T$$

The corresponding control input and the structure state variables, $\boldsymbol{\eta}_{\text{long}}$, responses are shown in Figure 5.28 and 5.29 respectively.

With the comparison between solution $\mathbf{p}_1$ and solution $\mathbf{p}_4$, especially the difference between Figure 5.18 and 5.27, even the difference of k_η between these two cases is just 0.0024, the matching between linear and non-linear models still have a difference that cannot be neglected.

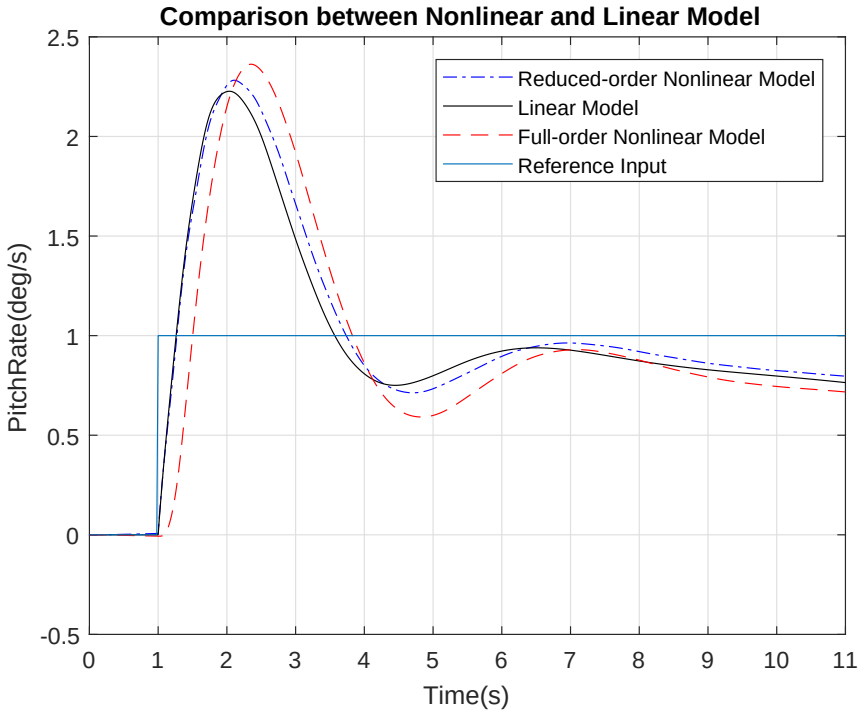

Figure 5.27: Pitch Rate Comparison : Case 4

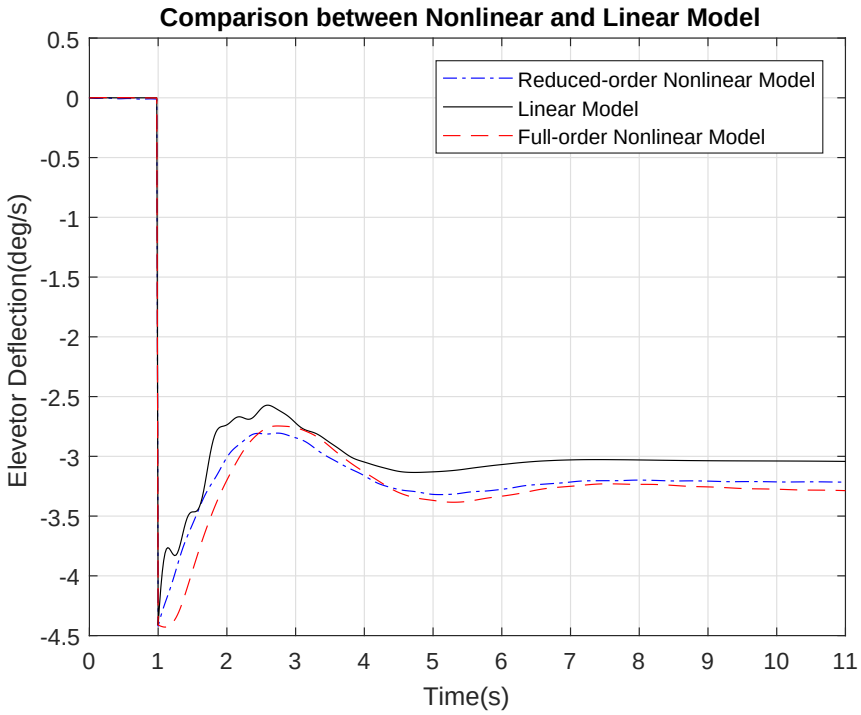

Figure 5.28: Control Input Comparison : Case 4

Thus it can be concluded that k_η plays a really important role for flexible system. The linear model cannot behave like non-linear models in the response of the

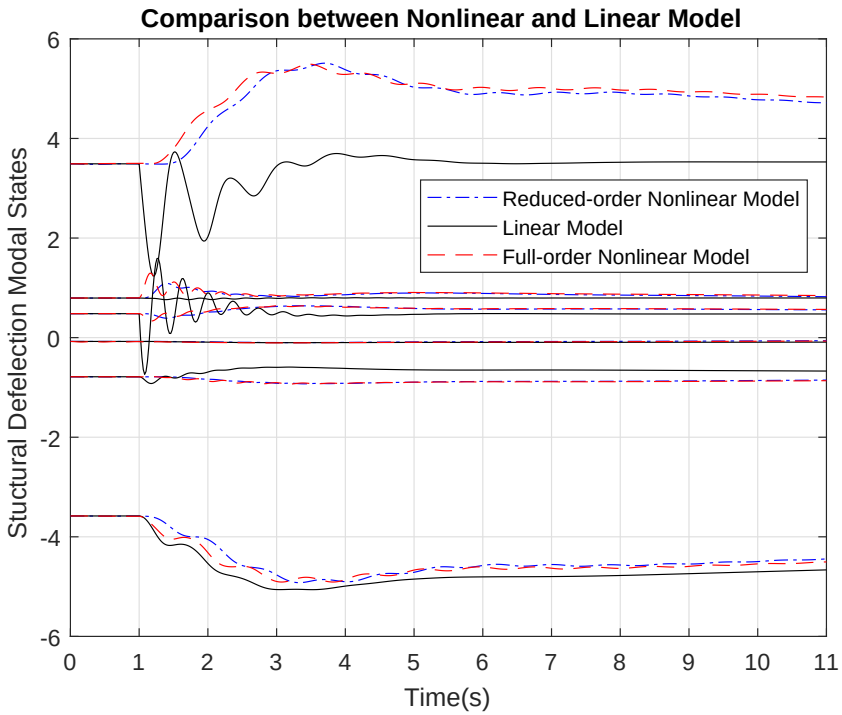

Figure 5.29: Structure Deformation Comparison : Case 4

structure state variables. Therefore, feeding back $\boldsymbol{\eta}_{\text{long}}$ will make the FCS sensitive, the performance of linear and non-linear model will have a large difference. This is because the $\mathbf{k}_{\boldsymbol{\eta}}$ will magnify the difference of structure state variables response between linear and non-linear models.

5.2.2 Comfort and Control Effort

This study is a multi-objective study, except handling quality performance, the performances under disturbance should also be tested in non-linear models. This section shows these performances of the four non-dominated solutions stated previously.

Open Loop Response

Before the closed-loop test, the differences in the open-loop response between full-order non-linear, reduced non-linear model and linear model should be examined. Figure 5.30 shows the normal acceleration responses for the three models.

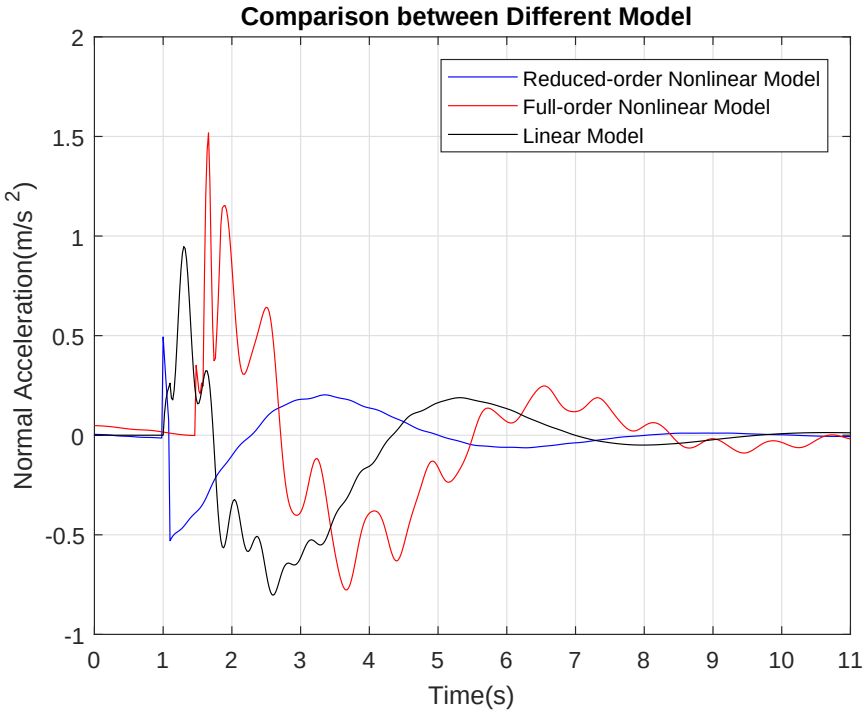

Figure 5.30: Normal Acceleration Comparison : Open Loop

The input is a pulse input of vertical velocity disturbance,

$$w_t = \begin{cases} 10m/s & \text{for t} \in [1, 1.1] \\ 0 & \text{else where} \end{cases} \tag{5.2}$$

It is clear the differences between them are large.

As explained previously (see Section 3.2.5), the full-order non-linear model can not perfectly trim with the reduced-order model trim condition, that caused the differences of the initial values. There also is a lag between the inputs, this is because the full-order non-linear model has time delay blocks (see Table 3.1) after wind disturbance inputs for considering the gust penetration effect that different nodes of aircraft will hit the wind disturbance at the different time. The response between linear model and reduced non-linear model is also very large.

The corresponding elevator deflections and $\boldsymbol{\eta}_{\text{long}}$ response are shown in Figure 5.31. The structure deformations $\boldsymbol{\eta}_{\text{long}}$ have relatively small differences between

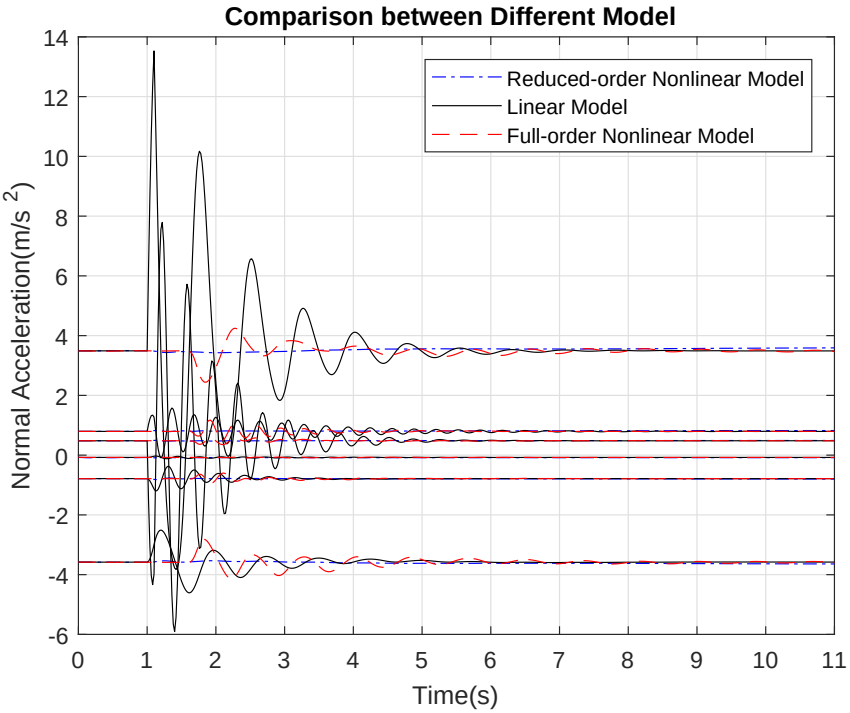

Figure 5.31: Structure Deformation Comparison : Open Loop

the two non-linear models, the response for the reduced order model basic remains same value, the full-order non-linear model have some oscillations but will trim to the same point as full order model. However, the linear model has large difference compared with the other two. This is because the dynamics relationship for $\boldsymbol{\eta}_{\text{long}}$ in the linear model is constant, that makes the linear model much more 'sensitive' than the others.

Closed Loop Test

Because the linear test of these comfort and control effort criteria have been tested in Section 5.1, and the full-order non-linear model's open-loop responses are very different with the other models, the closed loop non-linear test in this study use the reduced order non-linear model.

Figure 5.32 shows the normal acceleration responses for different solutions. The corresponding elevator deflections for different solutions are shown in Figure 5.33, the $\boldsymbol{\eta}_{\text{long}}$ responses are shown in Figure 5.34.

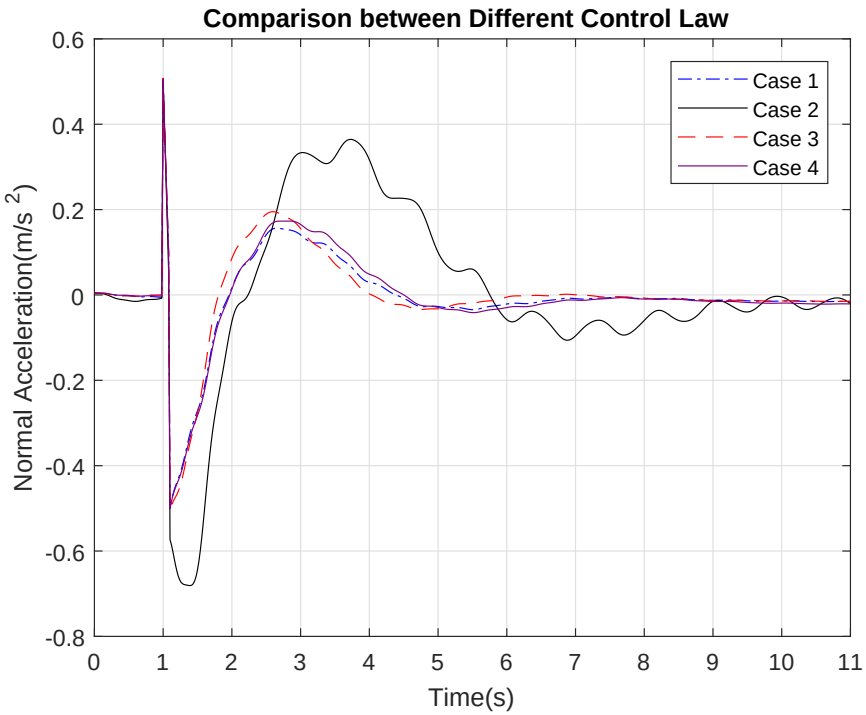

Figure 5.32: Normal Acceleration Comparison : Different Control Laws

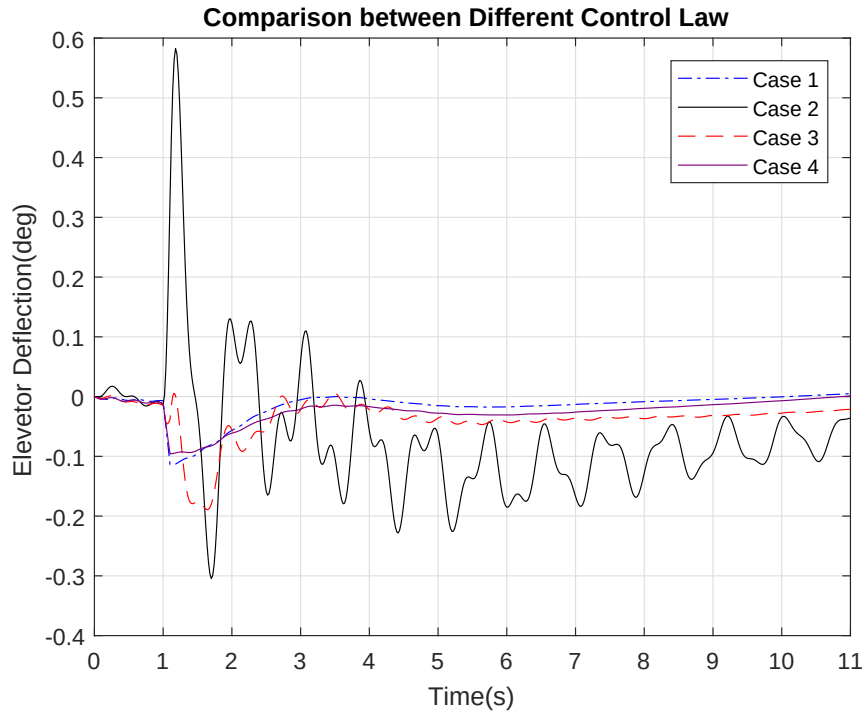

Figure 5.33: Elevator Deflection Comparison : Different Control Laws

From these figures, it is clear that the vertical wind disturbance did not give much influence to structure (Figure 5.34). The $\mathbf{p}_2$ solution control law has the

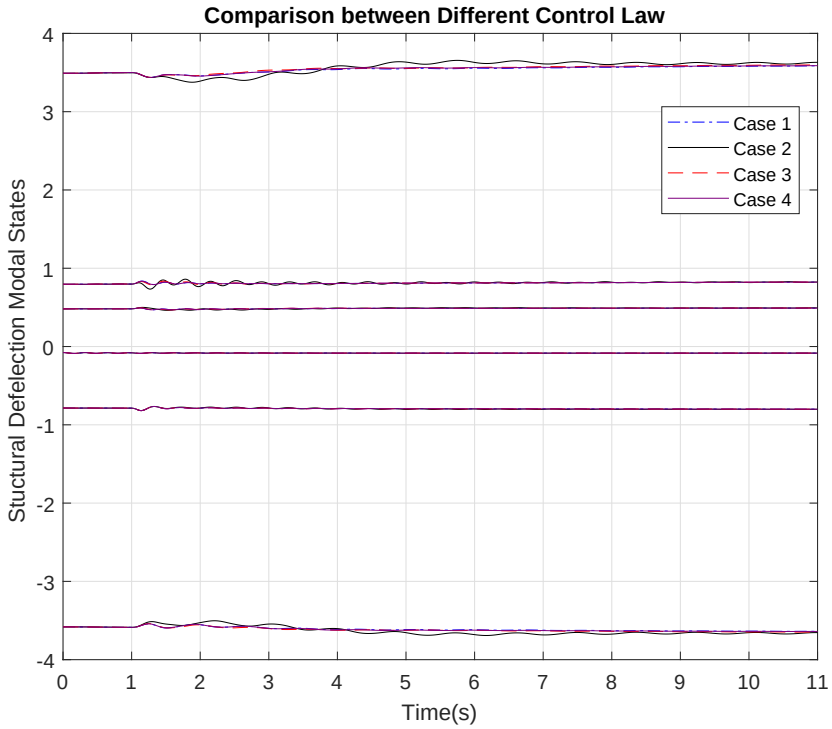

Figure 5.34: Structure Deformation Comparison : Different Control Laws

largest elevator deflection and the normal acceleration response also yhas the largest amplitude. This is mainly because of the high value of k_η in solution $\mathbf{p}_2$.

To compare the comfort and control effort criteria more accurately, rather than showing the time response, the H_2 norm of the time responses is used, which is also used as the objective functions (see Chapter 4) to show the performances.

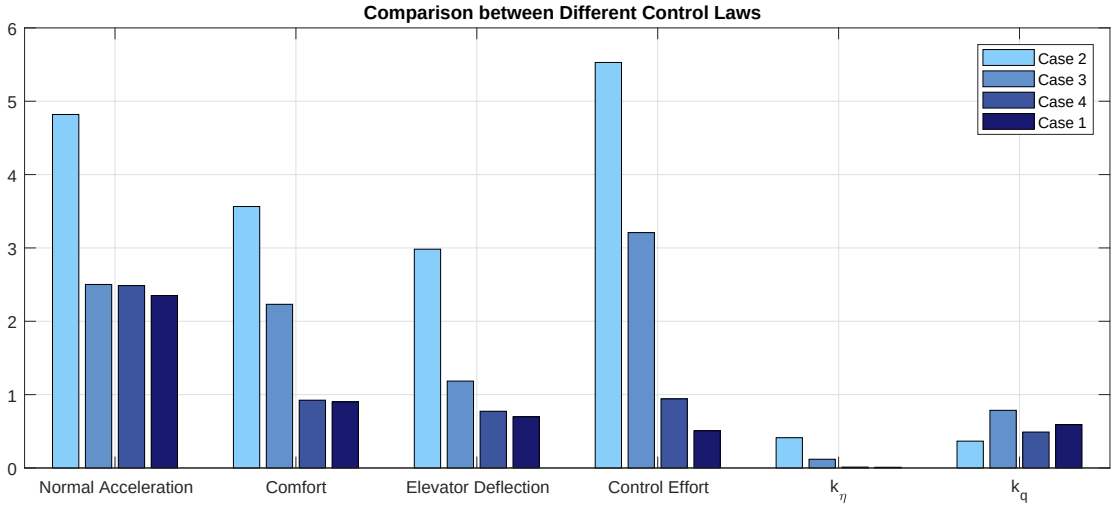

Figure 5.35: Comparison : Different Control Laws

Figure 5.35 shows the bar chart of different time response norms (normal acceleration and elevator deflection), objective indices (comfort and control effort) and the values of k_η and k_q. It is clear that the time response norms gives the same trend as the corresponding objective indices (normal acceleration with comfort and elevator deflection with control effort). Therefore, although the time response of the linear model and non-linear model do not match well, the linear indices are still reliable for at least these four cases.

However some concerns remain. A more accurate linear model which can capture the time response of non-linear model is still needed. Considering the limit of time, it is recommended as one of the future works.

Chapter 6

Conclusions and Future Work

6.1 Summary

The process of an RCAH flight controller design for a large flexible transport aircraft using a multi-objective mixed optimization (MOGA and LQR combination) approach is shown in this thesis.

A variety of objective criteria are used along with an LQR optimal controller. The approach allows trade-off studies to be conducted in order to assist the designer making the right choice of design parameters. The approach is flexible in its choice of criteria, in this case, these criteria included handling qualities with the respect of Gibson drop back criterion and rise time, passenger comfort and control effort indices that measure rejection of disturbances.

Several observations are made. For the linear system, the optimal control laws that are obtained by the proposed method work well. The Pareto-front of the non-dominated solutions in rise time and overshoot shows the 'separation'. It is shown that this 'separation' is caused by the gains on the structure deformation feedback (k_η). The variation of the gain on the pitch rate feedback (k_q) changes the rise time and overshoot of non-dominated solutions with similar k_η. It is also shown that higher k_η and lower k_q provides better handling qualities with the respect to

the Gibson Drop-back criterion. On the other hand, lower k_η and lower k_q provides better control effort and passenger comfort performance.

For the non-linear system simulation tests, because of the limits the model and the linearisation process, the optimal control laws obtained based on the linear model did not always work well on the corresponding non-linear model. With low k_η, the match between linear and non-linear model is acceptable, but the differences are large with the high value of k_η.

The responses of longitudinal structure deformation state variables ($\boldsymbol{\eta}_{\text{long}}$) between the linear and the non-linear model have very large differences for the simulation test. Although LQR is able to provide robust control laws, the control laws that obtained in this study do not work well on the non-linear model because of the large differences of $\boldsymbol{\eta}_{\text{long}}$.

6.2 Achievements

In summary, this research basically meets the aim and objectives that are set at the beginning.

1. A rich group of design specifications have been reviewed (especially for handling quality), using Gibson Drop-back criterion and rise time as the handling quality specifications and using an H_2 norm to represent the passengers' comfort and control effort criterion.

2. A mixed optimisation design method is proposed which is a the combination of LQR and MOGA, and uses an RCAH controller structure.

3. The performance of the designed controller has been evaluated on the non-linear model. The analyses of the trade-off among different objectives, the relationship between control law and objectives, control law and different models (the linear and non-linear models) are all represented.

6.3 Challenges and Limitations

To sum up, the proposed control system design method works well on the linear system, and because of the gap between the linear model and the non-linear model, not all of the control laws work well on the non-linear model. There are some challenges during the research and the proposed method also has some limitations.

Challenges

1. The first challenge is translating the Gibson Drop-back criterion into mathematical expressions. As explained before, for control problem, it is usually to convert objectives into a unique performance measure (e.g. H_2 norm for passengers' comfort and control effort). However, the Gibson Drop-back criterion is using some specific indices on the time response (q_{max}, q_{ss} and DB), which are hard to convert into mathematical norms. On the other hand, ideally, these indices are actually measured on the system without the phugoid mode. Unlike the rigid body model, the longitudinal model that used in this research has not four but eight modes. It is a challenge to find the phugoid mode for the closed-loop system and remove it during the design process.

   Therefore, the lowest frequency mode of the closed-loop linear system has been removed during the design process, and the performance indices are all measured based on the reduced-order linear system. This makes the design process more efficient and more accurate. And this is also one of the reasons to use RCAH controller structure in this study.

2. The second challenge is about constraints. Essentially, both LQR and MOGA are numerical methods, they are not that 'smart' to understand the real desired solution of the designer. Thus it is important to set suitable constraints for them, not only the linear constraints (e.g. searching space for MOGA) but also non-linear ones.

The constraint for the closed-loop phugoid mode prevents the algorithm to put too much effort to increase the damping of the phugoid mode, which is not necessary for a flight control system. The gains constraint limits the absolute value of gains that makes the control law possible to implement on the non-linear model. There also is a linear constraint to limit the searching space for MOGA, and this constraint helps MOGA to find enough rich set of optimal solutions within the desired region.

With these suitable constraints, the algorithm can actually give the designer desired solutions.

Limitations

1. The performances of the control laws on non-linear model are not always good enough. This is because of the gap between the linear model and the non-linear models. The flexible aircraft model that used in this study is very complex and highly non-linear. It is hard to use traditional way (trim and linearise) to get a reliable linear model for the original system. And the whole design approach is actually based on the linear model. That creates the gap between the performance of the control law on the linear model and the non-linear models. However, this design approach is good enough if the linear model is accurate enough.

2. This study just contains one flight condition. For a completed flight control system, it is necessary to expand the validation of the whole flight envelope of this aircraft.

3. Similar to the gap between the linear and non-linear models, there must be a gap between the simulation and the real aircraft. It is infeasible to do the flight test on the real aircraft because the model is a large commercial jet. But it is possible to validate it on a flight simulator. This validation does not

contain in this study also because of the limit of time.

Therefore, the recommendations for future work are listed next.

6.4 Recommendations for Further Work

There are three main recommendations for further work,

1. Linear model of the non-linear system: The linearisation process of this study is based on the reduced order simplified the non-linear model, that caused some problem when implementing the controller into the original non-linear model. The reason for this has not been determined. Hence the full-order non-linear model linearisation should be investigated to get a more accurate linear model for the controller design process.

2. Full flight envelope: This work can be considered as a template of one trim condition point inside the flight envelope of the AX-1 model. Using LPV models or gain-scheduling theory to expand the FCS usable range to the full flight envelope is an area for further work.

3. Further validation: Further work is needed to validate the controller designs using a flight simulator, this can be done through the CA^{2}LM framework by using the flight simulator in Cranfield University.

Appendix A

AX-1 Open-loop State-space Model

$$
A=\begin{pmatrix}
-0.0026 & 0.0257 & -5.5437 & -9.7562 & 0.0020 & -0.0082 & -0.0008 & 0.0107 & 0.0003 & -0.0073 & 0 & 0 & 0 & 0 & 0 & 0 \\
-0.0849 & -0.6172 & 170.4933 & -0.3214 & -0.0207 & -0.1852 & 0.0114 & 0.82 & 0.0031 & -0.0803 & 0 & -0.0001 & -0.0008 & -0.0001 & 0.0002 & -0.0001 \\
0.0001 & -0.0086 & -0.4469 & 0 -0.0001 & 0.0008 & 0.0006 & 0.0198 & 0.0001 & -0.0007 & 0 & 0 & 0 & 0 & 0 & 0 & \\
0 & 0 & 1 & 0 & 0 & 0 & 0 & 0 & 0 & 0 & 0 & 0 & 0 & 0 & 0 & 0 \\
-1.8833 & -14.3494 & -157.3141 & -0.0062 & -2.334 & -71.122 & 0.8886 & 48.2884 & 0.2624 & -0.5504 & 0.0016 & -0.0074 & -0.0244 & -0.0071 & 0.0081 & 0.0001 \\
0 & 0 & 0 & 0 & 1 & 0 & 0 & 0 & 0 & 0 & 0 & 0 & 0 & 0 & 0 & 0 \\
1.1678 & 10.6941 & 256.1085 & -0.0216 & 1.5518 & 5.7203 & -2.2422 & -295.614 & -0.3563 & -2.0993 & -0.0015 & 0.0049 & 0.0193 & 0.0067 & -0.0069 & 0.0029 \\
0 & 0 & 0 & 0 & 0 & 0 & 1 & 0 & 0 & 0 & 0 & 0 & 0 & 0 & 0 & 0 \\
-0.2884 & -1.2487 & -17.4599 & 0 -0.1134 & 0.1339 & 0.0483 & -0.7324 & -1.1666 & -383.6239 & 0.0002 & -0.0002 & -0.0021 & 0.0008 & 0.0006 & 0.0007 & \\
0 & 0 & 0 & 0 & 0 & 0 & 0 & 0 & 1 & 0 & 0 & 0 & 0 & 0 & 0 & 0 \\
-0.0003 & -0.0001 & -0.836 & 0 0.0019 & -0.0079 & -0.0028 & 0.0035 & -0.0632 & -0.0005 & -2.4072 & -62.3183 & -0.7793 & -43.9401 & -0.3605 & -27.3741 & \\
0 & 0 & 0 & 0 & 0 & 0 & 0 & 0 & 0 & 0 & 1 & 0 & 0 & 0 & 0 & 0 \\
0 0.0003 & -0.1572 & 0 0.0005 & -0.0016 & -0.0009 & 0.0008 & -0.0131 & -0.0001 & -0.5112 & -1.6432 & -1.2477 & -244.6658 & -0.169 & -8.1068 & & \\
0 & 0 & 0 & 0 & 0 & 0 & 0 & 0 & 0 & 0 & 0 & 0 & 1 & 0 & 0 & 0 \\
0 -0.0004 & -0.4671 & 0 0.0009 & -0.0019 & -0.0012 & 0.0037 & -0.0349 & -0.0001 & -0.5659 & -3.596 & -0.5904 & -27.0902 & -2.4666 & -359.9582 & & \\
0 & 0 & 0 & 0 & 0 & 0 & 0 & 0 & 0 & 0 & 0 & 0 & 0 & 0 & 0 & 1
\end{pmatrix}
$$

$$
B=\begin{bmatrix}0.2510 & -8.9534 & -1.0950 & 0 & 197.6270 & 0 & 335.2370 & 0 & -1.0284e-07 & 0 & -3.6323e-05 & 0 & 0.0019 & 0 & 0.0399 & 0\end{bmatrix}^T
$$

References

S. Ahmed and J.F. Whidborne. Integration of h-infinity and time domain specifications using the convex combination method. *IFAC Proceedings Volumes*, 40: 135–140, 2007.

S. P. Andrews. *Modelling and Simulation of Flexible Aircraft: Handling Qualities with Active Load Control*. PhD thesis, Cranfield University, Cranfield, Bedfordshire, U.K, 2010.

P. Apkarian and D. Noll. Nonsmooth h_∞ synthesis. *IEEE Transactions on Automatic Control*, 51(1):71–86, 2006.

D. Arzelier, D. Georgia, S. Gumussoy, and D. Henrion. h_2 for hifoo.

J. S. Baras, M. K. H. Fan, W. T. Nye, and A. L. Tits. DELIGHT.LQG: A CAD system for control systems design using LQG controller structure. In *18th Annual Conf. on Inf. Sci and Syst.*, Princeton, NJ, 1984.

Aharon Ben-Tal. Characterization of pareto and lexicographic optimal solutions. In Gnter Fandel and Tomas Gal, editors, *Multiple Criteria Decision Making Theory and Application*, pages 1–11. Springer, Berlin, Heidelberg, 1980. ISBN 978-3-540-09963-5. doi: 10.1007/978-3-642-48782-8.

S. Boyd and C. Barratt. *Linear Controller Design: Limits of Performance*. Prentice-Hall, Englewood Cliffs, N.J., 1991.

S. Boyd, C. Barratt, and S. Norman. Linear controller design: Limits of performance via convex optimization. *Proc. IEEE*, 78(3):529–574, 1990.

J.V. Burke, D. Henrion, A.S. Lewis, and M.L. Overton. Hifoo - a matlab package for fixed-order controller design and h_∞ optimization. *IFAC Proceedings Volumes*, 39:339–344, 2006.

C.E.S Cesnik and E.L. Brown. Modeling of high aspect ratio active flexible wings for roll control. In *AIAA Modeling and Simulation Technologies Conference*, Denver, Colorado, 2002.

M.V. Cook. *Flight Dynamics Principles*. Elsevier Ltd., Linacre House, Jordan Hill, Oxford OX2 8DP, 2007.

M.V. Cook. *Lecture Notes for Flying Qualities and Flight Control*. Cranfield University, Cranfield , Bedford MK43 0AL, U.K., 2012.

G. E. Cooper and R. P. Harper Jr. The use of pilot rating in the evaluation of aircraft handling qualities. Technical Report AD689722-567, Advisory Group for Aerospace Research and Development of North Atlantic Treaty Organization, Neuilly-sur-Seine,France, 1969.

T. R. Crossley and A. M. S. Dahshan. Design of a longitudinal ride-control systems by Zakian's method of inequalities. *J. Aircraft*, 19(9):730–738, 1982.

N. V. Dakev, J. F. Whidborne, A. J. Chipperfield, and P. J. Fleming. H_∞ design of an EMS control system for a maglev vehicle using evolutionary algorithms. *Proc. IMechE, Part I: J. Syst. & Contr.*, 311(4):345–355, 1997.

K. Deb, S. Agrawal, A. Pratap, and T. Meyarivan. A fast and elitist multi-objective genetic algorithm: Nsga-ii. *IEEE Transactions on Evolutionary Computation*, 2002.

Kalyanmoy Deb. *Multi-Objective Optimization Using Evolutionary Algorithms*. John Wiley & Sons, Inc., New York, NY, USA, 2001. ISBN 047187339X.

G. X. Dussart, M. Lone, and S.J Guo. Multidimensional discrete gust loads of a large civil flexible aircraft. In *AIAA Atmospheric Flight Mechanics Conference*, Grapevive, TX, January 2017. doi: 10.2514/6.2017-0016.

G. Ferreres and G. Puyou. Flight control law design for a flexible aircraft: Limits of performance. *J. Guid. Control Dyn.*, 29(4):870–870, 2006.

E. J. Field, K. F. Rossitto, and D. G. Mitchell. Landing approach flying qualities criteria for active control transport aircraft. Compilation Part Notice ADP011128 RTO MP-051, Defense Technical Information Center, 2000. Presented at the RTO AVT Symposium on "Active Control Technology for Enhanced Performance Operational Capabilities of Military Aircraft, Land Vehicles and Sea Vehicles", held in Braunschweig, Germany, 8-11 May 2000.

Edmund Field. The application of a c* flight control law to large civil transport aircraft. Technical Report College of Aeronautics NO. 9303, College of Aeronautics, Cranfield, 1993.

P. J. Fleming and A.P. Pashkevich. Application of multi-objective optimisation to compensator design for siso control systems. *Electronics Letters*, 22:258–259, 1986.

C. M. Fonseca and P. J. Fleming. Multiobjective genetic algorithms. In *IEE Colloquium on Genetic Algorithms for Control Systems Engineering*, number 1993/130, pages 61–65, London, U.K., 1993a.

C. M. Fonseca and P. J. Fleming. Genetic algorithms for multiobjective optimization: formulation, discussion and generalization. In *Genetic Algorithms: Proceeding of the Fifth International Conference*, pages 416–423, San Mateo, CA, 1993b.

C. M. Fonseca and P. J. Fleming. Multiobjective optimal controller design with genetic algorithms. In *Proc. CONTROL 94*, pages 745–749, Coventry, U.K., 1994.

C. M. Fonseca and P. J. Fleming. Multiobjective optimization and multiple constraint handling with evolutionary algorithms – part I: a unified formulation. *IEEE Trans. Syst. Man & Cybernetics – A*, 28(1):26–37, 1995.

F.W. Gembicki, C. Barratt, and Y.Y. Haimes. Approach to performance and sensitivity multiobjective optimization: The goal attainment method. *IEEE Transactions on Automatic Control*, 20:769–771, 1975.

M. Giacomán-Zarzar, R. Ramirez-Mendoza, P. J. Fleming, I. Griffin, and A. Molina-Cristóbal. Robust H_∞ controller design for aircraft lateral dynamics using multi-objective optimization and genetic algorithms. *IFAC Proceedings Volumes*, 41(2): 8834–8839, 2008. ISSN 1474-6670. doi: 10.3182/20080706-5-KR-1001.01493. 17th IFAC World Congress.

J. C. Gibson. Criteria for handling qualities of military aircraft,. Technical Report AGARD-CP-333, AGARD, Neuilly-sur-Seine, France, 1982.

J.C. Gibson. *Development of a design methodology for handling qualities excellence in fly by wire aircraft.* Delft University Press, 1999. ISBN 90.

D. P. Giesy. Calculation of Pareto-optimal solutions to multiple-objective problems using threshold-of-acceptability constraints. *IEEE Trans. Autom. Control*, 23(6): 1114–1115, 1978.

D. E. Goldberg. *Genetic Algorithms in Search, Optimization and Machine Learning.* Addison-Wesley, Reading, MA., 1989.

S. Gumussoy, D. Henrion, M. Millstone, and M.L. Overton. Multiobjective robust control with hifoo 2.0.

D. Haessig. Selection of LQR/LTR weighting matrices through constrained optimisation. In *Proc. 1995 Amer. Contr. Conf.*, pages 458–460, Seattle, WA, 1995.

ISO2631-1. Mechanical vibration and shock – evaluation of human exposure to whole-body vibration. Technical Report ISO2631-1, International Organization for Standardization, Geneva, Switzerland, 1997.

T.M. Kier and G.H.N. Looye. Unifying manoeuvre and gust loads analysis. *International Forum on Aeroelasticity and Structural Dynamics*, 2009.

G. Kreisselmeier and R. Steinhauser. Application of vector performance optimization to a robust control loop design for a fighter aircraft. *Int. J. Control*, 37(2):251–284, 1983.

F. Kubica and T. Livet. Flight control law synthesis for a flexible aircraft. *Guidance, Navigation, and Control Conference, Guidance, Navigation, and Control and Co-located Conferences*, 1994. doi: 10.2514/6.1994-3630.

F. Kubica and B. Madelaine. Passenger comfort improvement by integrated control law design. Compilation Part Notice ADPO10491 RTO-MP-036, Defense Technical Information Center, 1999.

J. G. Lin. Mutiple-objective problems: Pareto-optimal soultions by method of proper equality constraints. *IEEE Trans. Autom. Control*, 21(5):641–650, 1976.

G.P. Liu, Yang J.B., and J.F. Whidborne. *Multiobjective Optimisation and Control*. Research Studies Press, 2002. ISBN 0863802648.

T. Livet, F. Kubica, and J. F. Magni. Robust flight control design with respect to delays, control efficiencies and flexible modes. *Control Eng. Pract.*, 3(10):1373–1384, 1995. ISSN 0967-0661. doi: 10.1016/0967-0661(95)00140-P.

J. M. Maciejowski. *Multivariable Feedback Design*. Addison-Wesley, Wokingham, U.K., 1989.

J.M. Macirjowski. *Multivariable Feedback Design*. Addison-Wesley Publishing Company, Wokingham, England, 1989.

A. McCuish and B. Caldwell. Development and flight experience of the control laws and the aeroservoelastic solution in the Experimental Aircraft Programme (EAP). In M. B. Tischler, editor, *Advances in Aircraft Flight Control*. Taylor & Francis, London, U.K., 1996.

J. McKernan, J. F. Whidborne, and G. Papadakis. Linear quadratic control of plane Poiseuille flow - the transient behaviour. *Int. J. Control*, 80(12):1912–1930, 2007. doi: 10.1080/00207170701477764.

MIL-STD-1797A. Flying qualities of piloted aircraft. Technical report, Department of Defense, U.S.A, 1997.

A. Molina-Cristóbal, I. A. Griffin, P. J. Fleming, and D. H. Owens. Linear matrix inequalities and evolutionary optimization in multiobjective control. *Int. J. Syst. Sci.*, 37(8):513–522, 2006. doi: 10.1080/00207720600783942.

H. A. Mooij. *Criteria for low-speed longitudinal handling qualities*. Number NLR TR 83037 U. Springer, Dordrecht, Netherlands, 1985. doi: 10.1007/97817941701717193177.

D. J. Moorhouse and R. J. Woodcock. Background information and user guide for mil-f-878sc, military specificationflying qualities of piloted airplanes. Technical Report AFWAL-TR-81-3109, FLIGHT DYNAMICS LABORATORY ,AIR FORCE WRIGHT AERONAUTICAL LABORATORIES,AIR FORCE SYSTEMS COMMAND, 1982.

R. C. Nelson. *Flight Stability and Automatic Control*. WCB/McGraw-Hill, Notre Dame, IN, 1998.

Lucien W. Neustadt. Minimum effort control systems. *Journal of the Society for Industrial and Applied Mathematics Series A Control*, 1(1):16–31, 1962.

W. Y. Ng. *Interactive Multi-Objective Programming as a Framework for Computer-Aided Control System Design*, volume 132 of *Lect. Notes Control & Inf. Sci.* Springer-Verlag, Berlin, 1989.

J. E. Paddison, R. M. Goodall, J. Bals, and G. Grübel. Multi-objective design study for a maglev suspension controller using the databased ANDECS-MATLAB environment. In *Proc. IEEE Symp. on Comp. Aided Contr. Syst. Design (CACSD'94)*, pages 239–246, Tuscon, AZ, March 1994.

R. Palacios, J. Murua, and R. Cook. Structural and aerodynamic models in nonlinear flight dynamics of very flexible aircraft. *AIAA Journal*, 48(11):2648–2659, 2010.

R. V. Patel and N. Munro. *Multivariable System Theory and Design*. Pergamon Press, Oxford, U.K., 1982.

V. Portapas, A. Cooke, and M. Lone. Modelling framework for flight dynamics of flexible aircraft. *Aviation*, 20(4):173–182, 2016. doi: 10.3846/16487788.2016.1264719.

V. Portapas, S. Yusuf, M. Lone, and E. Coetzee. Modelling framework for handling qualities analysis of flexible aircraft. In *AIAA Modeling and Simulation Technologies Conference*, Grapevive, TX, January 2017. doi: 10.2514/6.2017-0577.

W.A. Porter and J.P. Williams. A note on the minimum effort control problem. *Journal of Mathmatical Analysis and Applications*, 13:251–264, 1966.

I. Postlethwaite, J. F. Whidborne, G. Murad, and D.-W. Gu. Robust control of the benchmark problem using H_∞ methods and numerical optimization techniques. *Automatica*, 30(4):615–619, 1994.

G. Puyou, G. Ferreres, C. Chiappa, and P. Menard. Multiobjective method for flight control law design. In *Proc. AIAA Guidance, Navigation, and Control Conference*, 2004a.

G. Puyou, G. Ferreres, C. Chiappa, and P. Menard. A multiobjective method for flight control law design. *AIAA Guidance Naviguation and Control Conference*, 2004b.

J. D. Schaffer. Multiple objective optimization with vector evaluated genetic algorithms. pages 93–100.

D. Tabak, A. A. Schy, D. P. Giesy, and K. G. Johnson. Application of multiobjective optimization in aircraft control systems design. *Automatica*, 15:595–600, 1979.

A. Galip Ulsoy. Utilization of control effort constraints in linear controller design. *Journal of Dynamic Systems, Measurement, and Control*, 111:251–264, 1989.

A. Varga. On computing 2-norms of transfer function matrices. *American Control Conference*, 1992.

J. F. Whidborne and G. P. Liu. *Critical Control Systems: Theory, Design and Applications*. Research Studies Press, Taunton, U.K., 1993. ISBN 0 86380 153 6.

J. F. Whidborne, I. Postlethwaite, and D.-W. Gu. Robust controller design using H_∞ loop-shaping and the method of inequalities. *IEEE Trans. Contr. Syst. Technol.*, 2(4):455–461, 1994. doi: 10.1109/87.338666.

J. F. Whidborne, G. Murad, D.-W. Gu, and I. Postlethwaite. Robust control of an unknown plant – the IFAC 93 Benchmark. *Int. J. Control*, 61(3):589–640, 1995a. doi: 10.1080/00207179508921920.

J. F. Whidborne, I. Postlethwaite, and D.-W. Gu. Multiobjective control system design – a mixed optimization approach. In R.P. Agarwal, editor, *Recent Trends in Optimization Theory and Applications*, volume 5 of *World Scientific Series in*

Applicable Analysis, pages 467–482. World Scientific, Singapore, 1995b. ISBN 981022382X. doi: 10.1142/9789812798862_0030.

J. F. Whidborne, I. Postlethwaite, and D.-W. Gu. A mixed optimization approach to multi-objective computer-aided control system design. In *Proc. IEEE Symp. on Comp. Aided Contr. Syst. Design (CACSD'96)*, pages 309–314, Dearborn, MI, 1996.

D. Wienke, C. Lucasius, and G. Kateman. Multicriteria target vector optimization of analytical procedures using a genetic algorithm. Part I. Theory, numerical simulations and application to atomic emission spectroscopy. *Analytica Chemica*, 265 (2):211–225, 1992.

J.R. Wright and J.E. Cooper. *Introduction to Aircraft Aeroelasticity and Loads*. American Institute of Aeronautics and Astronautics, U.S.A, 2007.

S. Yusuf, O. Chavez, and M. Lone. Application of multivariate orthogonal functions to identify aircraft flutter modes. In *AIAA Atmospheric Flight Mechanics Conference*, Grapevive, TX, January 2017. doi: 10.2514/6.2017-0695.

L. A. Zadeh. Optimality and non-scalar-valued performance criteria. *IEEE Trans. Autom. Control*, 8(1):59–60, 1963.

V. Zakian. A performance criterion. *Int. J. Control*, 43(3):921–931, 1986.

V. Zakian and U. Al-Naib. Design of dynamical and control systems by the method of inequalities. *Proc. IEE*, 120(11):1421–1427, 1973.